UNIVERSITY OF CAPE TOWN

FACULTY OF ENGINEERING AND BUILT ENVIRONMENT

Department of Civil Engineering

A study on ground improvement using a combination of stone and concrete columns

Geotechnical Engineering Group

Author: Yogendra Pudaruth

Supervisor: Dr Denis Kalumba

Co-supervisor: Laxmee Sobhee-Beetul

A thesis submitted in partial fulfilment of the requirement for award of the degree of Master of Science in Civil Engineering specialising in Geotechnical Engineering at the University of Cape Town

[October 2017]

Dissertation declaration form

1. I know that plagiarism is wrong. Plagiarism is to use another's work and to pretend that it is one's own.
2. I have used the Harvard convention for citation and referencing. Each contribution and quotation in this report from the work or works of the other people have been attributed and have been cited and referenced.
3. This report is my own work.
4. I have not allowed and will not allow anyone to copy my work with the intention of passing it off as his or her own work.

Student Name : Pudaruth Yogendra

Signature : Signed by candidate

Date : 3rd October 2017

Acknowledgement

Firstly, I would like to express my sincere gratitude to my parents who supported me both financially and morally throughout the course of this study.

I extend my gratitude to my Supervisor, Dr Denis Kalumba for his guidance and support. He has always been helpful throughout this research and his guidance was always showered upon his students. He is always cheerful and that often kept me wondering about his secret of being so lively. I also convey my thanks to Laxmee Sobhee-Beetul for her inputs that she had toward the end of my submission.

I also wish to thank Mr Charles Nicholas, workshop manager, for all his help, guidance in whatever technical issues I had and for all those mind puzzling discussions that we had from time to time. He was always welcoming and willing to help whenever I needed any kind of advice. I am also grateful to Mr Noor Hassen (Laboratory Manager), Mr Tahir Mukaddam (Senior Technical Officer) and all the other technical staff for their time, friendliness and sarcastic humour for always keeping the lab lively. They were always helpful in coordinating me when I had to switch between the different Civil Engineering laboratories for various testing and sample preparation purposes.

I extend my gratitude to Mr Norrin Stone who has supplied me the geocomposite for my experiments. I thank all my Geotechnical Engineering friends (Mark, Steven, Prospect, Katlego, Charles, Monica, Tracey, Motheo, Lita, Shaina and Sane) for making these two years at University of Cape Town a memorable one. A special note goes to Paul Mavundla and Ruben Aza-gnandji for the interesting discussions that we always had. I also seize this opportunity to thank Dr Karis Moxley, from the UCT writing centre, for her valuable feedbacks and comments.

Lastly, I would like to show my appreciation to the Committee-members of the UCT Canoe Club, UCT Yacht club, UCT Mountain and Ski club, UCT Underwater club and We are Animals Society for always keeping the various individual clubs lively. These clubs enabled me to find the right balance between my studies and keeping myself physically fit. It was a great pleasure to be part of this amazing family.

Yogen Pudaruth

(PDRYOG001)

Abstract

Stone column is a cost-effective ground improvement technique that is typically employed for low-rise buildings and road embankments. This technique mainly uses naturally occurring materials as its load transferring medium. However, stone columns have some constraints because of the loose interactions between their aggregates which can lead to uncontrolled settlements, especially in soft soils. As a result, their performance is usually improved by the inclusion of geosynthetics either in layers or as a confinement. However, there was a lack of studies that used a binder within the stone column aggregates with a view to limit the bulging/lateral spreading of its aggregates in such soils.

In this study, the upper portion of the stone columns was replaced by different grades of unreinforced concrete. The length of the concrete, as well as the depth of the soil beneath the columns, were varied. The effects of these different variables, when the resulting column was subjected to an applied load, were investigated. The optimum configuration of the above was identified and its resulting change in performance when it was combined with a reinforced bedding layer was studied. Considering application/installation procedures on site, it was best deemed to install and test a geosynthetic-reinforced bedding layer on top of, rather than within, the stone column.

It was observed that increasing the grades of concrete did not have any consistent influence on the performance of the resulting columns when there was a considerable layer of soil beneath them. The hybrid stone columns (combination of stone and concrete) performed better than the normal stone column and even to a full concrete column of the same length in several cases. Physical modelling revealed that the bulging length ranges from 2.0-2.4D (D is the diameter of the column). Test results for the optimum hybrid stone column yielded a maximum load improvement factor of 3 to 6 folds (200% to 500% increase in bearing capacity) depending on their respective configuration compared to the unreinforced soil. The improvement factor was further increased to 9.9-fold (nearly 900% increase in bearing capacity) when the optimum hybrid stone column was tested in combination with a reinforced bedding layer. The findings from this research can be used to enhance and promote the stone column ground improvement technique while still providing an economical advantage as well.

Contents

Figures

Tables

Notations and Abbreviations

ρ_{wet}	- Density of concrete mix (kg/m^3)
CBR	- California Bearing ratio
Cm	- Centimetre
C_u	- Cohesion of soil sample
D	- Diameter of stone column
D_e	- Effective diameter covered by stone column
DT	- Differential transducers
F_m	- Target mean strength
F_s	- Specified characteristic strength
FEA	- Finite Element Analysis
G10	- Grade 10 concrete
G20	- Grade 20 concrete
G30	- Grade 30 concrete
G40	- Grade 40 concrete
GC	- Geo-cell
GI	- Ground Improvement
Hz	- Hertz
k	- Constant, taken as 1.64 for 5 % defective samples
kJ	- Kilojoules
kN	- Kilonewtons
kPa	- Kilopascals
L	- Litres

LR - Load Ratio

m - Metre

M_{agg} - Mass of aggregate in concrete mix per m^3

M_{water} - Mass of water in concrete mix per m^3

M_{cement} - Mass of cement in concrete mix per m^3

Min - Minutes

MPa - Mega-Pascals

N - Newtons

No. - Number

OSC - Ordinary stone columns

S - Spacing of stone column

S5 - 100 % stone column

S4 - 80% stone column, 20% concrete

S3 - 60% stone column, 40% concrete

S2 - 40% stone column, 60% concrete

S1 - 20% stone column, 80% concrete

SC5 - 100 % Concrete column

s - Settlement

sd - Standard deviation, taken as 8 for less than 20 results

SSD - Saturated surface dry

T - Tonne

TNT - Trinitrotoluene explosive

Chapter 1: Introduction

1.1 Background

With ever-growing world population and urbanisation, land has become a valuable resource for which there is an increasing demand. Ideally, most constructions should be done on stable solid grounds and for long the strength of the soil dictated the type of foundations to be used. The soil is a nonhomogeneous material, which means that its characteristics (permeability, shear strength, bearing capacity, the rate of consolidation etc.) vary from one point to another hence, it may not always provide the best conditions for building purposes.

When faced with difficult ground conditions, the most suitable approach is to find another site but this is seldom the case. Another solution is to redesign the building, such as increasing the size of the foundation to distribute the load over a larger and safer area. It is also possible to remove the ground material and replace it with a more suitable one especially when the depth and the quantity of the problematic soil are relatively small (Kirsch and Bell, 2012).

The bearing capacity of the soil is one of the crucial factors to be considered when opting for the construction of major load-bearing structures (Bowles J.E, 1997). It must be ensured that the soil on the chosen site is of desired strength and can provide satisfactory performance. If this is not the case, then it should be improved using mechanical and/or chemical ground improvement techniques (Nicholson, 2015). Ground improvement is regarded as the modification of the physical properties of the ground (Kirsch and Bell, 2012). Various literature (Byrne and Berry, 2008, Kirsch and Bell, 2012, Nicholson, 2015) stated that the contributions of ground improvement are:

1. a net improvement in bearing capacity
2. reduced settlement
3. increased rate of consolidation
4. reduced possibility of liquefaction
5. Increased hydraulic conductivity

The techniques that are used for ground improvement differ according to the type of soils that need to be modified and the magnitude of the load that they need to support. Stone column is a ground improvement technique that provides all the five benefits mentioned earlier as well as a cost-effective approach (Xanthakos *et al.*,1994, Keykhosropur *et al.*, 2012, Asgari *et al.*, 2013, Nicholson, 2015). In addition, the use of stone columns is an environmentally friendly technique as they are usually made up of natural aggregates (stones) that act as a reinforcement within the soil.

According to Barksdale and Bachus (1983), the construction of stone columns involves the partial replacement (15-35 %) of soft soil material with compacted vertical columns of stones that normally penetrate the full layer of the weak strata. Each column is normally designed to carry between 20 - 50T of imposed load. Since the stone columns are made up of loose materials, with no binder in between them, their strength is governed by their circumferential confinement which, is normally provided by the surrounding soil (Murugesan and Rajagopal, 2006, Gniel and Bouazza, 2009, Keykhosropur *et al.*, 2012, Ghazavi and Javad, 2013). Figure 1-1 shows the drainage path by which groundwater gets dissipated through the stone column.

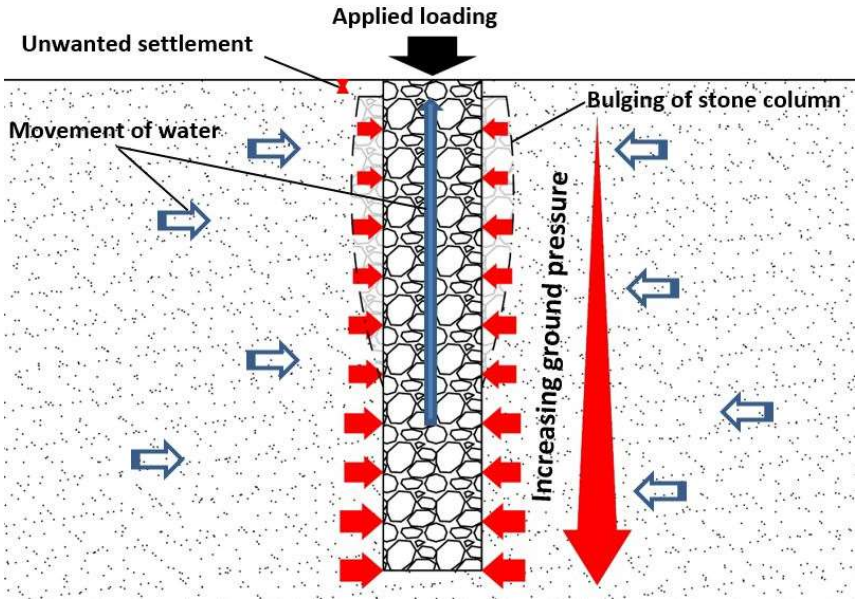

Figure 1-1: Dissipation of groundwater via the stone column.

When the column is loaded, it gains its axial stability when it bulges (Barksdale and Bachus, 1983). This bulging is governed by the confining pressure and transfers some

of the bearing load to the surrounding soil due to the interface shear friction. The insufficient lateral restraint in highly compressible soils can become of great concern because it can lead to considerable lateral spreading (bulging) of the stone column which in turn causes settlements and ground instability issues (Murugesan and Rajagopal, 2006, Gniel and Bouazza, 2009, Keykhosropur *et al*., 2012, Ghazavi and Javad, 2013).

To minimise associated problems related to settlements, stone columns are usually encased with geogrid/geosynthetic reinforcement to limit their bulging in these types of soil (Gniel and Bouazza, 2010, Keykhosropur et al., 2012, Ghazavi and Javad, 2013). However, from the literature review, it has been found that there is still room for improvement by an innovative approach that has not been studied so far.

1.2 Problem statement and research approach

As highlighted earlier, if the stone column experiences excessive lateral spreading (bulging), uncontrolled settlements will occur. This may be detrimental because it can lead to cracking and structural instabilities. Previous studies have confined the stone column materials with a geogrid/geosynthetic to control bulging and limit settlement. However, there is a lack of research that involved binding the stone column material together with a view to mitigating the bulging/settlement issues. This could be a useful focus for research because this could promote a better practical way of reinforcing stone column.

As a result, to better understand how a binding material can improve the performance of a stone column, this study focused on the use of concrete as a binder. This approach will be like combining two different methods of ground improvements (Concrete piling and stone column). Concrete piling is effective in bypassing weak ground and transferring the imposed load directly to a suitable load stratum but cost implications can be relatively high. On the other hand, the stone column is a cheaper approach to ground improvement. A combination of both could possibly enhance the performance of the stone column with a minimum rise in cost compared to other deep ground improvement techniques such as piling/compaction grouting.

1.3 Aim and Objectives

The aim of this research was to determine the optimum arrangement of the hybrid stone column (combination of concrete and stones) in different configurations whereby the effects of the depth of soil, the strength and length of the concrete reinforcement/plug will be studied. To achieve this aim, a series of tests were devised through which specific objectives were met. The objectives were as follows:

- Investigating how the length of the concrete plug/reinforcement within the hybrid stone column affects its performance while keeping the overall dimensions of the hybrid stone column and other variables constant.
- Assessing the performance of specific columns while varying the thickness of the soil beneath them.
- Analysing how different grades of the concrete plug/reinforcement affects the bearing capacity of specific hybrid stone columns.
- Studying the effects of a reinforced bedding layer on top of the optimum configuration with a view to increasing its performance.

1.4 Significance of study

This study is important as it embraced the idea of a relatively cost-effective ground improvement technique, stone column, by further enhancing its capabilities. The application of the findings of this research is vast and paves the way to various other studies that have been elaborated in Chapter 6. One of the major applications is for the construction of road embankments over soft ground but it can also be adapted for low-rise buildings or other load-bearing structures such as bridge piers.

1.5 Scope and limitations

This research involved laboratory experiments on a scaled model of stone columns. A unit cell was used for testing purposes which, considered the spacing ratio of stone column (with respect to its diameter) that is normally adopted for construction purposes. The soil used was prepared accordingly so that it mimics the performance of a soft soil and its moisture content was maintained throughout this study. Additional

information and details are found in the research methodology section (Chapter 4) of this dissertation.

The main limitation of this research was the lack of field testing. This could have been used to validate the findings from the laboratory results for practicability purposes. These should be done to back up and support the findings of this research with a view to proceeding with the recommended application as elaborated in Chapter 6 (Application and conclusions). Moreover, due to time constraints, a numerical model to predict the behaviour of these hybrid stone columns could not be fully developed. However, the results obtained from this research could be adopted to develop and calibrate such model which will be useful for design purposes.

1.6 Hypothesis

If the concrete acts as a reinforcement, the bearing load will be transferred to a deeper level within the stone column, which might contribute to an increase in performance. In the absence of punching failure, increasing the strength of the concrete should have a positive impact on the performance of the column. In addition, a reinforced bedding layer might also help to increase the load carrying capacity of the configuration as it will enable sharing of load between the soil and the column. However, it is anticipated that the inclusion of a soil layer beneath the tested columns will lead to a decrease in performance compared to if it was on a stiff ground, due to end bearing failure.

1.7 Organisation of the study

Following this chapter, Chapter 2 introduces the necessity of ground improvements and some of the different techniques available. Chapter 3 focuses more on the stone column as a method of ground improvement. It highlights the studies that have been done so far. The methodology that has been adopted in this study is detailed in Chapter 4. Chapter 5 presents the results that were obtained throughout this research. Chapter 6 elaborates on the different objectives that were met through this dissertation. It also presents relevant discussions, application and recommendations for further studies. This section is followed by the appendices where additional details about the experiments carried out can be obtained.

Chapter 2: The need for ground improvement

2.1 Introduction

This chapter presents a general overview of the importance of ground improvement and some of the various techniques available for diverse types of soils (Figure 2-1). It is necessary to ensure that buildings/roads are structurally sound; however, it is of utmost importance to verify whether the ground can provide sufficient bearing capacity for support (Bowles J.E, 1997).

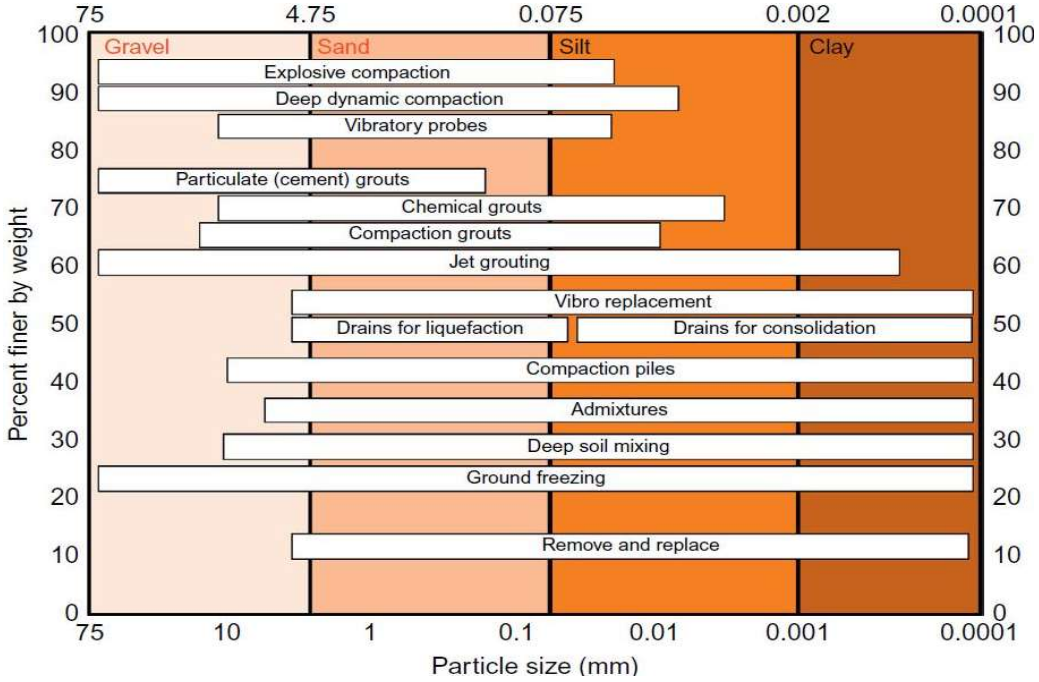

Figure 2-1: Ground improvement techniques and their suitability to different types of soil (Nicholson, 2015).

Craig and Knappett (2012) defined the bearing capacity as the ultimate load that will cause failure of a supporting soil just below or adjacent to the foundation. If insufficient investigations are carried out, catastrophic failures can occur due to poor design and unforeseen conditions. Sadly, in some cases, this can lead to loss of life as well. In the following sections, a few cases of geotechnical failures will be elaborated to fully highlight the importance of ground improvement/investigations.

During the early twentieth century, with the advancement in heavy machinery and a better understanding of soil properties, several methods of ground reinforcements have been developed by Terzaghi and others (Kirsch and Bell, 2012). A brief overview of these different techniques has been highlighted hereafter. Their approaches and suitability for various soil types will be considered.

2.2 Cases of Geotechnical Engineering Failures

The following sections will present cases of geotechnical engineering failures. The projects that will be highlighted are as follows:

1. Transcona Grain Elevator Canada
2. Leaning Tower of Pisa- Italy
3. Lotus Riverside Apartments- Shanghai
4. Ring Road Project- Mauritius
5. Global slope instability issues in a residential area- Cape Town

These failures cases were picked out from several others as each one of them brought forward a unique way through which instabilities occurred. These cases gave a general idea of the various aspects that must be considered when assessing the stability of a ground.

2.2.1 Transcona Grain Elevator-Canada

The construction of the 36400m^3 grain tower in the north of Transcona (near Winnipeg), Manitoba, Canada began in 1911 (Bosela *et al*., 2013) and ended in September 1913 (Puzrin *et al*., 2010). On the 18th of October of the same year, after uniformly filling the silos with grains to around 87.5% of their capacity, a slight settlement was observed. Within 1 hour, about 30cm settlement occurred. However, it ceased after around 24 hours but by then the structure was tilting by approximately 27 degrees from the vertical as shown in Figure 2-2 (Puzrin *et al*., 2010).

Unfortunately, at that time, no correlations/equations were available to check the bearing capacity of the soil underlying the structure. In 1951, after a thorough

geotechnical study was carried out, it was found that the structure tipped due to insufficient ground bearing capacity resulting from a soft underlying soil stratum.

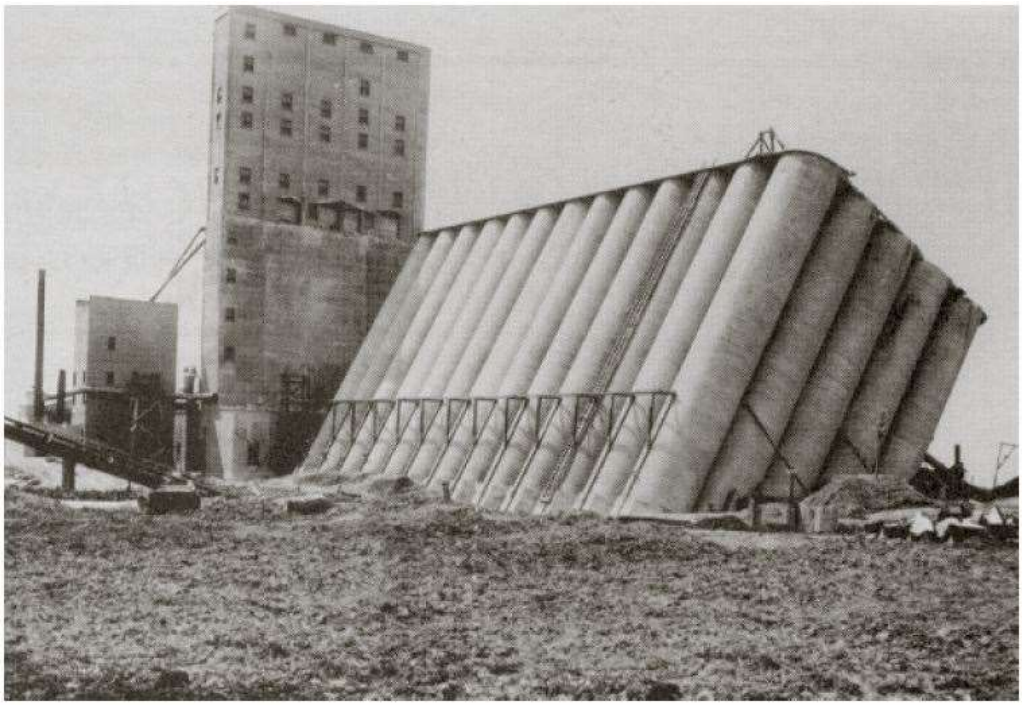

Figure 2-2: Transcona Grain Elevator, Canada (Puzrin *et al*., 2010).

2.2.2 Leaning Tower of Pisa-Italy

Located in the city of Pisa in Italy is the Romanesque Leaning Tower (Figure 2-3). Its construction was carried out in three stages, with nearly a century gap in between them. It started in 1173 and ended in 1370. Initially funded by the treasure from six heavily loaded boats, it was built as a bell tower to show the power of the Church and Republican around that time. At the beginning of stage 2 in 1272, the tilt was around 0.2˚ and by its end in 1276, it was noted that the building was tilting by 0.6˚. At the start of the 3rd stage in 1360, the tilt was around 1.6˚. Currently, the 56m high tower tilts at an angle of 5.5 degrees from the vertical (Puzrin *et al*., 2010). However, the tower has now been stabilized with the use of grouting technique and is a major tourist attraction (Bosela *et al*., 2013).

Figure 2-3: The leaning tower of Pisa, Italy (Wonderopolis, 2012).

Puzrin *et al*. (2010) reported that the instability was not a foundation failure because there was a lack of heaving of the surrounding soil and rate of tilting was slow over the course of years after construction. They stated that the cause was due to the differential settlement of the various soil layers onto which the tower is founded (Figure 2-4).

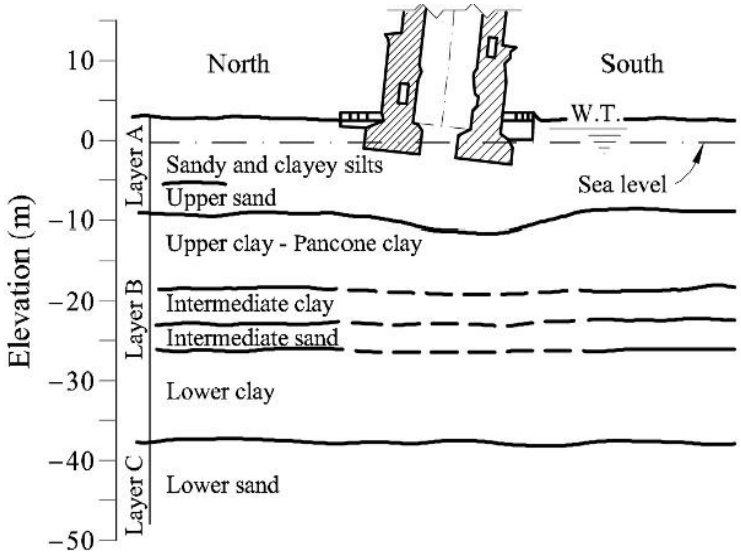

Figure 2-4: Different soil strata underlying the Leaning Tower of Pisa (Puzrin *et al*., 2010).

2.2.3 Lotus Riverside Apartment- Shanghai

This Block No. 7 apartment was part of a residential complex consisting of 11 buildings each between 11-13 storeys high. After the construction, excavation was being carried out on the southern side of the building for a proposed underground parking space and consequently, the dugout soil was temporarily dumped on the Northern side of the building. At the time of the collapse, the excavation was around 4.6m deep and the soil had been piled up to 10m high (Chai et al., 2014).

On the 27th June 2009, the whole building overturned in the direction of the excavation. It was noted that the building was predominately intact, although it was resting on its side, indicating that this was a possible foundation failure and not a structural failure (Figure 2-5).

Figure 2-5: Lotus apartment, Block 7, collapse (Chai *et al*., 2014).

A retaining wall formed by the deep mixing method was constructed up to a depth of around 10m to assist the excavation by supporting the soil next to it. It was also reported that this wall was in turn supported by 6-9m long soil nails. Moreover, after a Finite Element Analysis (FEA) simulation performed by Chai *et al*. (2014), from available data, it was found that the foundation pile was adequate. However, the

concrete hollow piles that were used for the foundation snapped, due to lateral forces that were created by the temporary soil stockpiling next to the building (Figure 2-6). Furthermore, it was also reported that it had been raining several days prior to the collapse which may have contributed to a seepage force that added to the lateral pressure experienced by the pile foundation (Chai *et al*., 2014).

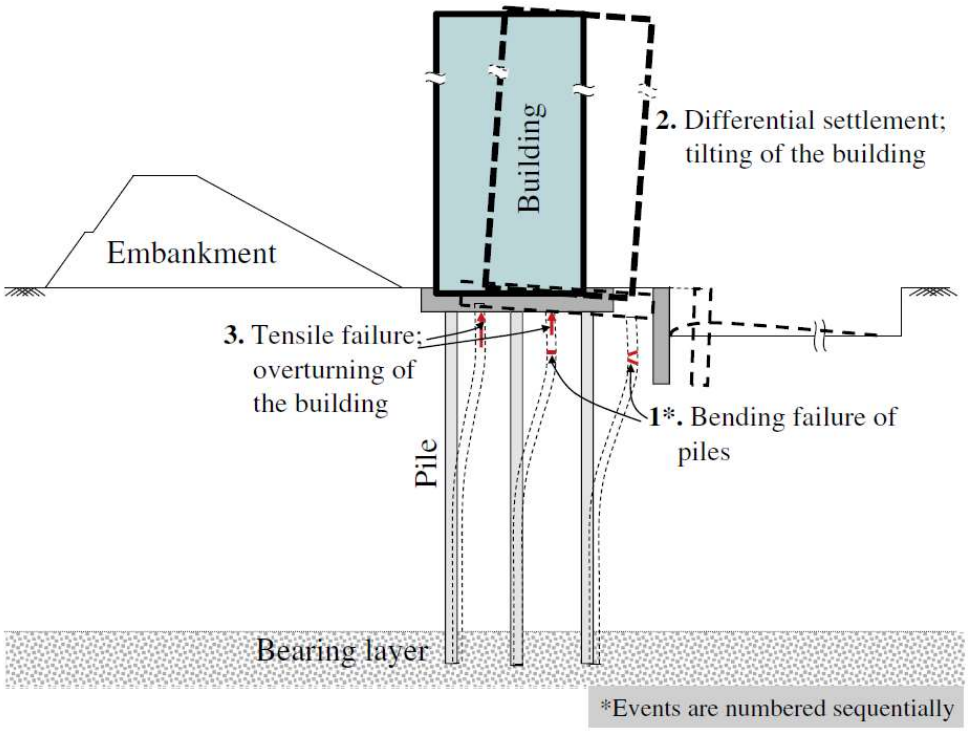

Figure 2-6: Illustration of failure mechanism that triggered the collapse of the lotus apartment collapse (Chai *et al*., 2014).

2.2.4 Ring Road project- Mauritius

The Ring Road is situated near the city of Port Louis, Mauritius. It was built to alleviate the congestion problem in the capital. The construction started in 2010 and was completed by 2013. In early 2014, prior to its operation, cracks started to appear on the road surface. This was followed by a massive failure of a 15m high mechanically stabilised earth wall (Figure 2-7). At that time, the cracks extended for a length of over 750m. The contractor carried out an investigation of the ground up to 5m deep before construction. However, after the failure and a thorough geotechnical research, the contractor attributed the failure to a weak soil strata of 1-1.5m thickness at 21m deep

from the ground surface (Government information service, 2015). This weak soil layer triggered a slide that in turn caused the failure of the retaining wall. Anchors of over 40m length and as deep as 8m into solid bedrock were used to stabilize the whole fill material hereafter.

Figure 2-7: Ring Road, Mauritius. The bottom right picture shows the construction of the MSEW (ARQ, 2014).

2.2.5 Global slope instability issues in a residential area- Cape Town

The residential area was constructed in the Southern Cape of South Africa between 2004 and 2006. Roughly 10 years after the completion of the project, residents observed cracks in their houses. After a geotechnical investigation, it was found that the houses were built on a massive slope that had global instability issues (Figure 2-8). This means that the slope on which the houses were constructed was moving. As a result, some of these houses had to be evacuated due to safety concerns (Le Roux, 2016). This case showed that it is also not sufficient to design and cater for specific structures. Although the design could be adequate, there are other factors/uncertainties that might render the design unsafe. It is crucial to check the suitability of the whole area around it especially when constructions are done on a slope.

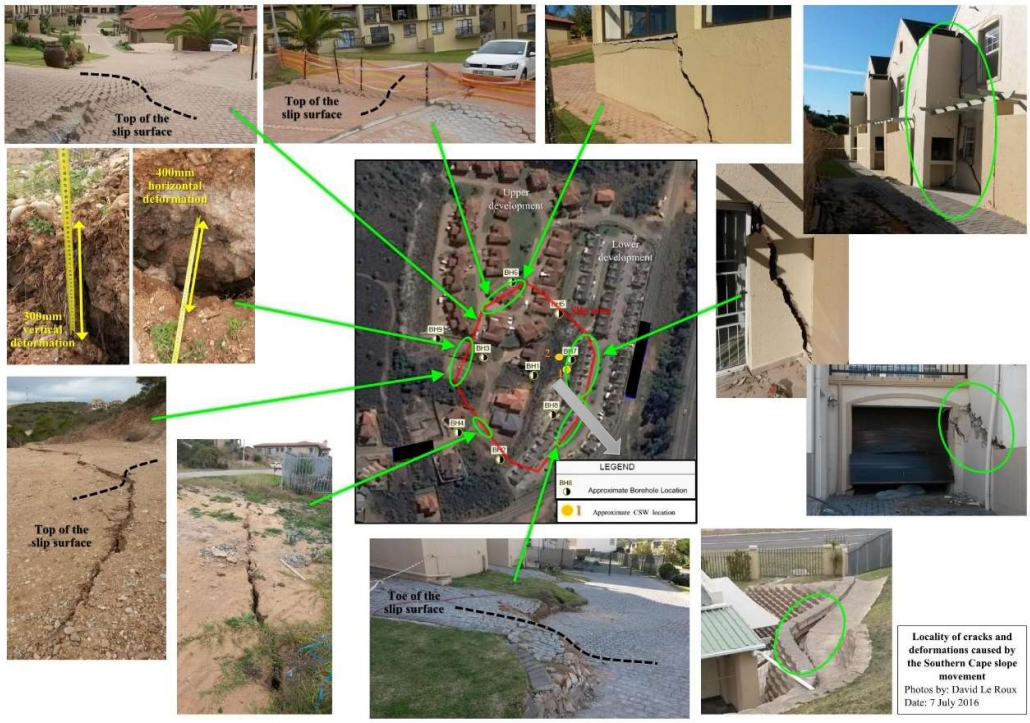

Figure 2-8: Global instability failure of the slope on which several residential buildings were constructed (Le Roux, 2016).

For most of these cases, the failure could have been prevented if thorough geotechnical surveys were conducted prior to construction. The cost implication of these surveys would have certainly increased the cost of the project but it would definitely be less than the repair cost encountered to remedy the situation. These initial ground investigation surveys would have helped to forecast the ground conditions earlier. Therefore, necessary measures could have been considered during the construction phase to prevent disaster.

If a problematic soil is encountered on site, there are several ways in which it can be improved. These will be explained by introducing some of the different ground improvement techniques available.

2.3 Ground improvement techniques

Ground improvement techniques refer to the processes used to modify existing site soil conditions in such a way as to improve its characteristics until it exhibits

satisfactory performance under design loading conditions. They mostly aim at increasing the bearing capacity of a ground, limit its settlement and increase its drainage capabilities. The International Society for Soil Mechanics and Geotechnical Engineering classified ground improvement techniques into 5 major categories (Huybrechts and Denies, 2013), these are shown in Table 2-1.

Table 2-1: Ground improvement techniques and their classification according to ISSMGE-TC211 (Huybrechts and Denies, 2013).

Classification	Description	Example of Ground Improvement (GI) techniques
A	GI without admixtures in non-cohesive soils or fill materials	Dynamic compaction, Vibro-Compaction
B	GI without admixtures in cohesive soils	Replacement, Preloading, Vertical drains (accelerated consolidation), Vacuum consolidation
C	GI with admixtures or inclusions	Vibro-Replacement, Stone columns, Sand compaction piles, Rigid inclusions
D	GI with grouting type admixtures	Particulate and chemical grouting. Deep mixing, Jet grouting
E	Earth Reinforcement	Geosynthetic or Mechanically Stabilized Earth (MSE), Ground anchors, Soil nails

The following sections will elaborate on the different ground improvements practices used, their methods of operation and application to respective soil types. However, it was outside the scope of this research to give in-depth details of every method available.

2.4 Compaction

Compaction may be categorized as the simplest method of ground improvement. The earliest method of compaction was herding sheep back and forth on newly placed ground which, has now been replaced by sheep's foot rollers (Xanthakos *et al*., 1994). Compaction refers to the densification of an in-situ soil due to the expulsion of air and is normally achieved by mechanical means. This technique should not be mistaken with consolidation that involves an increase in density due to the expulsion of water. In addition, compaction occurs almost immediately whereas consolidation is a time-dependent process. The main factors that affect the degree of compaction are:

- The type of soils being compacted
- The moisture content of the soil

- Methods of compaction
- Compactive effort (compaction energy per unit volume of soil)

Besides, different methods and equipment are used depending on the depth and type of soils that need to be improved. Compaction can be categorized into two separate classes namely: Shallow compaction and Deep compaction.

Shallow compaction refers to the ground that needs to be worked on the surface. These include transport, earth dam projects and general compaction for fill materials. The soil is normally compacted in layers of 20-30cm thick (Nicholson, 2015) until desired height.

Deep compaction refers to an in-situ process where great depth (>30m) of soil can be improved simultaneously. There is a wide range of techniques available for this, such as explosive compaction, dynamic compaction, rapid impact compaction, Vibro compaction, compaction grouting etc. These are explained hereafter.

2.4.1 Shallow compaction

There is a variety of rollers available for shallow compaction. The choice of these machines is principally dependent on the type of soil to be compacted and required depth of compaction.

For fine-grained soil, such as silty clay, sheep's foot rollers (Figure 2-9) is preferable. The way this roller compacts the soil is known as kneading compaction. It is a process by which fine-grained soil is worked, sheared and manipulated leading to a better compaction (Nicholson, 2015).

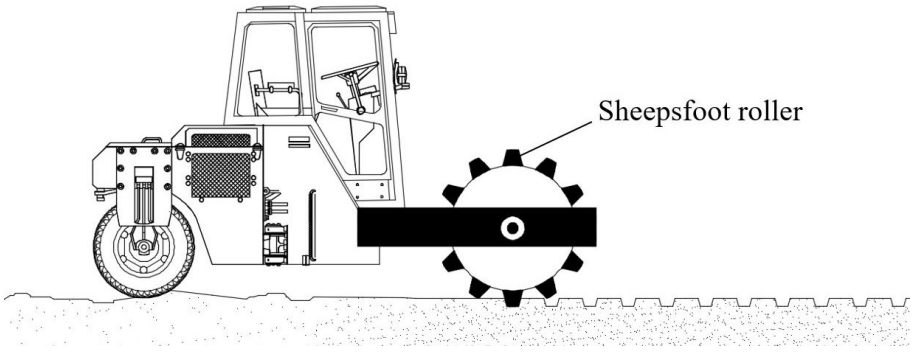

Figure 2-9: Sheep's foot roller.

Vibratory rollers are preferred for compaction of coarser materials such as that of a road base. These rollers have a vibration frequency of approximately 16-60Hz (Nicholson, 2015). Xanthakos *et al*. (1994) stated that the frequency of vibration that is most effective for clean sand compaction lies between 25-30 Hz.

On the other hand, an impact roller (Figure 2-10) can be used to compact a wide range of soil, including saturated silty material. This method of compaction by the impact roller, also known as rolling dynamic compaction, can generate enough compaction energy to densify soil up to 2-3m deep (Nicholson, 2015).

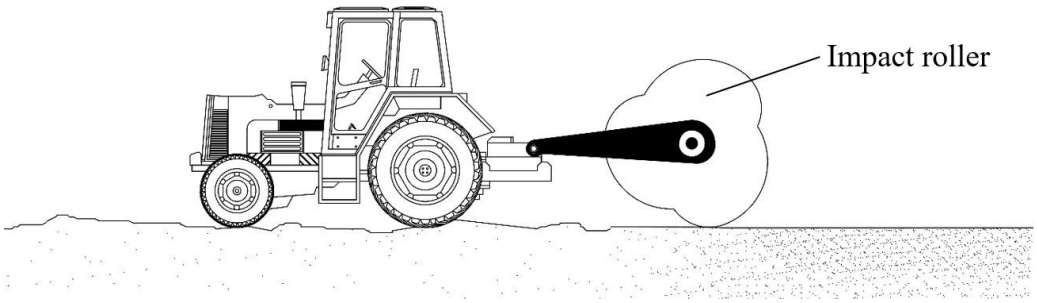

Figure 2-10: Impact roller.

2.4.2 Explosive compaction

Explosive compaction is generally limited to granular soil and those having fines not more than 15-20% (Kirsch and Bell, 2012). This method has been around since the 1930s, though it is seldom used (Nicholson, 2015). Nicholson (2015) stated that it is effective for granular soil having a density of 50-60% of their maximum value and for saturated, free draining soil. It can achieve a relative density of around 70-80% up to 35m deep. The blasting creates a compression followed by rarefaction waves that generate shear waves which assist in collapsing of the soil structure. For saturated soil, there is a sudden increase in pore-water pressure, which sometimes shoots up from the ground. After the pore-water pressure is dissipated, there are rearrangements of the soil particles leading to densification. However, due to environmental concerns, noise pollution, production of fumes, far-reaching shock waves and possible groundwater contamination, its use is limited. Figure 2-11 shows a diagrammatic representation of an explosive compaction.

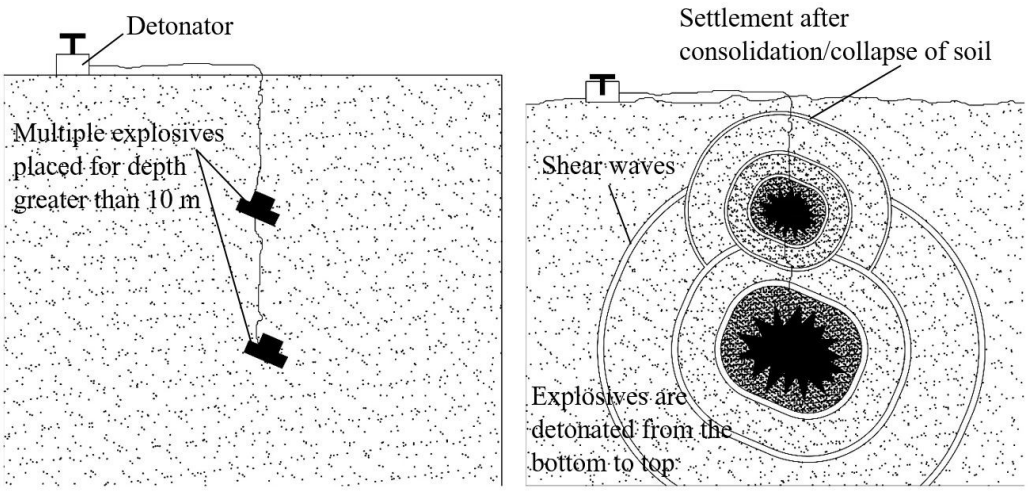

Figure 2-11: Explosive compaction.

The explosive charges are usually placed at 2/3rd of the depth that needs to be treated, up to a maximum of 10m. After 10m penetration, multiple charges are recommended. These charges are detonated from the bottom to top to take advantage of the shear wave generated (Raj, 1999). Kirsch and Bell (2012) stated that 10-15kg of TNT is needed for improvement up to 10 m deep and the effect of compaction can reach up to 20% - 50% deeper than the installation depth. Mitchell and Soga (2005) suggested the following relationship for estimating the weight of explosive needed:

$$W = 164CR^3$$

Where,

W: Weight of explosive needed in Newtons (N)

C: Coefficient of 0.025

R: Radius of influence in meters (m)

2.4.3 Dynamic compaction

According to Xanthakos *et al*. (1994), Dynamic compaction was first developed by the Romans before it was used in the United States as early as 1871. For this process, the degree of compaction is dependent on the weight of the pounder and the height from which it is dropped. Xanthakos *et al*. (1994) stated that the weight can be over 20T and

can be dropped from a height of over 30m. Kirsch and Bell (2012) reported that weights as heavy as 170T have been used. The spacing between compaction points is normally between 4-10m (Byrne and Berry, 2008). Each drop produces a shear wave that penetrates the ground and causes the soil particles to rearrange themselves to a more densely packed configuration. Figure 2-12 shows a diagrammatic representation of the dynamic compaction.

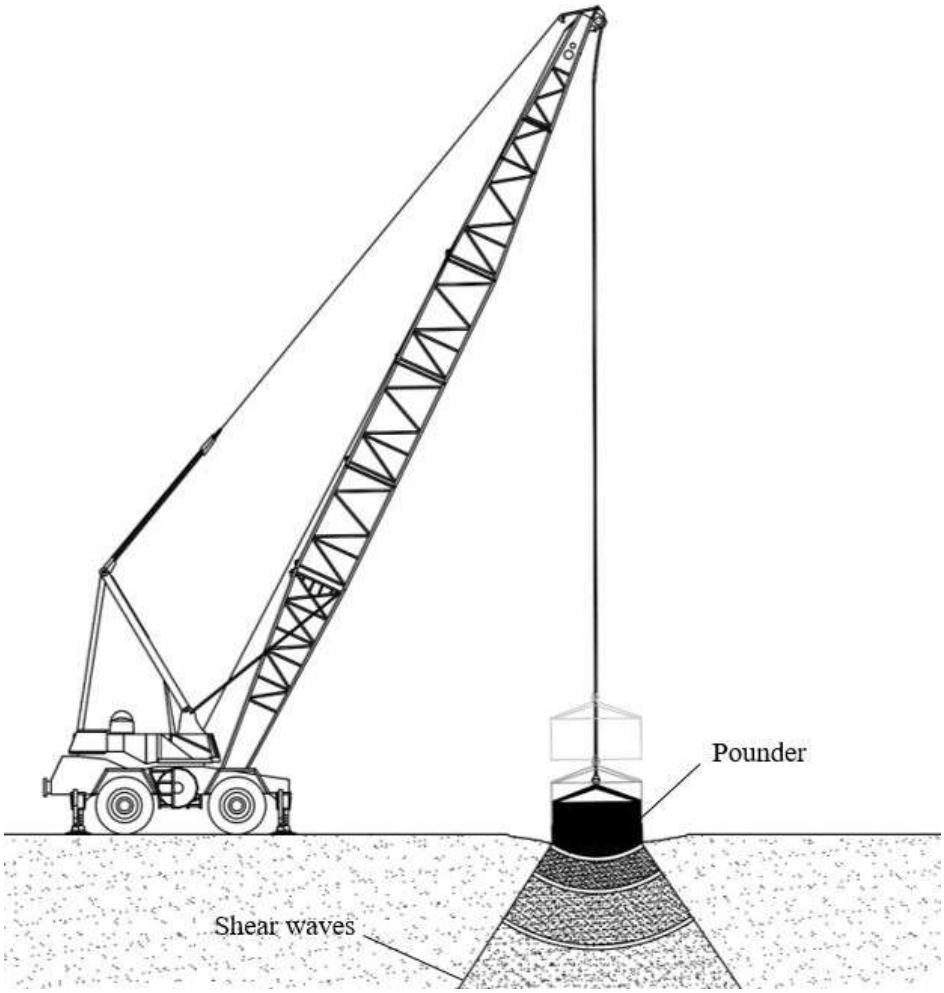

Figure 2-12: Dynamic compaction of soil.

Xanthakos *et al*. (1994) provided a relationship between the height of the drop, weight of the pounder and depth of improvement as shown in Figure 2-13. The depth of compaction depends on the energy imparted into the ground and can be related by the following equation.

$$D = k\sqrt{Wh}$$

Where,

D : the depth of compaction in metres

k : an influence factor which varies between 0.375 and 0.7

W: the weight of the pounder in tonnes

H: the drop height in metres

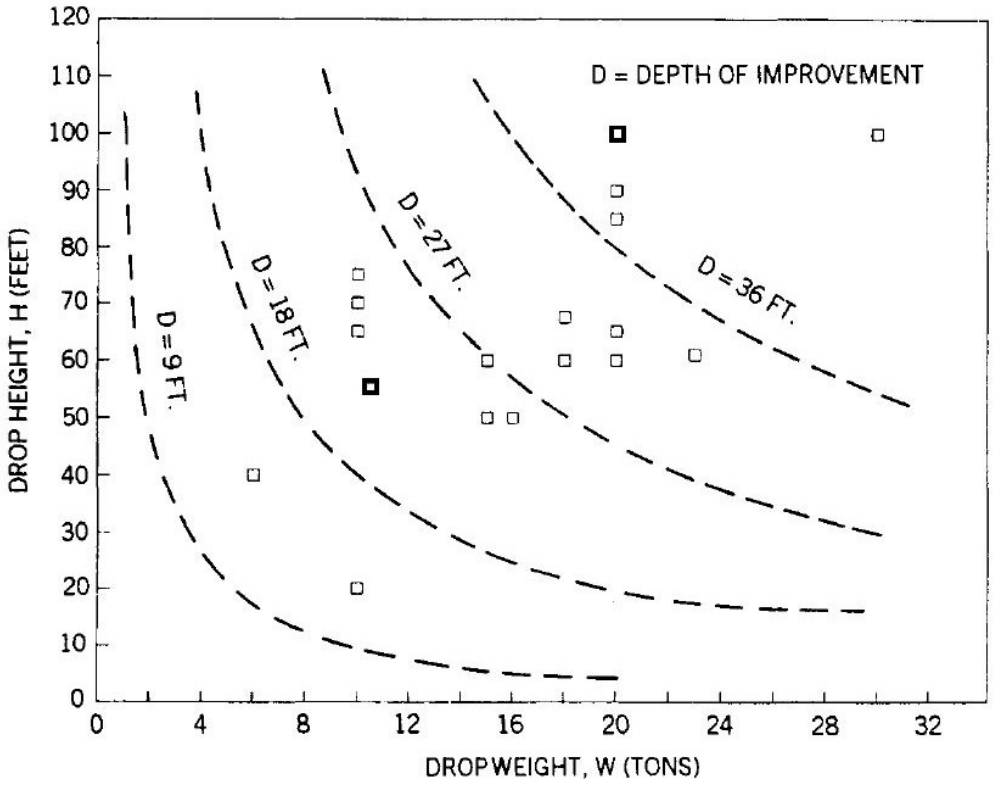

Figure 2-13: Relationship between the weight of pounder and the height of drop (Xanthakos *et al*., 1994).

Byrne and Berry (2008) added that the depth of improvement is limited to around 3-4 times the diameter of the pounder. Dynamic compaction is best suited for light loaded structures such as low-rise residential buildings, road embankments and dams. Its effectiveness is dependent on the depth of groundwater level and the type of soils that need to be densified. This technique increases the pore water pressure thus, it will not be appropriate for soils of low permeability. This process is normally done in 3 phases (Figure 2-14) namely:

1. Primary phase : The deepest layer is compacted during this phase
2. Secondary phase : Intermediate layers of soil is compacted
3. Ironing phase : Compaction is done between prints, compacting the shallow layers

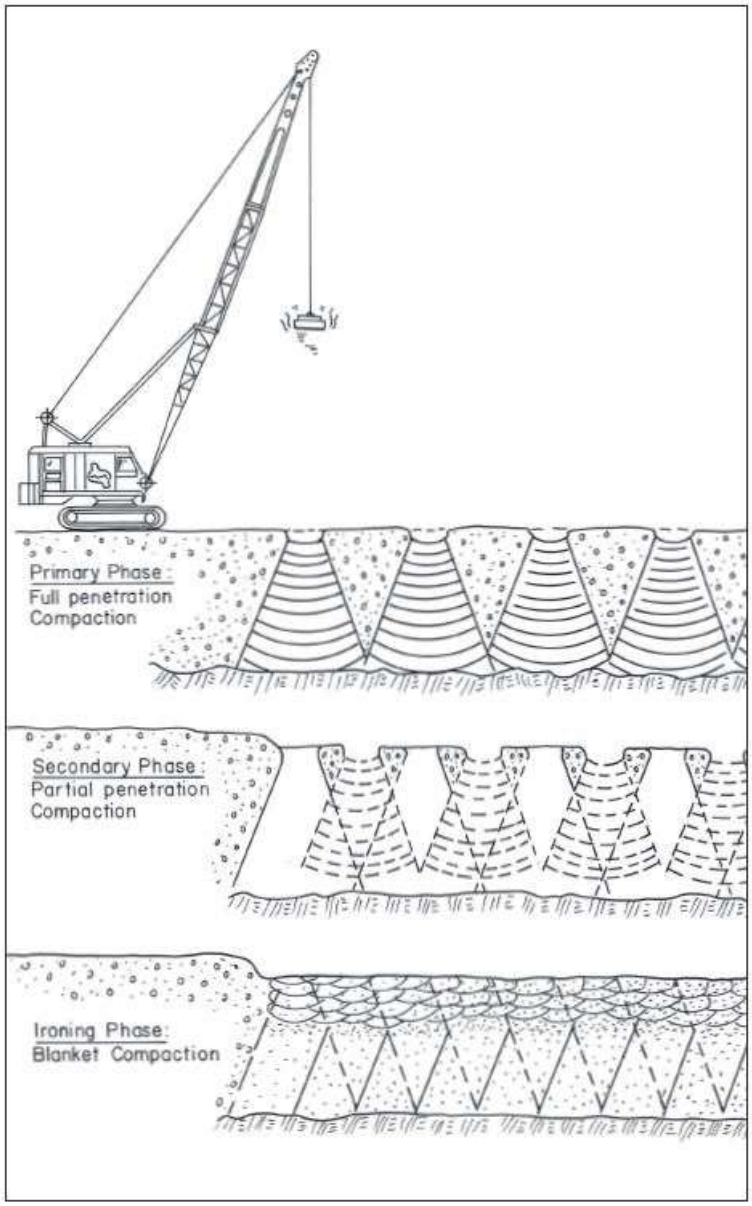

Figure 2-14: Phases of dynamic compaction (Byrne and Berry, 2008).

The process of dynamic compaction creates lots of noise and vibrations which must be taken into consideration. In addition, the shock waves generated can cause damage

to surrounding infrastructures (Byrne and Berry, 2008, Kirsch and Bell, 2012) while flying debris can be ejected up to 60m from the point of impact. If work is done near existing roads and other structures, necessary measures should be taken, such as a providing a movable screen, to intercept debris (Kirsch and Bell, 2012).

2.4.4 Rapid impact compaction

Rapid impact compaction was reported to have been developed in England during the 1990s (Nicholson, 2015). It normally consists of a hydraulic hammer which drops a mass of 7-9T from a height of 1m on an impact plate at a rate of approximately 0.6-1.3Hz. These create shock-waves (shear waves) that travel through the soil and densifies it. This method allows compaction between 4-7m deep. However, it is not suitable for soil containing more than 15% fine (soil passing 63µm sieve) (Nicholson, 2015).

Compaction should be done in stages as illustrated in Figure 2-14. Moreover, Kirsch and Bell (2012) stated that a recovery period should be kept after each stage to allow for dissipation of pore-water pressure. This can vary between 1-2 days for well-graded sands and gravel and 1-2 weeks for sandy silts. Figure 2-15 shows a diagrammatic representation of the Rapid impact compaction process.

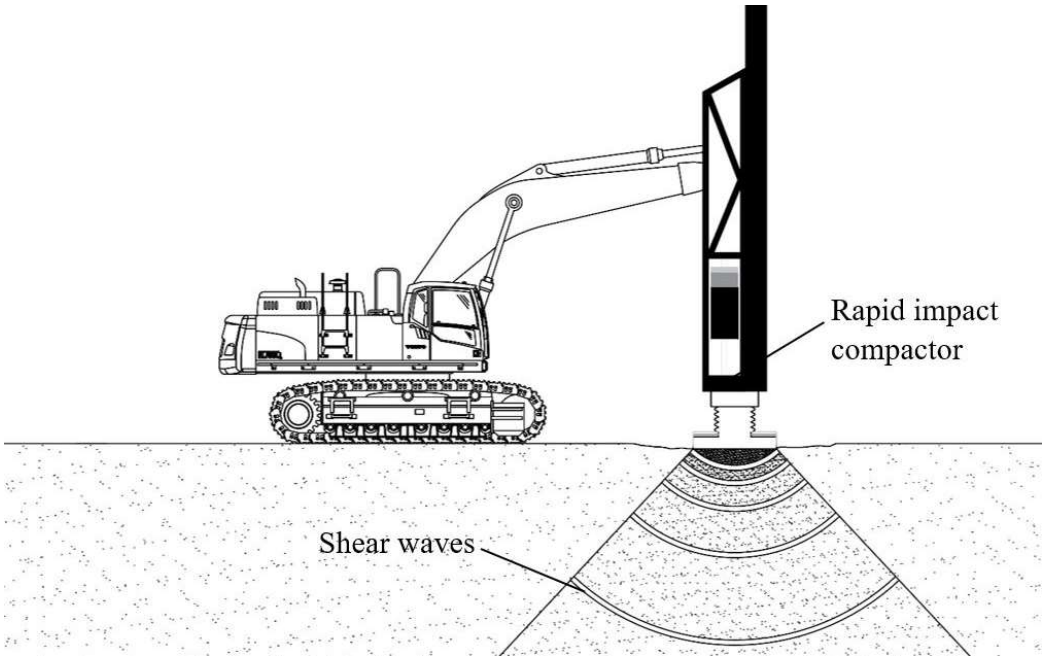

Figure 2-15: Rapid impact compaction.

2.4.5 Vibro-Compaction/Vibro-displacement

Vibro-Compaction is a wet process that has been developed and patented in Germany during the 1930s (Xanthakos *et al*., 1994). It uses a jet of water to guide the probe into the ground. This method is typically used for coarse soils, having negligible fines content. The efficiency of this method is dependent on the type of material that needs compaction.

Figure 2-16 shows the suitable particle size range for Vibro-compaction. Franki (2010) and Nicholson (2015) stipulate that soil up to 50m depth can be compacted using this method. The compaction points are either in a square or in an equilateral-triangular arrangement, spaced at 2.5-5.0m apart (Kirsch and Bell, 2012). According to Byrne and Berry (2008), these columns can carry loads between 300 and 500kN. Figure 2-17 illustrates the Vibro-Compaction process. The vibration is caused by the rotation of an eccentric weight about the axis of the probe. Its layout is shown in Figure 2-18.

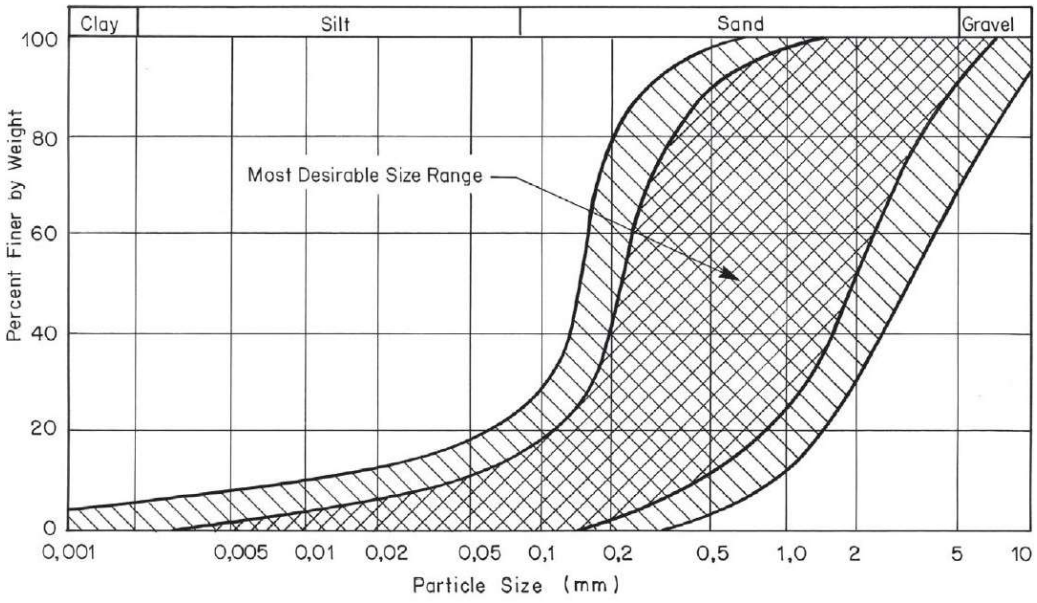

Figure 2-16: Soil grading range suitable for Vibro-compaction (Franki, 2010).

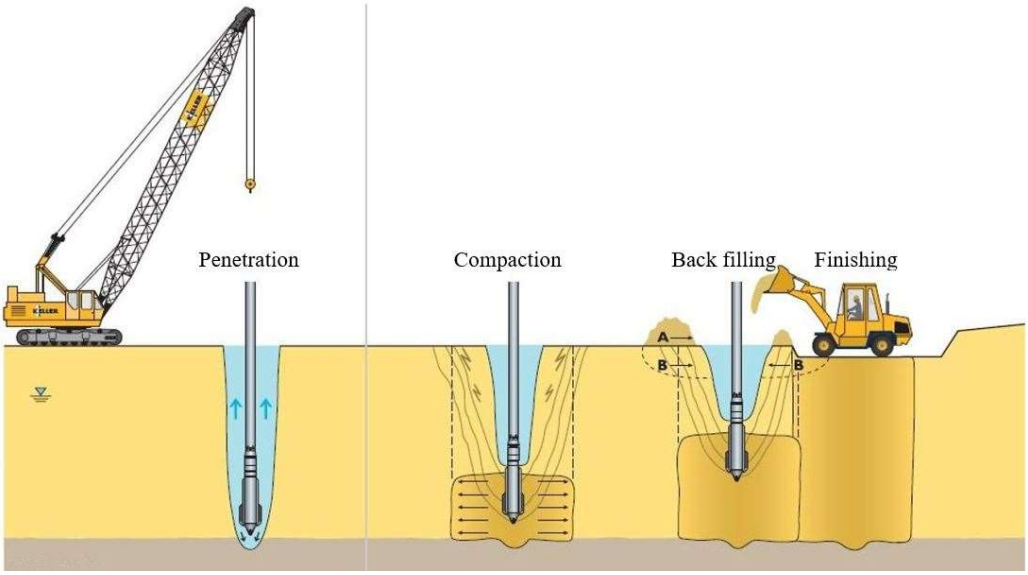

Figure 2-17: Construction phases of Vibro compaction process (adapted from Franki, 2010).

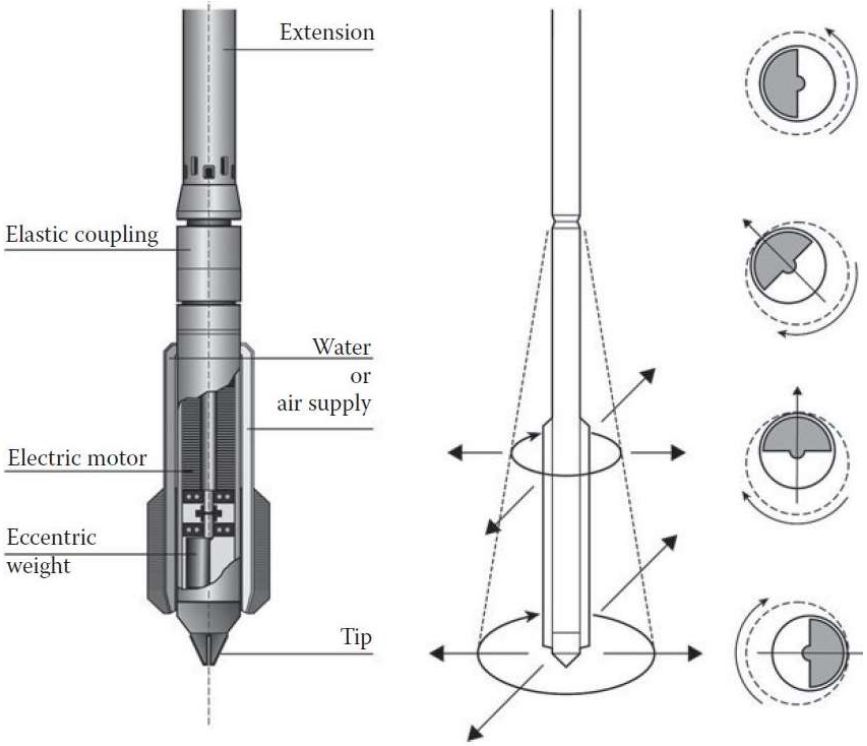

Figure 2-18: Layout of vibrating probe (Byrne and Berry, 2008).

The advantages of Vibro-compaction as highlighted by Byrne and Berry (2008) are:

- It is a fast and economical system
- Noise and vibration levels are low
- Deep compaction up to 20m can easily be reached
- Compaction can be done on soil having a high-water table
- Degree of compaction of the soil can easily be checked

The disadvantages are:

- The method is not suitable for soil having high silt and clay content.
- The degree of compaction is dependent on the grading of the material

2.5 Admixture soil stabilization

Admixture soil stabilization refers to any improvement where some materials are added to the soil to increase its engineering properties. These materials may be cement, fly-ash, lime, asphalt, chemical additives and other waste products. This technique has been around for thousands of years. Shallow surface mixing has proved to reduce maintenance cost and improve the bearing capacity of embankments/road and foundations for low-rise buildings (Nicholson, 2015). With the advancement of technology and machinery, this process has been extended for deep soil up to 30m and more. (Nicholson, 2015)

Xanthakos *et al*. (1994) stated that lime stabilised clay can bring an increase of 10-50 times in shear strength after few months following the mixing. They attributed the gain in shear strength to the pozzolanic reactions of the lime with silicates and aluminates within the clay. They also stated that an undrained shear strength of over 10.0MPa may be achieved with the use of a cement binder. Lime, however, is not desirable for long-term solution. If the soil is rich in sulphates, secondary reactions may occur which can lead to undesirable products such as ettringites and thaumasite. These products swell when in contact with water and expand. This can have damaging consequences due to the heaving of the soil over an extended period. Cement, on the other hand, may be inefficient for cohesive soil and uneconomical due to high dosage requirements (Nicholson, 2015). Figure 2-19, shows a representation whereby this technique can be

used to mix a stabilizer, such as lime, to a subgrade to improve and increase the life expectancy of a road.

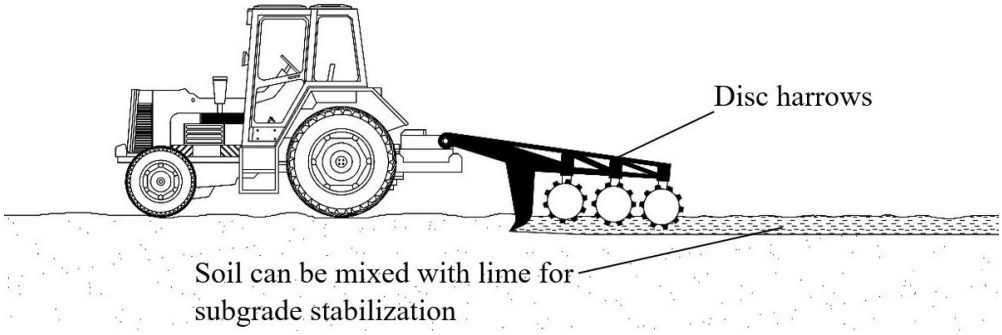

Figure 2-19: Shallow soil mixing of soil with a stabilizer such as lime.

2.6 Compaction grouting

Compaction grouting was invented in the United States around the 1950s. It can be used to strengthen the ground, reduce its permeability and for remedial works such as underpinning and levelling structures (Xanthakos *et al.*, 1994). It is a technique that forces a low mobility grout under high pressure, up to 3.5MPa (Xanthakos *et al.*, 1994), into the soil at a rate of 28-142L/min (Kirsch and Bell, 2012).This forms a bulb that expands and compresses the surrounding soil. A mixture of sand and cement is normally used for the grout, thereby densifying and strengthening the in-situ soil. Kirsch and Bell (2012) suggested a range of soil that is suitable for compaction grouting, this is as shown in Figure 2-20.

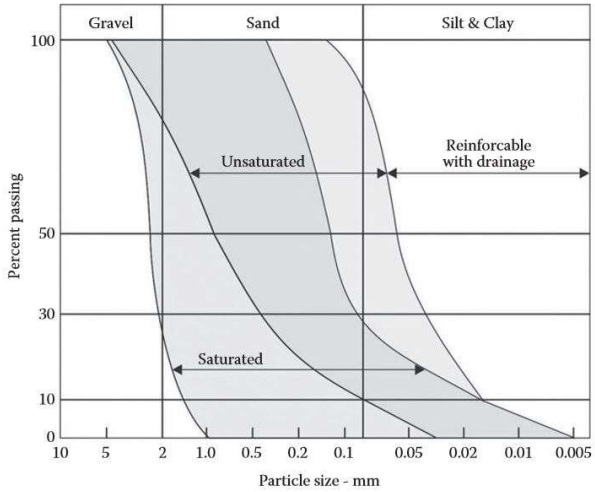

Figure 2-20: Range of soil suitable for compaction grouting (Kirsch and Bell, 2012).

Byrne and Berry (2008) stated that this method is suitable for soils with good drainage characteristics and cannot be used for saturated clays. The maximum depth of soil that can be treated is around 10m. Figure 2-21 shows a representation of the technique.

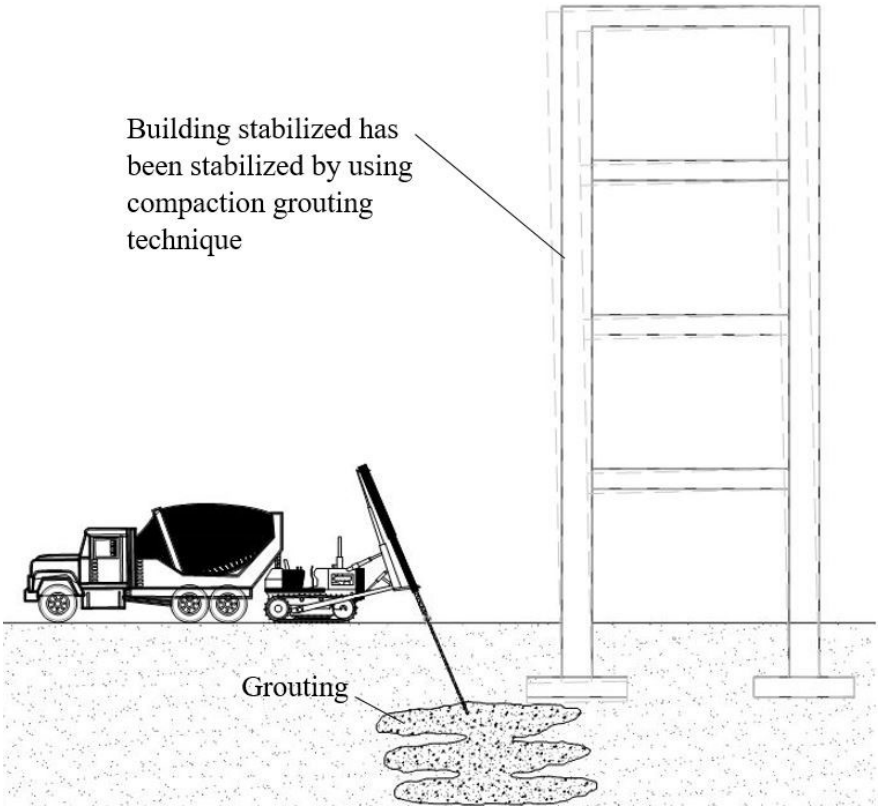

Figure 2-21: Compaction grouting used for remedial work.

It was reported that this is a relatively expensive method that can lead to ground heaving if not controlled properly. It is suited for small contract work due to its low rate of production. The advantages are that the equipment is relatively small and thus can squeeze into tiny working space. Moreover, it does not produce vibrations that can interfere with surrounding areas (Byrne and Berry, 2008).

2.7 Jet grouting

Jet grouting was developed in Japan around the mid-1960s (Xanthakos *et al*., 1994). It is a relatively expensive technique that involves partial replacement of fine soil particles with a cement slurry. A hole is normally pre-drilled into the ground through which a probe is driven. The soil is held by either Bentonite slurry or a temporary

casing. A high-velocity cement slurry is sprayed under pressure, over 8Mpa (Xanthakos *et al*., 1994), via a rotating nozzle situated at the end of the probe. High-pressure water jet, ejected at a pressure of over 50Mpa (Xanthakos *et al*., 1994), can be used simultaneously to help erode the soil. The jet will force the cement to be mixed with the soil in a radial direction. The rotating grout tube is slowly retracted, forming a large diameter grout column. Columns up to 3m in diameter (Byrne and Berry, 2008) and 45m depth (Xanthakos *et al*., 1994), can be formed using this method

This technique is best suited for sandy soils. However, if used in cohesive soil, the diameter of the column produced will be reduced hence lowering its efficiency (Byrne and Berry, 2008). Besides improving the bearing capacity of the ground, this technique can also be used for groundwater control, underpinning of foundation and to provide lateral earth support. According to Byrne and Berry (2008), this method is costly and ground heaving may occur under insufficient control. Figure 2-22 shows a diagrammatic representation of the Jet grouting process.

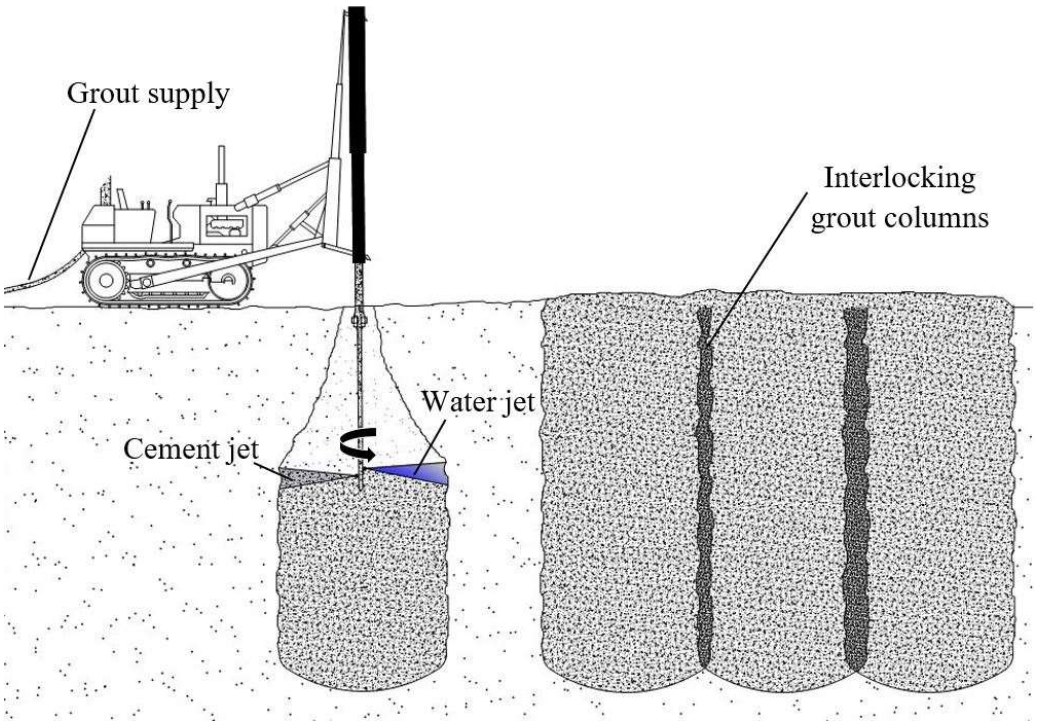

Figure 2-22: Jet grouting.

2.8 Accelerated consolidation

When a saturated soil is loaded, there is an immediate increase in pore-water pressure. This pressure takes time to dissipate depending on the permeability of the soil, coefficient of consolidation and the drainage path available (Kirsch and Bell, 2012). The lower the permeability of the soil and the longer the drainage path, the more time it will take for the pressure to normalise. Accelerated consolidation is a ground improvement technique whereby drains are introduced into the soil hence decreasing the drainage path. This will favour pore-water pressure dissipation and as a result, accelerate consolidation.

There are three main types of drains that are used for this technique, namely:

- Sand Drains: These are 150-250mm diameter drains filled with highly permeable sands.
- Sandwick drains: These are like sand drains except that the highly permeable material is confined in a geo-fabric of around 50-75mm in diameter.
- Band drain: These are cardboard or plastic bands that are around 100mm wide and 2-7mm thick. They provide a longitudinal channel that facilitates pore-water dissipation.

Drilling method is normally used to install the sand-drain and sandwick drain while vibratory techniques are used to drive and anchor the band-drain into the ground. Byrne and Berry (2008) stated that the band drain is usually the preferred one since the speed of installation is fast, usually under 3 minutes for each of them. They also added that band-drain offers less operational problem such as squeezing, necking and buckling which normally reduce efficiency. This is a low-cost method of ground improvement however, it is a time-dependent process (Byrne and Berry, 2008). Nicholson (2015) added that these drains can be used with ease, up to a depth of above 65m. Figure 2-23 shows a diagrammatic representation of accelerated condition.

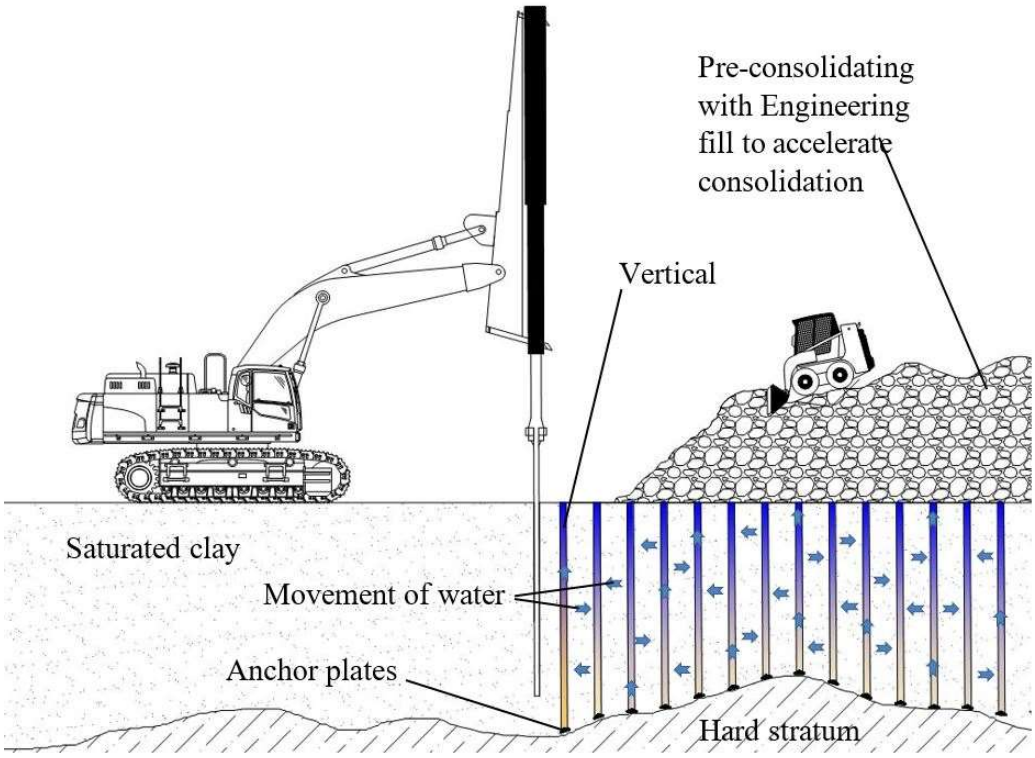

Figure 2-23: Installation of band drain for accelerated consolidation.

2.9 Deep Soil Mixing (Wet Soil Mixing)

Deep soil mixing has been developed around the 1960s and can be used to reinforce the ground at a depth of more than 30m (Nicholson, 2015). It is a technique whereby a powerful drill drives an auger rig into the ground as a cement grout is pumped into it. The rotating action of the rig mixes the grout with the soil creating a stiffer material that is normally used to transfer loads to a convenient bearing stratum. These columns can also be linked together to form a dense wall. Moreover, it can be used on any type of soils. Nicholson (2015) stated that this method of ground reinforcement has replaced many conventional techniques such as slurry walls, concrete cut-off walls and sheet piles. Byrne and Berry (2008) stated that the cost benefit of this method depends principally on the bulk economic availability of the binder material. Figure 2-24 shows a diagrammatic representation of the process.

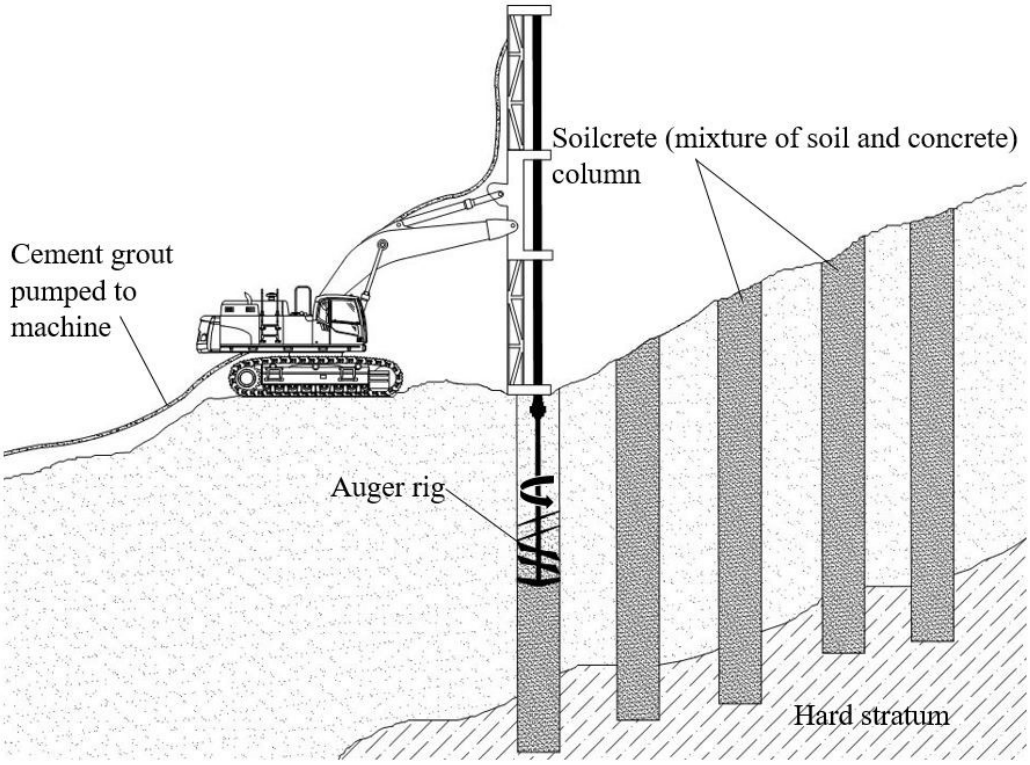

Figure 2-24: Deep soil mixing process.

2.10 Vibro-Concrete column

The installation of a Vibro-concrete column uses a method of injection whereby a cementitious material is pumped into a soil via a probe of 40-60cm. This technique was first reported to have been used in Sweden and Japan simultaneously during the mid-1970s. Columns formed by this method usually have diameters of 0.5-1m and a length of up to 25m (Kazemian and Huat, 2010). The same construction techniques as used for Vibro-Replacement column is adopted in this case. The only difference is that instead of using crushed stones, a concrete mix is used as the material making up the stone column. Franki (2010) states that normally a concrete mix ranging from C8 to C30 is used for this specific construction purpose. However, it has been reported that the column then mainly behaves like a pile. The Vibro-Concrete column is often combined with the Vibro replacement column thus eliminating the use of concrete in the upper section of the column (Franki, 2010).

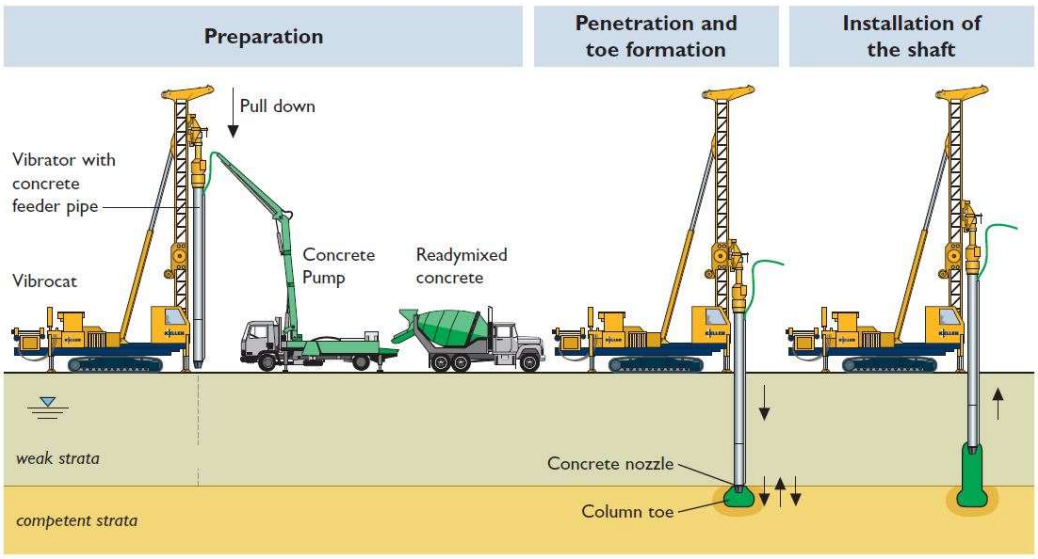

Figure 2-25: Installation of Vibro replacement method (Franki, 2010).

2.11 Geosynthetics

The use of natural fibres for soil stabilization can be traced back to thousands of years where coir and papyrus were used to reinforce the soil (Nicholson, 2015). Geosynthetic is a generic term that refers to man-made materials used in conjunction with soils/rocks. It can be classified into several common synthetic products such as geotextiles, geogrids, geomembranes, geocomposites and geonet. Geotextiles, geogrids and geocomposites are principally used to reinforce the ground by transferring /absorbing the tensile forces experienced by the ground. They have a huge degree of applications in geotechnical, environmental, transport and hydraulic engineering. Geosynthetics normally exhibit several functions (Erosion control, Filtration, Drainage, Fluid barrier, Reinforcement, Separation. etc) based on their applications (Shukla, 2002): Figure 2-26 illustrates some of the different applications of geosynthetics.

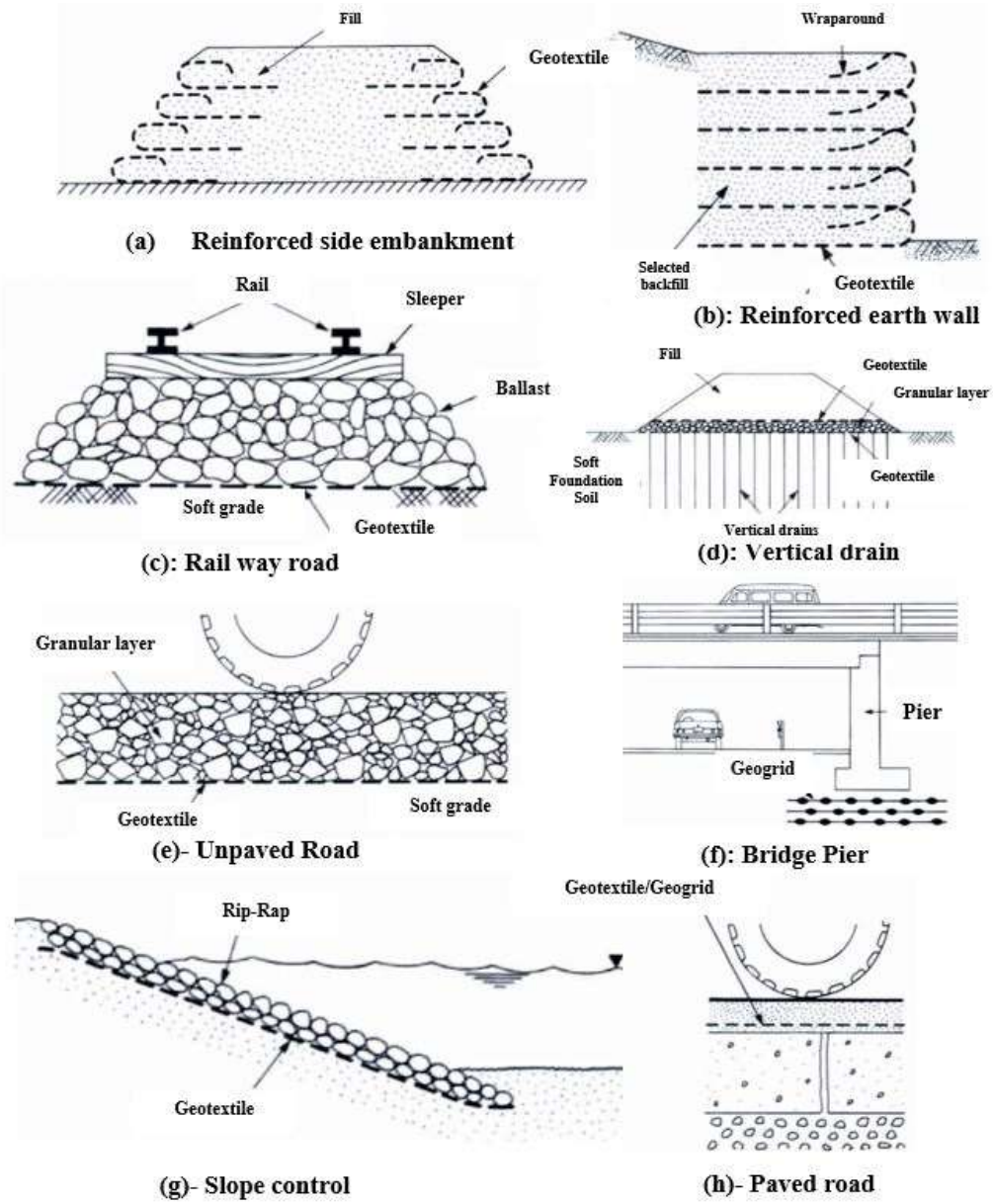

Figure 2-26: Typical Geotechnical applications (Adapted from Shukla, 2002).

2.12 Cost implications and General comment

Xanthakos *et al*. (1994) generated a rough estimation for the cost implications of different common ground improvement techniques. The cost has been reported as United States Dollars per cubic yard of treated soil. These are as follows:

Conventional compaction	1.0 - 5.0
Dynamic Compaction	0.5 - 3.0
Vibro-compaction	1.0 - 7.0
Stone columns	5.0 - 11.0
Compaction grouting	15.0 - 100.0

Kirsch and Bell (2012) added that techniques such as stone columns, vibro compaction and dynamic compaction, which do not use manufactured materials have various advantages in several situations. Vertical drains and grouting still have better advantages than other methods such as piling in terms of environmental sustainability. However, the sustainability of these methods is continuously being improved to limit their environmental impacts.

Stone column is a versatile ground improvement technique as it can perform several geotechnical functions at the same time. It is basically a column of stone, within a specific grading, compacted to the required density. The stone columns and the surrounding soil forms a composite material with a higher density. As a result, this brings several benefits such as an increase in bearing capacity and porosity among several others. Further details will be elaborated in the following chapter.

Chapter 3: Stone column as a ground improvement technique

3.1 Introduction

In this chapter, more attention will be drawn to the use of stone columns as a ground improvement technique as it was the focus area for this research. Its history, methods of construction, advantages, optimum length and different methods of failure/problems associated with it will be elaborated. The studies that have been done so far to remedy its constraints will also be assessed. By the end of this chapter, a mind map highlighting all the studies elaborated in this dissertation has been presented. The gap in research was henceforth made clearer consequently, the proposed approach was discussed.

Stone columns are granular piles consisting of crushed aggregates, gravel, sand or recycled material. They are ideally suited for improving clay, silt and loose silty sand soils. The first documented use of the stone column was in France around the 1830s (Barksdale and Bachus, 1983). They have successfully been used in several projects such as embankment fill support, reinforcement of railroad/wharf support, foundation reinforcement for buildings and various other structures (Gniel and Bouazza, 2009, Asgari *et al*., 2013) . As reported by Barksdale and Bachus (1983), the extensive use of stone columns across Canada, Europe, United States and Asia have proved their efficiency over ages. Nicholson (2015) added that stone columns may provide up to a 20-50% savings over traditional deep foundations. Over the years, according to several studies (Xanthakos *et al*., 1994, Keykhosropur *et al*., 2012, Asgari *et al*., 2013), stone columns have proven to:

- Increase stability of both natural and man-made slope
- Increase bearing capacity of in-situ soil
- Increase consolidation rate
- Reduce liquefaction in soil
- Reduce differential settlement

3.2 Construction of stone column

Stone columns are constructed by replacing part of the soft soil material with a compacted fill material which exhibits better properties. They are usually constructed by using the vibro-replacement method (vibro compaction), the vibro-displacement method (dynamic replacement), or the ramming process (driven stone column/compacted aggregate piers). Figure 3-1 shows the area of application of vibro Replacement and vibro Compaction method respectively (Franki, 2010).

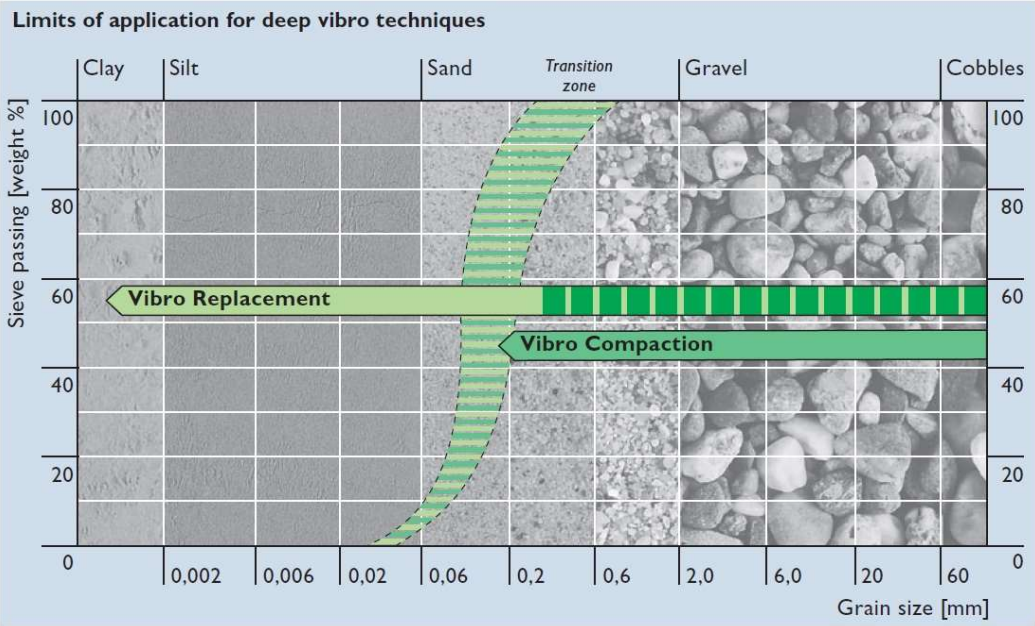

Figure 3-1: Limits of application for Vibro Replacement and Vibro Compaction (Franki, 2010).

Care should be taken in soft soil layers (such as organic/peat soil) as they do not provide adequate lateral restraint consequently, high settlements may be obtained. Figure 3-2 illustrates the bulging failure that may occur in a soft soil layer. Byrne and Berry (2008) stated that if the soft soil layer is greater than one-third the diameter of the stone column, then its stability should be checked. Barksdale and Bachus (1983) added that if such layer is greater than 1-2 times the diameter of the stone column, the Vibro-replacement method should not be used.

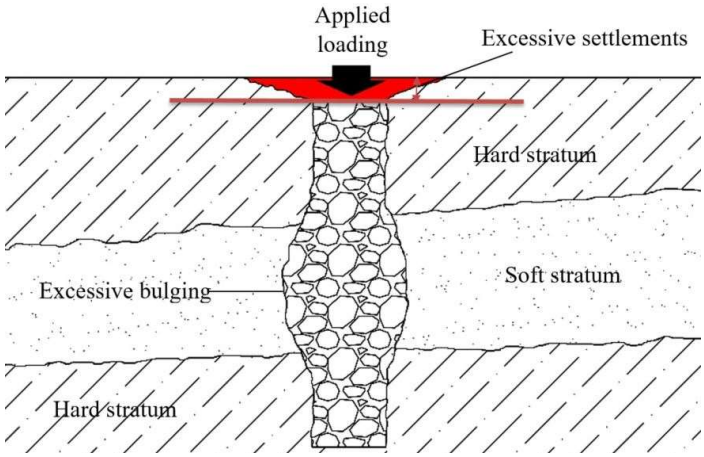

Figure 3-2: Bulging of the stone column in a very soft soil layer.

3.2.1 Vibro displacement (Vibro -compaction)

This method is like the vibro-compaction method discussed earlier. The only difference is that graded stones are dumped into the hole to form a stone column. Figure 3-3 shows a diagrammatic representation of the process. Kirsch and Bell (2012) reported that stone column over a length of 43m can be formed using this technique. They also added that when a bottom feed method is used (as shown in Figure 3-4), the grading of the stones is limited between 10-40mm otherwise it should be between 30-80mm.

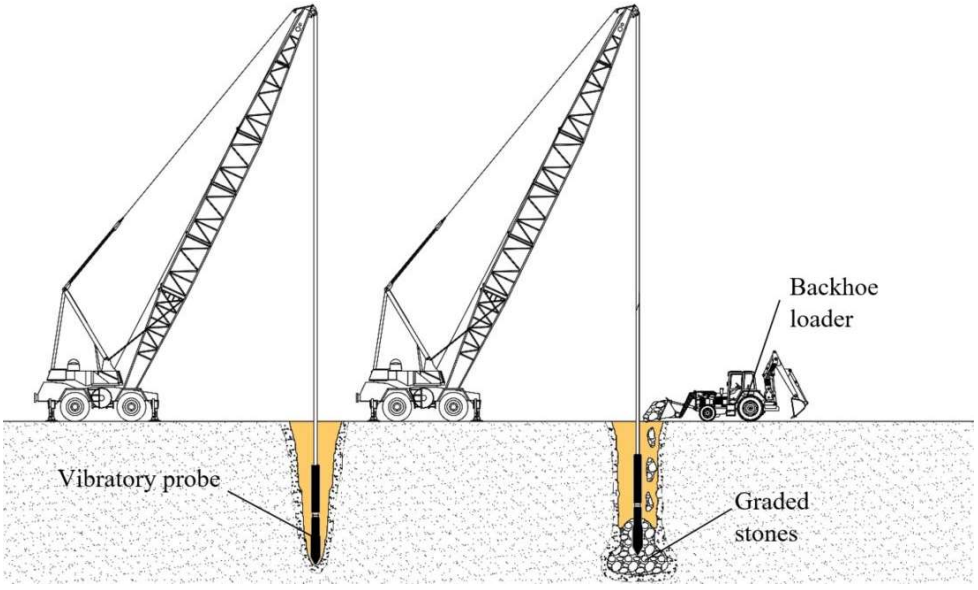

Figure 3-3: Installation of stone columns via the Vibro-replacement method.

3.2.2 Vibro-replacement (Dynamic replacement)

This method was patented in Germany around 1972 (Kirsch and Bell, 2012). It is an economical ground improvement technique that can produce stone columns, 0.6-1m diameter (Nicholson, 2015), at a high installation rate. These columns can carry a load between 300-600kN and should ideally be constructed on a hard rock stratum (Byrne and Berry, 2008). For the Vibro-replacement (dry process) method, a jetting probe is vibrated into the ground up to the desired depth. As the probe is gradually lifted from the ground, stone fills up the cavity. The penetration of the probe coupled with the vibration process causes the stones to densify (Figure 3-4). Hence, it produces stone columns that are tightly interlocked with the surrounding soil (Kirsch and Bell, 2012).

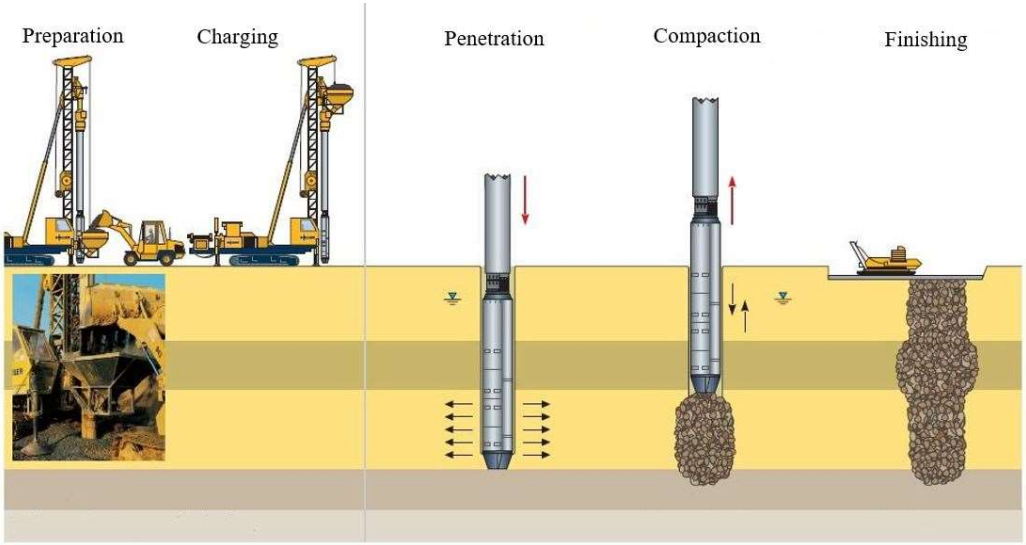

Figure 3-4: Vibro-replacement technique used to construct stone columns, using bottom feed method (Adapted from Franki, 2010).

Byrne and Berry (2008) stated that this method can be used for warehouses foundations, road embankments and even for multi-storey buildings. The depth of improvement is generally limited to around 8m using conventional equipment (Kirsch and Bell, 2012).

According to Byrne and Berry (2008), this method is economical in a wide range of soils and significant load carrying capacity can be attained with columns of large diameters (1.5-2.5m). However, with the conventional equipment available, only a

maximum depth of 8m of soil can be improved. Moreover, shockwaves produced upon installation can damage adjacent structures and should be monitored.

3.2.3 Compacted Aggregate Piers (Rammed aggregate piers/Driven stone column)

These stone columns are either constructed by driving an open/closed end pipe into the soil or by simply boring to create a hole. The diameter of the hole dug out is generally between 410-610mm, with a centre to centre spacing of greater than 2.5 times its diameter. The allowable working load is reported to be around 350-750kPa (Byrne and Berry, 2008)

IS 15284 (2003) came out with a standard procedure for placing a rammed stone column. It was reported that as a bailer/auger drills the borehole, an encasement is gradually forced into the ground up to the desired depth. This encasement provides a temporary support to hold the surrounding soil as the graded stones (Crushed aggregates) of 2-75mm are poured into the empty space in increments. These are used to fill the hole up to a maximum height of around 1-1.5m. The casing is then gradually removed until a minimum of 0.5m remains into the aggregates.

A weight of adequate mass and fall is dropped onto the crushed aggregates so that each blow delivers a minimum of 20kJ (kJ: kilojoules). The penetration of the rammer after each blow is noted. A satisfactory compaction is obtained when a set of 5 blows yields a cumulative settlement of 10mm or less (Byrne and Berry, 2008). The process is repeated until the rammed stone column is formed. Figure 3-5 illustrates the driven pile method. Byrne and Berry (2008) stated that a depth of up to 18m can be effectively treated using this method and moreover it generates low noise level. However, the production rate is slow and its cost implication can be relatively high compared to other techniques.

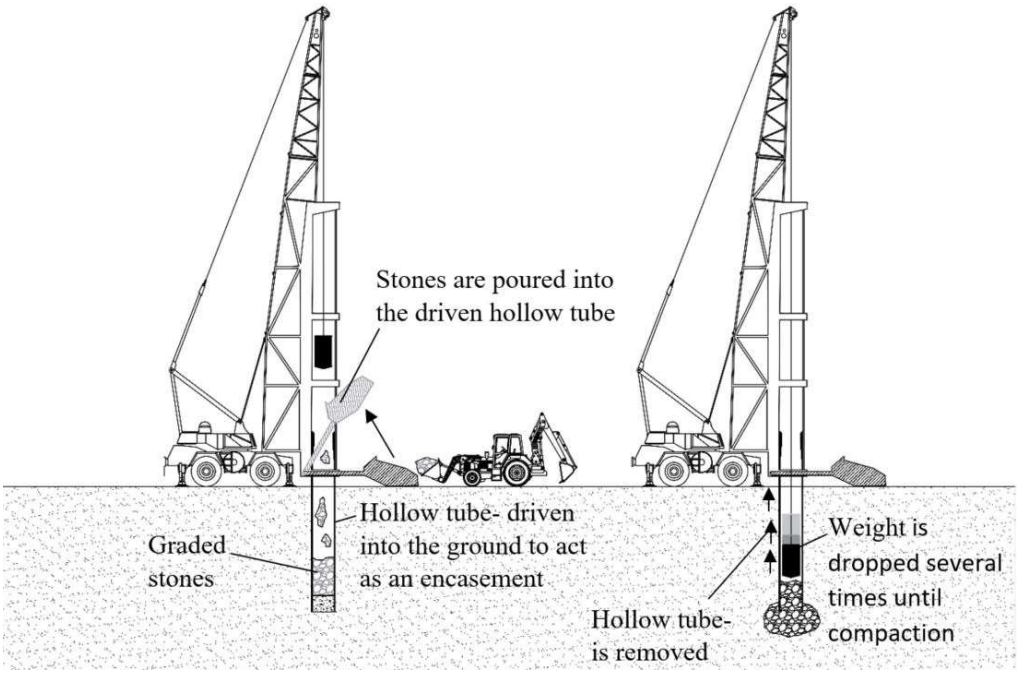

Figure 3-5: Driven pile method used to construct stone column.

3.2.4 Choice of material for stone columns

Barksdale and Bachus (1983) proposed several alternatives for the choice of grading to be used for the construction of stone columns. Table 3-1 shows the grading of aggregates for the Vibro replacement process as proposed by them.

Table 3-1: Several alternative grading for the stone column as proposed by Barksdale and Bachus (1983).

Sieve Size (inches)	Sieve Size (mm)	Alternative 1 (% passing)	Alternative 2 (% passing)	Alternative 3 (% passing)	Alternative 4 (% passing)
4	101.6	-	-	100	
3.5	88.9	-	-	90-100	-
3	76.2	90 -100	-	-	-
2.5	63.5	-	-	25-100	100
2	50.8	40-90	100	-	65-100
1.5	38.1	-	-	0-60	-
1	25.4	-	2	-	20-100
0.75	19.05	0-10	-	0-10	10-55
0.5	12.7	0-5	-	0-5	0-5

According to Barksdale and Bachus (1983), alternative 1 should ideally be used. If this is not suitable, alternative 3 should be utilized. However, if the large top-size

aggregates are not available, alternative 2 or 4 should be considered. Moreover, it was added that for rapid construction purposes, alternative 2 is preferred over alternative 1.

Most recently, IS 15284 (2003) and Kirsch and Bell (2012) stated that stone column materials should between 2-80mm. However, it should be restricted to a maximum size of 40mm if bottom feed method (Vibro-replacement method) is chosen for construction (Kirsch and Bell, 2012, IS 15284, 2003). A suitability number was also devised in order to assess the quality of the stone column materials (Dheerendra Babu *et al*., 2012). Table 3-2 shows the suitability number based on parameters from a sieve size analysis of the materials.

Table 3-2: Brown's suitability number (Dheerendra Babu *et al*., 2012).

Suitability no	0 - 10	10 - 20	20 - 30	30 - 50	>50
Rating	Excellent	Good	Fair	Poor	Unsuitable

$$Brown's suitability\ no. = 1.7\sqrt{\frac{3}{{D_{50}}^2} + \frac{1}{{D_{20}}^2} + \frac{1}{{D_{10}}^2}}$$

D_{50}, D_{20} and D_{10} are in mm at 50, 20 and 10 % passing by weight respectively.

3.3 The spacing of stone column (Centre to centre)

Stone columns grouped within a specific area undergo less bulging compared to a single loaded column. Barksdale and Bachus (1983) stated that the optimum spacing of the stone column generally varies between 1.8-2.7m centre to centre. They also added that a spacing of less than 1.5m should not be used due to construction problems. However, Byrne and Berry (2008) suggested that the spacing between compaction points should be between 1.5-2.5m. In contrast, more recently, Kirsch and Bell (2012) advised that the spacing should generally be between 2.5-5.0m, centre to centre.

Stone columns are mainly arranged either in an equilateral arrangement or in a square arrangement as shown in Figure 3-6 and Figure 3-7 respectively. However, it was reported that the equilateral arrangement gives better packing (IS 15284, 2003). This can also be observed from the comparison of Figure 3-6 and Figure 3-7. Moreover, IS 15284 (2003) added that there is no specific guideline for the exact spacing of the stone columns as this normally depends on the site conditions, settlement tolerances, and

arrangements of the stone columns, installation techniques and the stiffness of the stone column. However, a typical spacing of 2-3D (D is the diameter of the stone column) is normally adopted (Mani and Nigee, 2013). In contrast, Dash and Bora (2013) reported that a spacing of 2.5D gave the maximum performance.

$$\frac{\pi {D_e}^2}{4} = Effective\ area\ covered\ by\ a\ single\ column$$

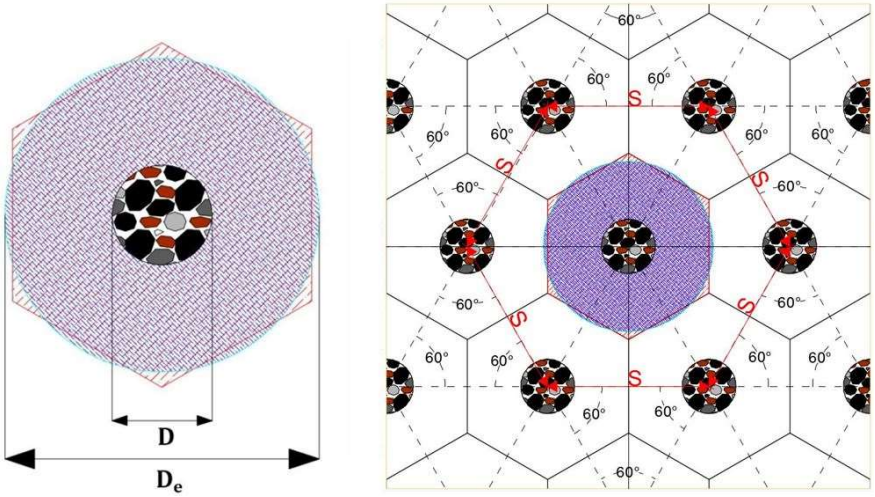

Figure 3-6: Equilateral arrangement of the stone columns, giving De = 1.05S.

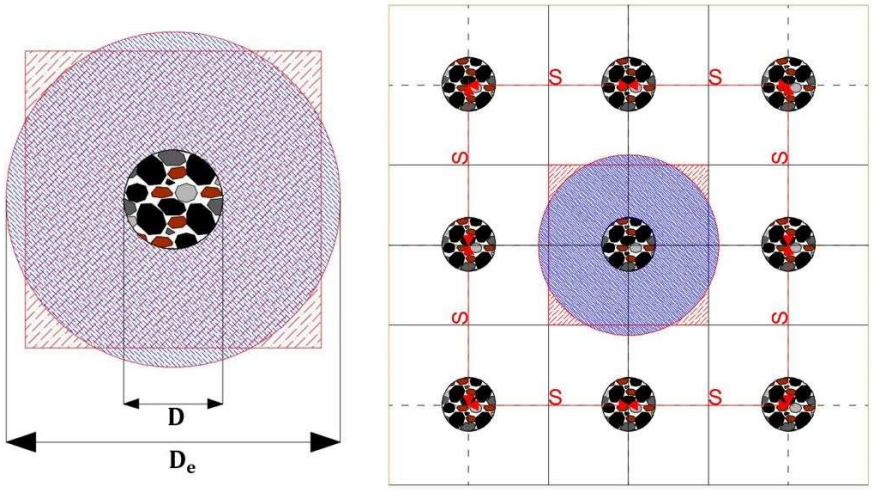

Figure 3-7: Square arrangement of the stone columns, giving De = 1.13S.

For the equilateral triangular configuration, the effective area is the area of the hexagonal shape. The value of D_e (D_e: effective diameter) in such case is 1.05S (S: spacing of stone column) whereas that of the square arrangement is 1.13S. Hence, it can be concluded that the former is better. The tributary soil area covered by the

effective diameter, D_e, is known as the unit cell of the stone column. Nevertheless, the performance of the columns is also influenced by other factors such as their stiffness, length and diameter which will be elaborated in the following sections.

3.4 Length and diameter of stone column

A stone column having a length between 4-6D (D in the diameter of the stone column) is generally used for construction purposes. Its diameter normally ranges between 0.8-1.2m whereas its length typically varies between 4-10m (Barksdale and Bachus, 1983, Deb *et al*., 2011, Nicholson, 2015).

If the centre to centre spacing and the length of the columns are unchanged, increasing their diameter will lead to an increase in the overall area replacement ratio which in turn will have a positive influence on their performance of the column (Deb, 2008, Keykhosropur et al., 2012, Deb and Mohapatra, 2012, Mani and Nigee, 2013, Aza-Gnandji and Kalumba, 2014,). Basically, this means that more and more soil will be replaced by the stone columns. Since the stone columns have better performance than the soil itself, an increase in area replacement ratio will lead to an overall increase in performance.

Dash and Bora (2013) did a series of lab tests with various variables, among which the length of the stone columns was also varied. Figure 3-8 shows the results obtained from their investigation where only the length of the stone columns was varied with respect to the diameter while all other variables were kept constant.

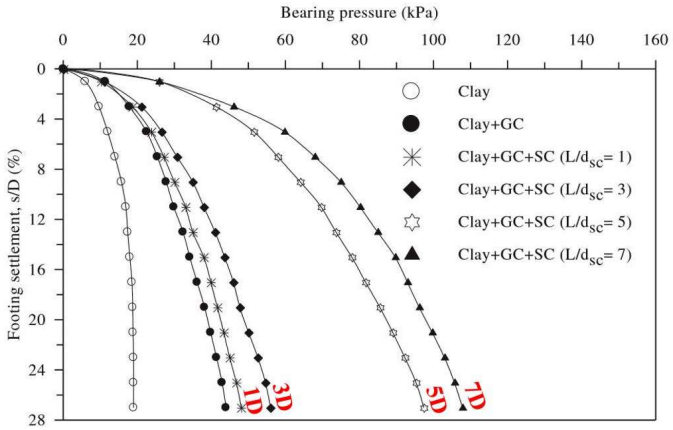

Figure 3-8: Settlement response of stone column with respect to different bearing pressures (Dash and Bora, 2013).

It was found that there was a significant improvement in the settlement response of the column as its length changed from 3D to 5D. However, it was noted that increasing the length further, from 5D to 7D, did not result in a significant improvement in performance of the column. Hence, it can be said that using a stone column length of 5D is generally satisfactory.

3.5 Modes of failure

The failure mechanisms of a stone column are normally dependent on its length. The most common mode of failures of the stone columns are shear failure, punching failure and bulging. Barksdale and Bachus (1983) observed that a column greater than 4D essentially fails by bulging (Figure 3-9a), irrespective of whether it is resting on a solid surface or not.

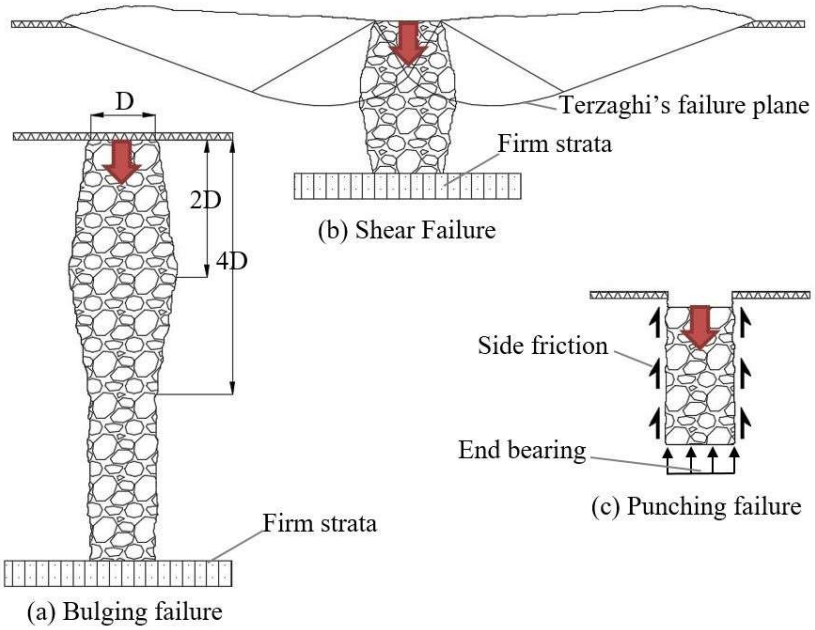

Figure 3-9: Failure mechanisms of stone columns (Adapted from IS 15284 (2003)).

It was also reported by Barksdale and Bachus (1983) that the length of bulging normally varies between 2-3D while IS 15284 (2003) adopted a length of 4D. Murugesan and Rajagopal (2006) stated that the bulging length is 2.5D while Ghazavi and Javad (2013) reported it is between D-2D from the head of the column. Murugesan and Rajagopal (2006) added that the bulging of the stone column is normally resisted

by the passive pressure of the surrounding soil. Hence the stone column material at a deeper level will normally experience a better confining pressure. If the stone column is less than 4D and stands on a firm stratum, it will fail by shear failure (Figure 3-9b). However, if the column is less than 4D and is in a 'floating' condition, it will normally experience punching failure (Figure 3-9c).

Other modes of failure, such as bending failure, can also be experienced by columns that are greater than 4D in length such as that observed by Chen *et al*. (2015). They used sand columns (diameter 32 mm and length 400mm) to reinforce an embankment support. Therefore, the length of their columns was 12.5D. Moreover, it was noted that the stone column was not loaded axially due to the embankment which could have contributed to the bending failure as well. The bending failure of the column obtained from their experiments is shown in Figure 3-10.

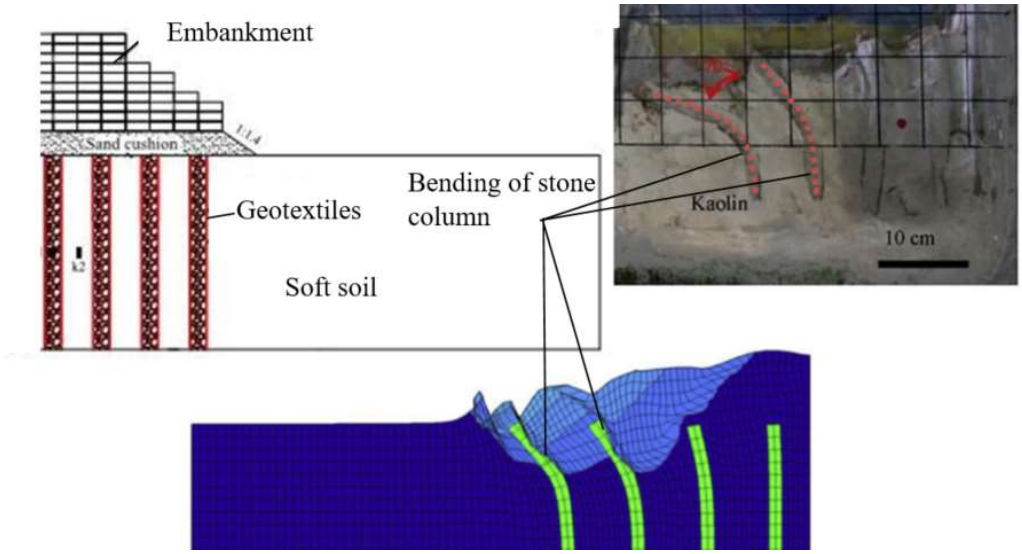

Figure 3-10: Results and modelling obtained from experiments carried out by Chen *et al*. (2015).

Terzaghi proposed a failure mechanism of the soil beneath a foundation footing (Das and Sobhan, 2014), as shown in Figure 3-11. This model was used to generate the failure mechanism for soils having various friction angles. It is observed from Figure 3-12 that a soil with a higher friction angle will be able to mobilise a greater frictional force due to its lengthier plastic zone. Hence it is expected that such soil will be able

to carry more load as it will provide a better passive resistance (Mani and Nigee, 2013). On the contrary, soft soils do not have a good friction angle and are problematic to stone columns.

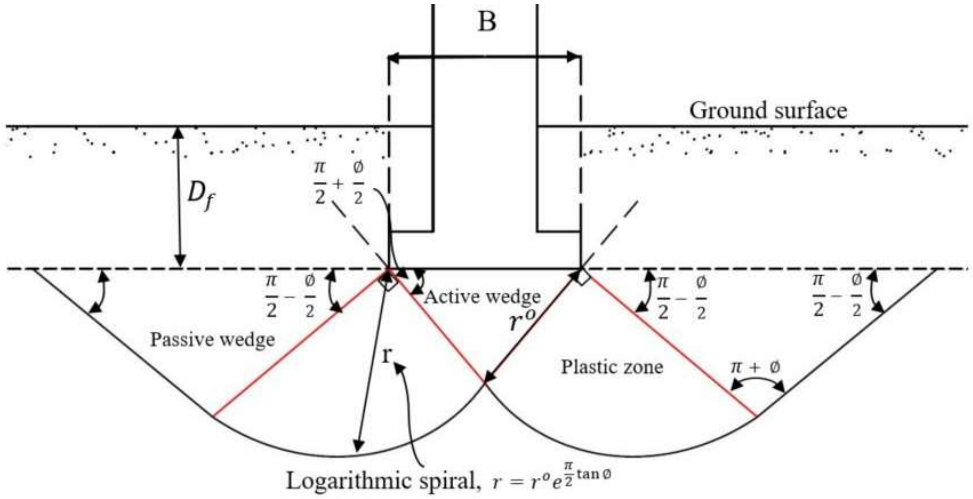

Figure 3-11: Terzaghi's failure mechanism. (adapted from Das and Sobhan (2014)).

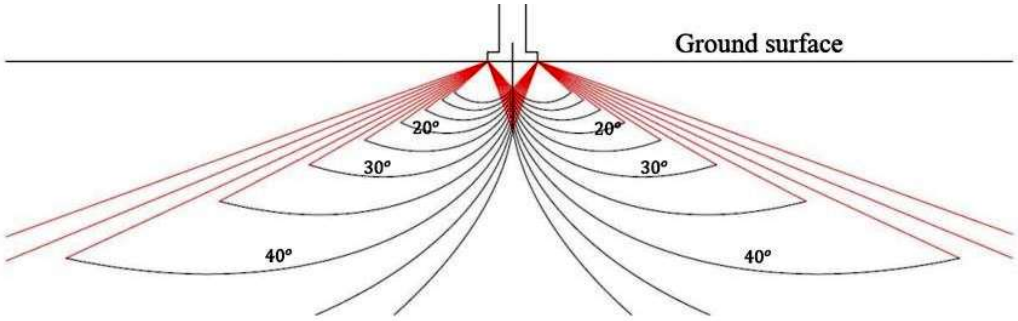

Figure 3-12: Terzaghi's generated model of the different active wedge with respect to different friction angles.

3.6 Problems associated with stone columns and remedial measures adopted

It is not recommended to use normal stone columns in very soft soil (C_u < 15 kPa) due to the lack of lateral confinement. Stone columns constructed in very loose/soft soils can bulge excessively and as a result, considerable settlement can be obtained (Murugesan and Rajagopal, 2006, Gniel and Bouazza, 2009, Keykhosropur *et al.*, 2012, Ghazavi and Javad, 2013,). Byrne and Berry (2008) stated that stone columns in

such soils need lateral support to effectively carry their applied load. Numerous studies (Murugesan and Rajagopal, 2006, Gniel and Bouazza, 2010, Deb and Mohapatra, 2012, Ghazavi and Javad, 2013, Chen et al., 2015) have been done to optimise the performance of such stone columns so far. These include encasing the stone columns with geosynthetic/geogrid reinforcement and as well as placing a reinforced bedding layer over them. The encasement of a stone column increases its stiffness by holding its constituting material together and thus limits bulging/settlements. Kirsch and Bell (2012) reported that the first documented use of a geotextile to reinforce stone columns was in 1993 for a dam project in Austria. This was used to avoid lateral spreading of the columns and to maintain their filterability.

3.6.1 Geogrid/Geotextile encasement

Geogrid encasement sleeves are typically made by welding a frame to make a rigid structure. Gniel and Bouazza (2009) investigated the use of geogrid to ameliorate the stone columns. They used several geogrids and assessed each of them respectively. They observed that increasing the tensile strength of the encasement significantly increased the bearing capacity of the stone column as shown in Figure 3-13.

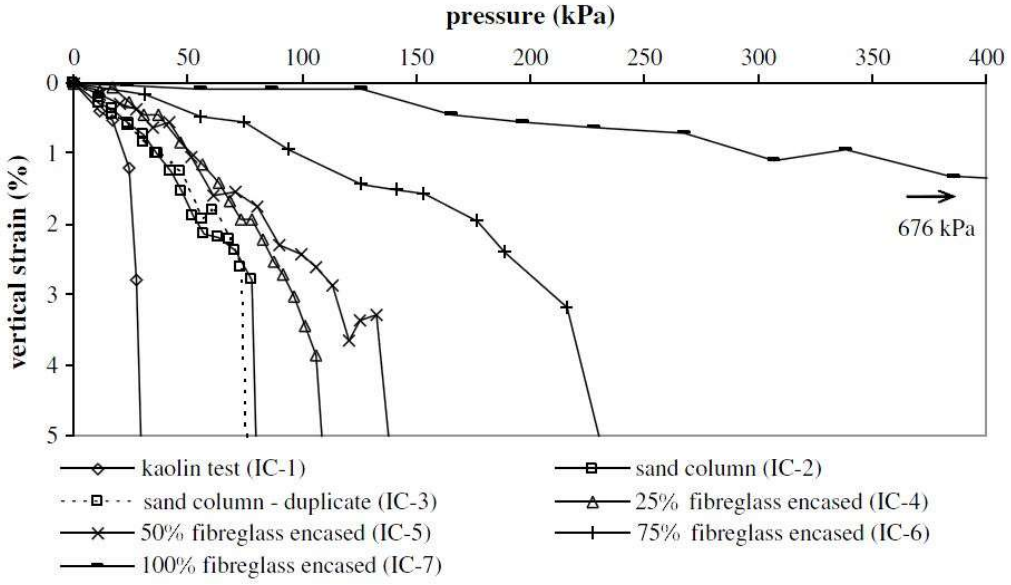

Figure 3-13: Vertical strain response of stone column with different type and length of fibreglass (Gniel and Bouazza, 2009).

The Kaolin clay had a maximum bearing pressure of about 25 kPa before failure but a 100% fibreglass reinforced geogrid achieved its maximum bearing pressure after 676 kPa had been applied. This accounts for over 27-folds increase in strength. Gniel and Bouazza (2010) found that by effectively overlapping the geogrid, a good economical approach can be brought forward. Cable ties were used to fix the geogrid into position and it was found that a 100% circumferential overlap encasement had the best performance. Figure 3-14 shows a typical encasement sleeve used by Gniel and Bouazza (2010).

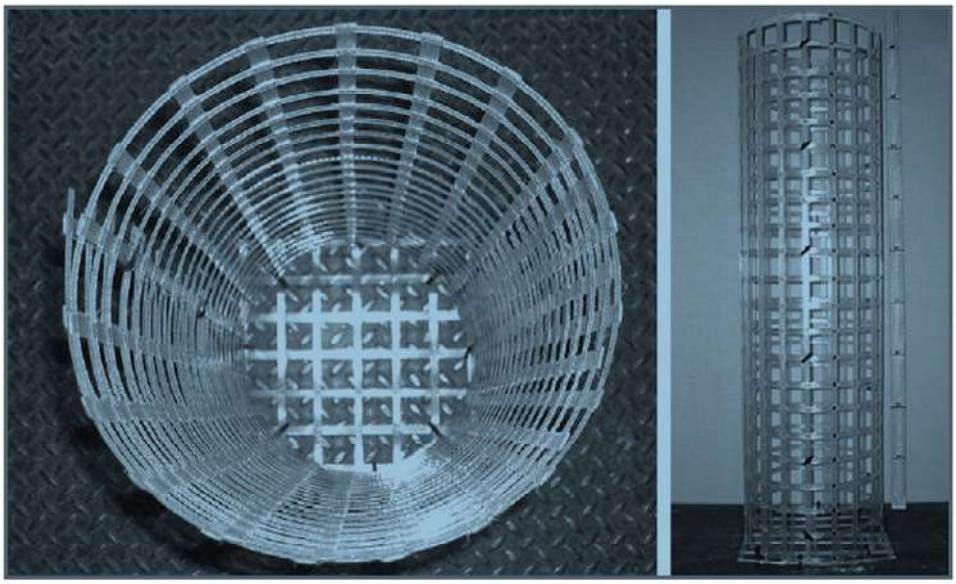

Figure 3-14: Encasement sleeve of stone columns used for model testing (Gniel and Bouazza, 2010).

Ghazavi and Javad (2013) obtained comparable results with geotextile reinforcements. Keykhosropur *et al*. (2012) used 3D numerical analysis to predict the performance of encased stone column below an embankment. They also found that by effectively increasing the encasement strength of the geosynthetic encasement, the performance of the stone column can be increased. Likewise, from numerical analysis, Murugesan and Rajagopal (2006) obtained considerable improvement of the stone columns when the strength of their geosynthetic encasement was increased. An extract of their results is shown in Figure 3-15.

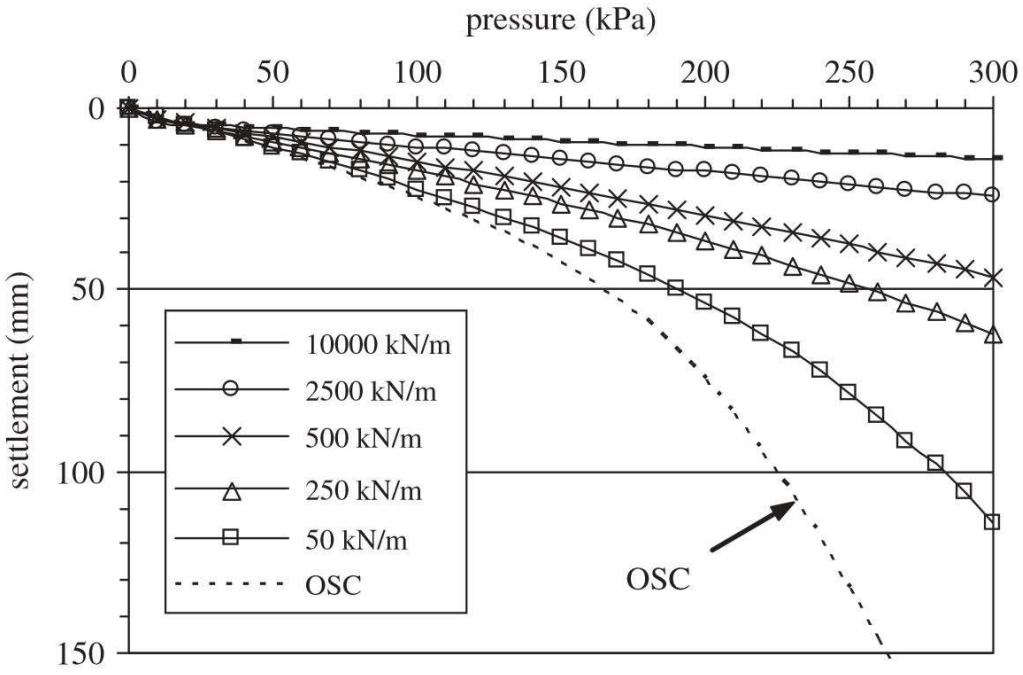

Figure 3-15: Response of stone columns with different levels of the encasement. (Murugesan and Rajagopal, 2006).

It was also reported that geotextiles can be damaged by crushed aggregates and vibration during installation (Gniel and Bouazza, 2010). However, even if the geotextile ruptured, the column will still perform better than an uncased one. Furthermore, Hong *et al*. (2015) added that a stronger geotextile encasement will force the bulging to occur at a deeper depth. It was shown through numerous studies that increasing the strength of the encasement leads to an improvement in the bearing capacity of the column, however, the same cannot be said with regards to its length.

Gniel and Bouazza (2009) reported that an increase in the length of the encasement increased the column's overall stiffness. Consequently, a column having a greater length of encasement will exhibit better performance. However, from their numerical analysis (using GEOFEM software), Murugesan and Rajagopal (2006) found that increasing the depth of encasement above 3D brought limited improvement in the bearing capacity of the column as shown in Figure 3-16.

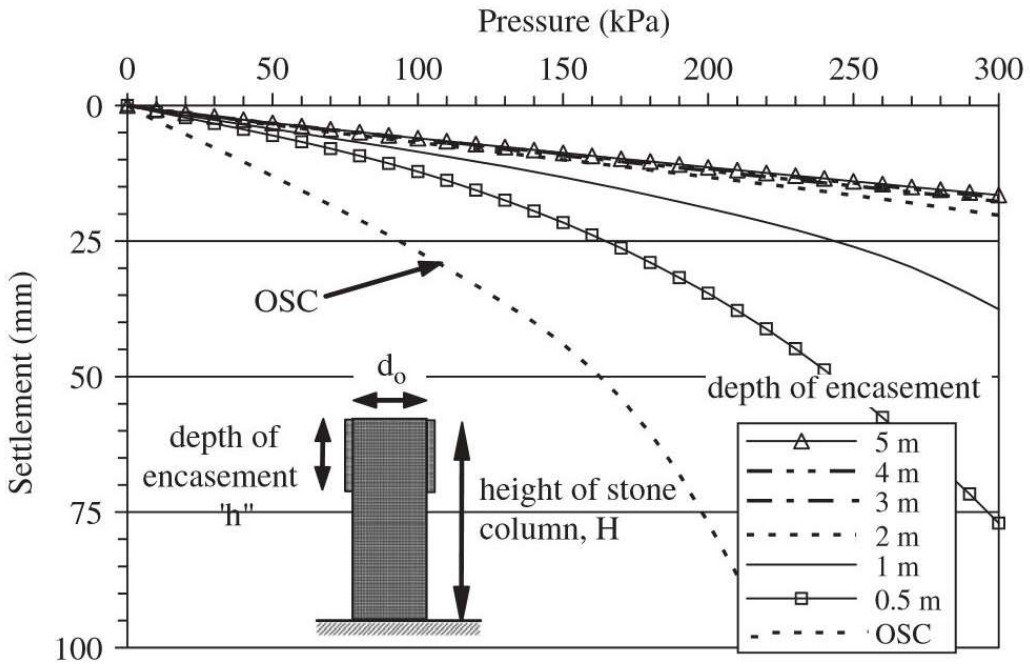

Figure 3-16: Encasement depth of a 0.6m diameter stone column (Murugesan and Rajagopal, 2006).

The lateral confinement of the stone columns can also be increased by increasing the surcharge load around the footing. This can be achieved by placing a layer of material such as a sand bed above stone column.

3.6.2 Bedding layer

Barksdale and Bachus (1983) stated that the performance of the stone column can be improved by placing a granular blanket (bedding layer) over it. This bedding layer will increase the bearing capacity and reduce settlement of the stone column (Barksdale and Bachus, 1983, Tafreshi and Dawson, 2010, Deb *et al.*, 2011, Deb and Mohapatra, 2012, Dash and Bora, 2013,). IS 15284 (2003) reported that, for construction purposes, the blanket/bedding layer should be compacted to a relative density of 75-80% and that its minimum thickness should be 0.5m. However, the underlying soil should be first compacted by means such as rolling/tamping to a minimum depth prior to placing the bedding.

Deb and Mohapatra (2012) stated that the use of a geosynthetic layer in an embankment above a stone column enhanced the load transfer between the stone

column and its surrounding the soil. Deb et al. (2011) used sand as a bedding layer and reported that an increase of 233 % in bearing capacity was obtained when the layer was reinforced with geogrid compared to an unreinforced one.

Tafreshi and Dawson (2010) reported that a reinforced bedding layer acts as a thick slab, minimising surface heaving of the soil and increasing its bearing capacity. They observed that increasing the horizontal span of reinforcement by greater than 3.2D brings no additional benefit to the bearing capacity of a column. Thus, excess length of reinforcement should not be wasted. They showed that the bed layer reinforced with geocell performed better compared to that of a geosynthetic reinforced layer for equal or less quantity of material. The geocell reinforced layer exhibited a better bearing capacity and lower settlement. They added that by increasing the height of the geocell, the bearing capacity can be increased and settlement can be reduced.

Dash and Bora (2013) observed that the stone column alone can increase the bearing capacity by 3-folds however, combined bedding layer reinforced with geocell, a bearing capacity of 10-folds can be achieved. They also observed that the optimum thickness of the geo-cell layer is equal to that of the footing diameter, after which the increase in performance is minimal. Figure 3-17 shows the setup used by Dash and Bora (2013).

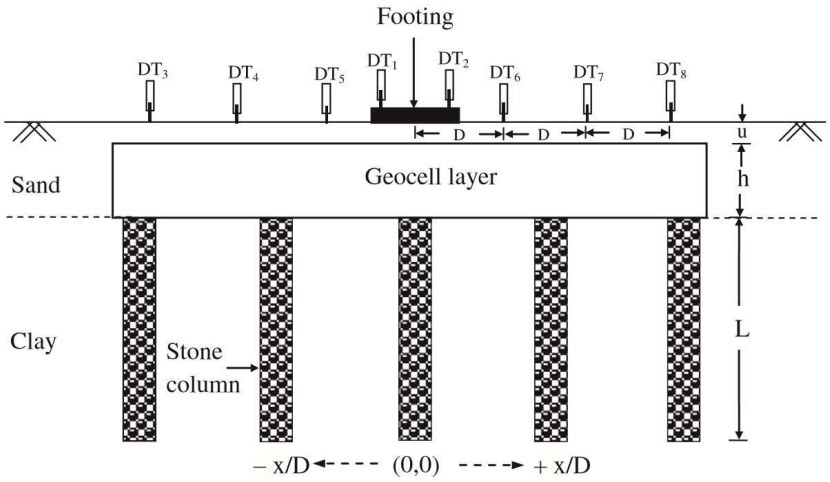

Figure 3-17: Stone column with Geocell layer on top (Dash and Bora, 2013).

3.7 Summary of findings

As elaborated in this Chapter, numerous studies have been conducted to increase the bearing capacity of the stone columns and limit their settlements. Encasement with geosynthetics is the main approach normally adapted to confine the stone column's materials in a view to increase their stiffness and control bulging. Through the different studies discussed earlier, it was noted that the tested stone columns were in contact with the base of the mould (which represents a firm stratum). However, this was an ideal condition because the firm stratum provided a reaction force that resisted end bearing failure. Ground conditions on site are variable and there was a lack of studies to investigate the effect on the performance of the stone columns if the bearing stratum layer was deep. None of the studies addressed so far investigated what will happen if the stone column cannot be constructed on a firm stratum.

Moreover, it was understood that the geogrid/geotextile reinforcements increase the stiffness of the stone column. As a result, bulging is controlled. Nevertheless, it was anticipated that increasing the cohesion of the stone material will also bring an improvement in stiffness. This can be achieved by using a binder, such as concrete, to hold the stone column material together in order to increase its stiffness/performance. So far, none of the previous studies used this approach. The concrete is expected to behave as a stiff encasement and transfer the bulging to a deeper level within the column thus, increasing the performance of the stone column as predicted by Hong *et al*. (2015).

This research aimed at exploring a new way in which the performance of stone columns can be improved. Different grades of concrete of varying lengths were used to systematically replace part of the stone column, and its settlement behaviour with respect to the applied load was then monitored. In addition, the behaviour of these columns was also studied in different conditions whereby the depth of soil beneath them was varied. To conclude the set of experiments, a geosynthetic reinforced bedding layer was used in combination with the column having the optimum performance to verify if additional improvements could be achieved. Details about how the experiments were planned and carried out will be explained in the following

chapter. Figure 3-18, shows a summary of the main aspects that were identified with regards to stone columns.

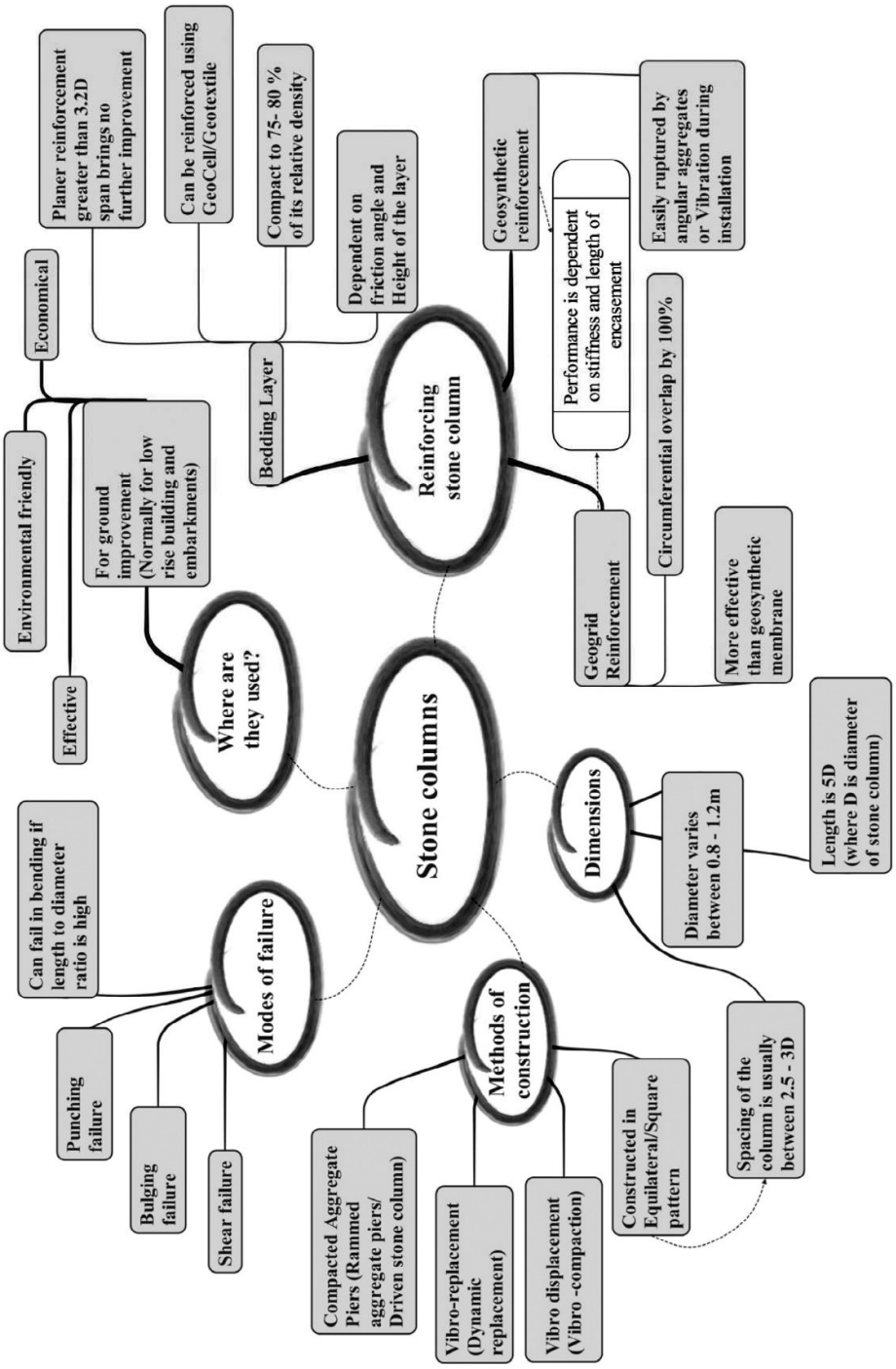

Figure 3-18: Summary of the main aspects of stone columns.

Chapter 4: Research Methodology

4.1 Introduction

In this chapter, the methodology adopted for the course of the experiments were defined and elaborated. Considering the actual dimensions of the stone column (average diameter of 1m and length of 5D) used on site, it was difficult to test such under lab conditions. Hence, a model of the stone column was constructed and tested using an adequate unit cell (Defined in section 4.4). As a result, the stone column material was carefully selected to match an appropriate scale used for the lab testing purposes. The soil was also prepared to a convenient moisture content, having a CBR value of 4%, modelling the properties of a weak soil.

4.2 Properties of materials used for testing

4.2.1 Soil material

Cape Town clay was the base material that was adopted for testing. It was excavated from a construction site in Green Point area, near the city centre of Cape Town, South Africa (Sobhee-Beetul, 2012). It was relatively dry, reddish-brown and fine-grained mass as shown in Figure 4-1.The classification of the soil and its properties were determined in the UCT Geotechnical Engineering laboratory.

Figure 4-1: Soil material used for testing.

Table 4-1 shows a summary of all the soil properties determined through lab tests according to their respective standards. The importance of the relevant tests and the method of how the tests were carried out are elaborated in Appendix D.

Soil Properties	Test	Standards	Summary of results
Liquid limit	Standard test methods for Liquid Limit, Plastic Limit, and Plasticity Index of Soils	ASTM D4318 (2010)	37%
Plastic Limit			18%
Plasticity Index			19%
California bearing ratio (CBR)	Standard test method for California Bearing Ratio (CBR) of laboratory-compacted soil	ASTM D1883 (2016)	4.01%
Maximum Dry Density	Compaction effort of soil using standard effort	ASTM D698 (2012)	1850kg/m^3
Optimum moisture content			14.20%
Soil Grading	Particle size distribution (Gradation) of soils using sieve analysis	ASTM D6913 (2009)	26% Clay 26% Silt- 48% Sand
	Standard test method for particle size analysis of soil	ASTM D422 (2007)	
Shear strength	Direct Shear Test of soils under consolidated drained condition	ASTM D3080 (2011)	c'= 13.1 kPa
Friction angle			$\emptyset'_p = 27.0^0$
Specific gravity	Standard test methods for Specific Gravity of soil solids by water pycnometer	ASTM D854 (2014)	2.68

Table 4-1: Summary of results obtained from various lab tests.

4.2.2 Angular stone material for the stone column and bedding layer

It was stated that the average column size is normally 1m in diameter (Barksdale and Bachus, 1983). However, this was scaled down by 20 to obtain a stone column of 50mm diameter which was used for testing. The same approach was used to obtain a convenient aggregates size grading that was utilized for a 50mm diameter stone column. Figure 4-2 shows the stone column aggregates that were selected for testing.

The typical sieve size of the aggregates used on site was elaborated in section 3.2.4. Alternative 1, as elaborated in section 3.2.4, was chosen from Table 3-1 from which a convenient grading range used for testing purposes was calculated. Table 4-2 shows a summary of the scaled down grading for construction of a 50mm diameter column after Barksdale and Bachus (1983).

Figure 4-2: Angular stone column materials.

Table 4-2: Aggregate size for 50 mm diameter column, based on alternative 1 from Barksdale and Bachus (1983).

Alternative 1				
Sieve size (1m diameter column) / inches	**Sieve size (1m diameter column) /mm**	**Sieve size (50mm diameter column) /mm**	**Min % passing**	**Max % passing**
3	76.2	3.81	90	100
2	50.8	2.54	40	90
0.75	19.05	0.95	0	10
0.5	12.7	0.64	0	5

These values were further compared with various research done in the respective field. Table 4-3 shows a summary of the aggregates sizes used by several authors using a stone column of around 50mm diameter. The stone column's material was prepared in such a way to satisfy both the limits proposed by Barksdale and Bachus (1983) and the aggregate sizes adopted by different authors as stipulated in Table 4-3.

Table 4-3: Summary of various column aggregates sizes for stone column around 50 mm diameter.

Column diameter / mm	**Aggregate size used/ mm**	**Author name and year**
60mm	2.36 - 4.75mm	Sharma *et al.* (2004)
50, 75 and 100mm	2 - 10mm	Murugesan and Rajagopal (2006)
51mm	1.6mm uniform size	Gniel and Bouazza (2009)
50mm	2 - 6mm	Deb *et al.* (2011)

Figure 4-3 shows the grading of the stone aggregates used for the construction of the stone columns model. The analysis was done as per ASTM D6913 (2009). Further details can be found from the Appendix C.

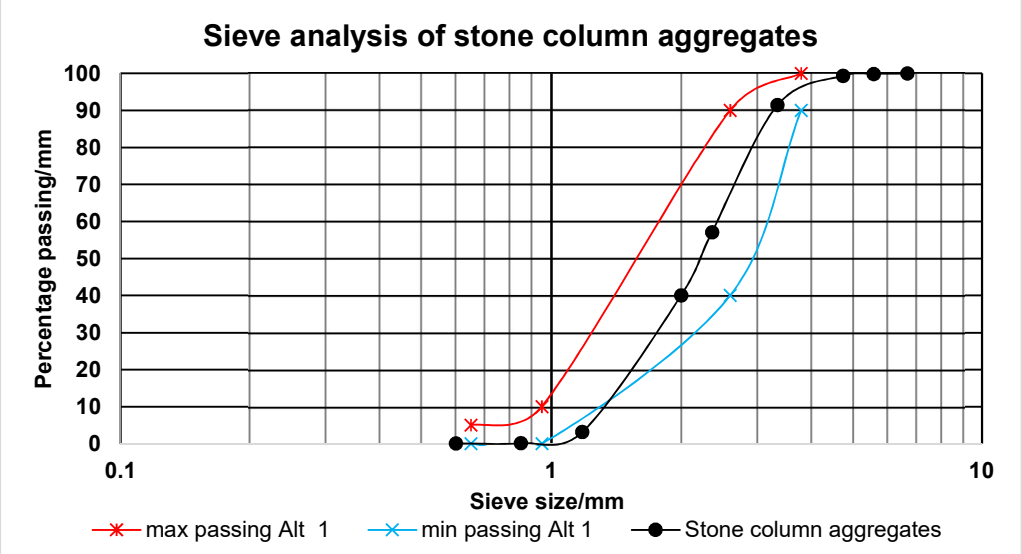

Figure 4-3: Grading of aggregates used as stone column material.

Referring to Figure 4-3 and Table 3-2 (from section 3.2.4) Brown suitability number was found to be 2.05. Hence, according to Dheerendra Babu et al. (2012), the material prepared for testing was rated as excellent.

4.2.3 Geosynthetic- Rockgrid

Although from the literature it was found that a bedding layer reinforced with a geocell was best suited to increase the performance of the stone column, it was difficult to test such for the lab model selected. Due to the small size of the model, an adequate industrially available geocell could not be obtained. Similarly, an adequate geogrid could not be found to reinforce the bedding layer. However, it was deemed adequate to use the industrially available geocomposite, as shown in Figure 4-4, for testing purposes due to its relatively small thickness (around 1mm) and grid spacing (roughly 1.5cm). The geocomposite reinforced the bedding layer that was used in conjunction with the stone column to investigate if any additional improvements can be brought forward.

The material was obtained from a local supplier, Kaytech Engineered fabric. This is a combination of a geogrid and geotextile henceforth, it had superior properties. Table 4-4 shows the properties of the geocomposite material (Rockgrid 50/50) used for testing.

Figure 4-4: Geo-composite (Rockgrid) used to reinforce the bedding layer of the stone column.

Table 4-4: Properties of Rockgrid (Geocomposite) 50/50, 100/100 and 200/200 (Kaytech Engineered Fabric, 2015).

			50/50	100/100	200/200	
Material		200 g/m^2 needle punched, polyester nonwoven				
Short Term Tensile Strength (T_u)	Machine	kN/m	50	100	200	SANS 1525:13 / ISO 10319
	Across	kN/m	50	100	200	
	Elongation	%	10	10	10	
Long Term Design Strength (LTDS)① (114 yrs)		kN/m	30	60	120	
Creep Limited Strength (10^6 hrs or 114 yrs)②		kN/m	35	70	140	ISO 13431
Water Flow Rate	Normal to Plane @50mm head	ℓ/s/m^2	60			SANS 11058:13 / ISO 11058
	In Plane 20 kPa (i=1)	l/hr/m-width	112			ISO 12958:10
Roll Dimensions		m	5 x 100			

① $LTDS = \frac{T_u}{f_c \cdot f_d \cdot f_e \cdot f_m}$

f_c (creep) = 1.40 (10^6 hrs or 114 yrs)②

f_d (damage) = 1.05 (sand, silt, clay, yarn facing soil)

f_e (environment) = 1.10 (pH 4-9)

f_m (material) = 1.00

4.2.4 Concrete mix design

A suitable design approach, as elaborated in Appendix A.1, was identified to produce four different grades of concrete (G10, G20, G30 and G40 having an average compressive strength of 17.3MPa, 33.4MPa, 41.6MPa and 52.2MPa respectively). The materials used to prepare the concrete mix is shown in Figure 4-5.

Figure 4-5: Coarse aggregate, Cement and Dune sand used for concrete design.

The most commonly available Cement in the area, CEM II 42,5N was used throughout the design. The dune sand and aggregates were obtained from a local supplier. The detailed analysis/tests of the concrete mixes and relevant tests on the aggregates are attached in the Appendix A.1. After the curing process as per BS EN 12390-2 (2000), 50mm diameter concrete plugs were cored through the cylindrical concrete mould as shown in Figure 4-6. The concrete cores were then cut into respective lengths needed for the experiments.

Figure 4-6: Coring of 50mm concrete cores.

4.3 Determining adequate moisture content to run experiment

The compacted soil sample was prepared so that it exhibits the properties of a weak soil and is workable enough so that it can be easily removed using the manual auger. It is not advisable to use normal stone columns in very soft soil (Cu < 15 kPa) due to lack of lateral confinement (Murugesan and Rajagopal, 2006, Gniel and Bouazza, 2009, Keykhosropur *et al.*, 2012, Ghazavi and Javad, 2013,). From the direct shear test experiment carried out on the soil sample at optimum moisture content (as determined from the proctor test), it was found that the cohesion (c') of the soil was 13.1kPa. Hence, the stone columns in such a soil should be reinforced.

CBR tests were carried out on the soil sample according to ASTM D1883 (2016) and ASTM D698 (2012). The value of the CBR after soaking the sample for 4 days, ASTM D1883 (2016), was found to be around 4 %. However, the unsoaked CBR value was found to be over 10 %. Since the prepared samples were tested just after compacting the soil and installing the appropriate columns, the soil was prepared at a CBR value of 4 % as determined by ASTM D1883 (2016).

To obtain such a condition, the moisture content of the soil was increased until the unsoaked CBR value was the same as that of a compacted sample at OMC soaked for 4 days and tested according to ASTM D1883 (2016). Figure 4-7 shows the CBR graph obtained for different moisture contents.

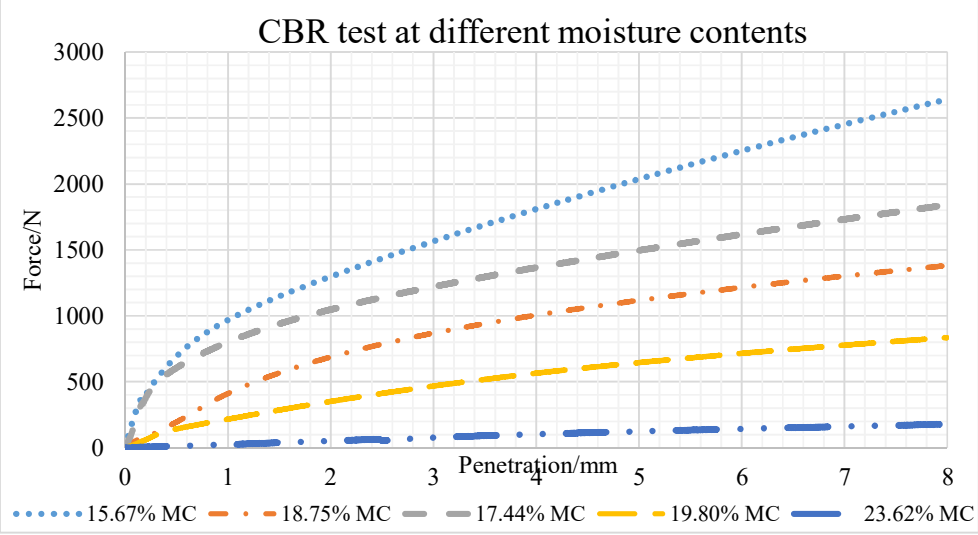

Figure 4-7: CBR graph at different moisture contents.

This is not an uncommon practice, in fact, Ghazavi and Javad (2013) used the same approach to lower the strength of the soil that they have used for their experiments. Deb *et al*. (2011) also used a similar relationship to choose the suitable moisture content to carry out their experiments.

Figure 4-8, shows a summary of the CBR values obtained from the series of experiments performed on the soil samples at different moisture contents. From the results obtained, it was concluded that the soil should be prepared at 20% moisture content for it to have similar behaviour to the same soil prepared at OMC, cured for 4 days in water, and tested accordingly.

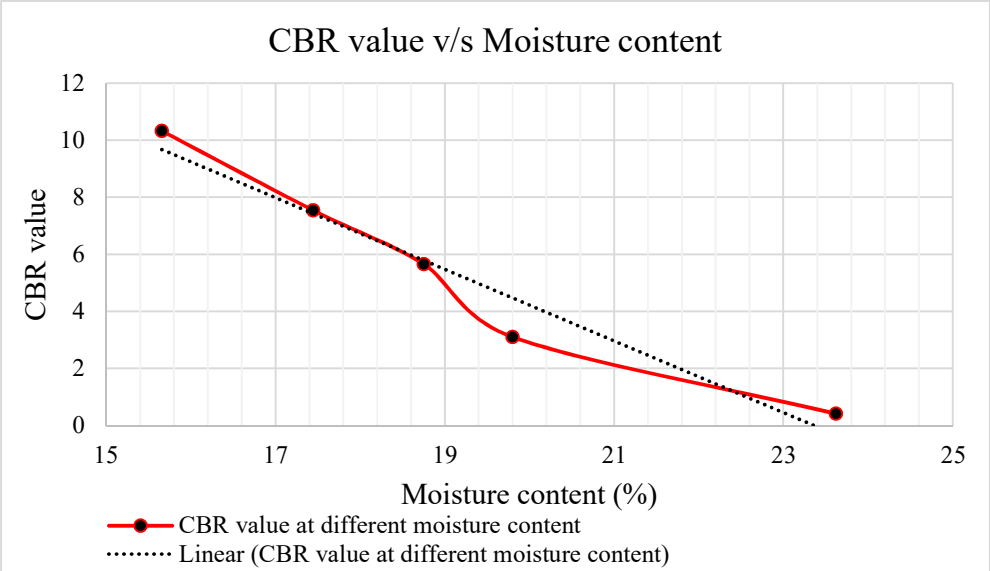

Figure 4-8: Variation of CBR with different moisture contents of the soil samples.

4.4 The dimensions of the bespoke mould and justification

As elaborated in section 3.3, stone columns are much more effective if they are arranged in a triangular configuration (equilateral arrangement) compared to a square arrangement since it will give a higher compaction ratio. For the investigation on the performance of stone columns in lab conditions, a unit cell arrangement is normally adopted if a properly scaled model cannot be investigated. For this research, a conventional CBR mould was found suitable to be used as a unit cell. Moreover, its height could also be varied accordingly, depending on the test setup, by removing or

adding extension collars. The typical diameter of a CBR mould is around 152mm and that of the stone column used was 50mm in diameter. Therefore, the mould was ideal for the planned experiments. Figure 4-9, shows the typical diameter of the column and the unit cell.

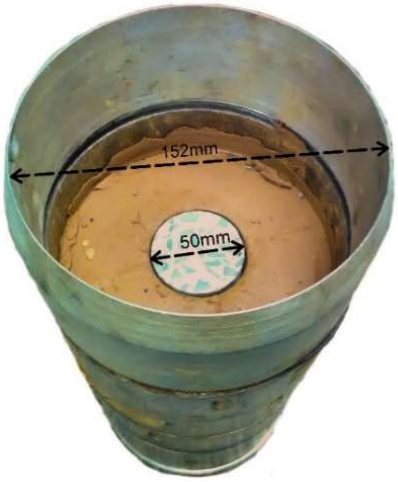

Figure 4-9: Position of the hybrid stone column and the typical diameter of the unit cell.

4.4.1 Spacing in an equilateral arrangement and square arrangement

The unit cell can be used to represent the sample either in an equilateral or square column arrangement. Since D_e is 152mm, in the case of a CBR mould, the spacing of the stone columns can be elaborated as follows:

1. ***Equilateral arrangement:*** $\boldsymbol{De = 1.05S}$

The representative spacing, S, of the column is 144.76mm (around 2.90 D) in the case in an equilateral arrangement.

2. ***Square arrangement:*** $\boldsymbol{De = 1.13S}$

The representative spacing, S, of the column is 134.51mm (around 2.69 D) in the case of a square arrangement.

According to the IS 15284 (2003), an optimum spacing between 2.5 and 3D is normally adopted for construction purposes. Hence, the unit cell is adequate for testing 50mm diameter stone column.

4.5 Planning of experiment

An outline of the experimental setup and the different columns/moulds arrangement used for this research have been illustrated in Figure 4-10. The different configurations /models were chosen as necessary for testing purposes. Table 4-5 shows the annotations used to label the different hybrid stone columns and configurations in which they were tested.

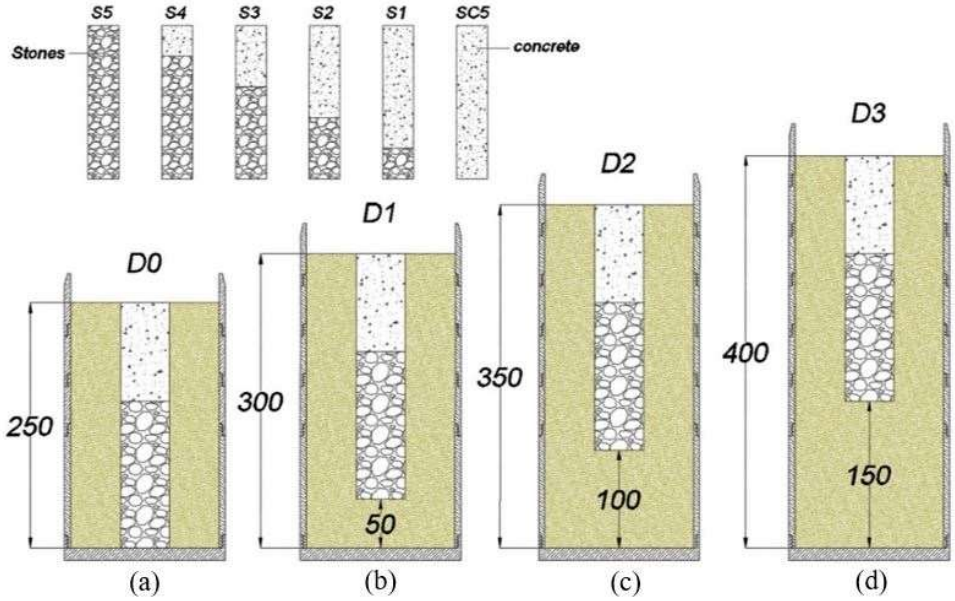

Figure 4-10: Models adopted for carrying out testing of the stone columns (All dimensions shown are in millimetres).

Table 4-5: Summary of annotations used to designate the hybrid stone column and the different configurations.

	Annotations	Description
Stone columns	**S5**	100% stone column (L=250mm), 0 % concrete (L=0mm)
	S4	80% stone column (L=200mm), 20 % concrete (L=50mm)
	S3	60% stone column (L=150mm), 40 % concrete (L=100mm)
	S2	40% stone column (L=100mm), 60 % concrete (L=150mm)
	S1	20% stone column (L=50mm), 80 % concrete (L=200mm)
	SC5	0% stone column (L=50mm), 100 % concrete (L=250mm)
Soil	**D0**	0mm of soil below column
	D1	50mm of soil below column
	D2	100mm of soil below column
	D3	150mm of soil below column

The optimum stone column obtained from the above testing configurations was isolated and further modifications were made in a view to increasing its performance. A bedding layer of 50mm was chosen as Dash and Bora (2013) stated that the optimum thickness of such a layer, reinforced with a geocell, is equal to the diameter of the footing. Figure 4-11 illustrates the testing patterns adopted to investigate the improvement brought by a reinforced/unreinforced bedding layer.

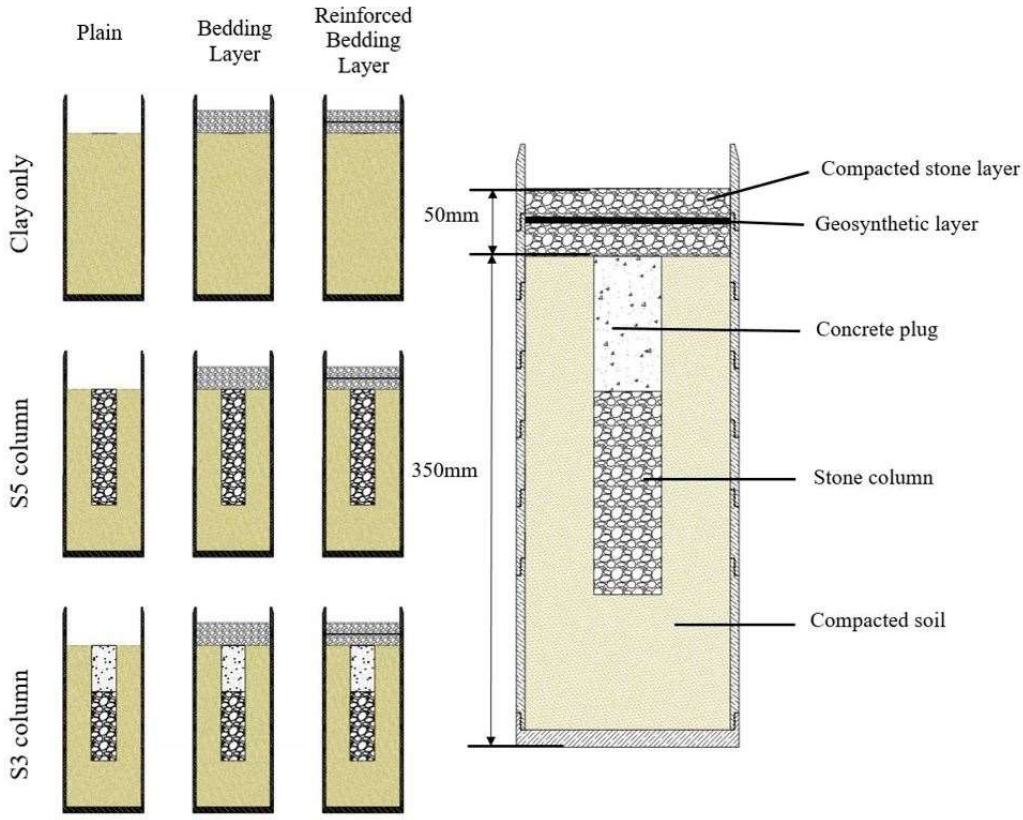

Figure 4-11: Testing patterns adopted to further reinforce S3 column in D2 configuration.

4.6 Preparation of soil for testing

4.6.1 Compaction of clay and stone column materials.

The soil material was compacted using the standard laboratory compaction effort (600kN-m/m^3) as described in ASTM D698 (2012). This can be achieved using the standard rammer of 24.5N (dropped from a height of about 305 mm) and 56 blows per layer (each about 40cm in height). However, a modification to the procedure was brought forward to minimise the preparation time while keeping the same compaction effort. A hammer of 4532g (44.5N) was dropped 24 times from a height of 510mm to compact a soil layer to a thickness of 50mm. The soil was compacted at 50mm thickness until the desired height was reached. To prevent any variation in the procedure, the thickness of the stone columns materials to be compacted at a time was kept at 50 mm. A compaction hammer having a weight of 2050g (20.1N) was dropped 5 times from a height of 600mm to deliver the same compaction energy as that used to compact the soil. Details about the calculations can be found in Appendix B.

4.7 Preparation of stone column for testing

4.7.1 Installing stone column

The soil material was compacted in the mould in layers of 50mm thickness. To ensure uniformity throughout all the test, the soil material was all prepared at once. Henceforth, they all had roughly the same moisture content (around 20%). Using the compaction rammer devised for the experiment, the respective soil was compacted in a standard CBR mould and its compacted density was calculated. This value was then used to measure the mass of the soil sample needed to form a layer of 50 mm thickness. This was found to be around 1.86kg. This predetermined mass was weighed for each layer and compacted using the 4.532kg rammer released from a height of 510mm, imparting an energy of 600kNm/m^3 on the soil sample. Figure 4-12 shows a diagrammatic representation for the preparation of the specimen for testing. Figure 4-13 shows the different tools that were used to install the stone column.

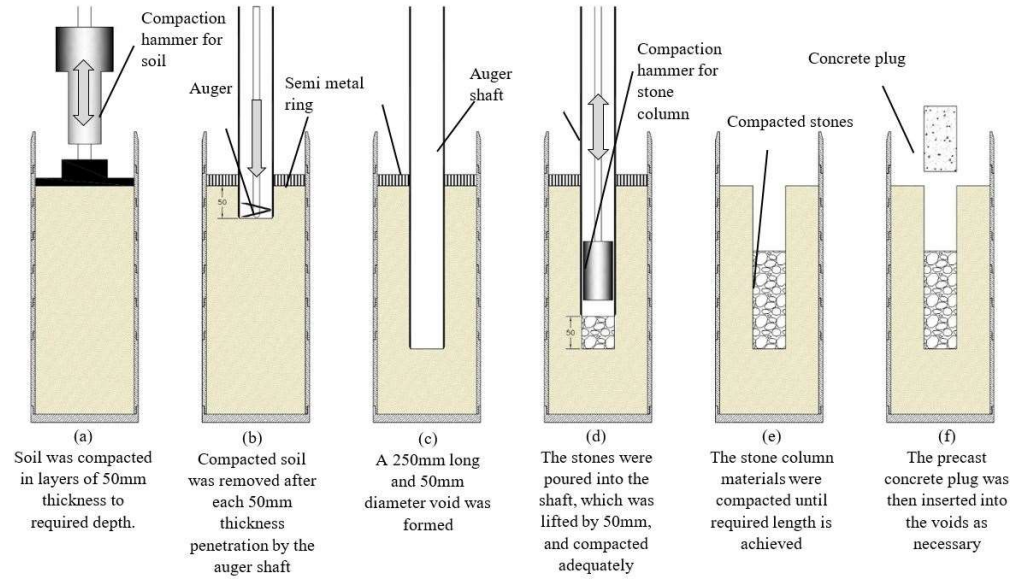

Figure 4-12: Method adapted for installation of the stone columns.

Figure 4-13: Tools used to install stone column.

Once the soil was compacted to the required thickness, the semi-metal ring (surcharge ring from CBR test) was placed on top (as shown in Figure 4-14). This served as a guide to ensure that the penetration of the auger shaft was perpendicular. The shaft was driven manually up to a penetration of 50mm after which the soil was removed to minimise any suction force. The process was repeated until a depth of 250mm was reached.

Figure 4-14: Position of auger shaft held centrally by the semi-metal ring (left) and the hammer used for compacting the soil layer (right).

After some trials, the amount of compacted stone aggregates required to create a stone column of 50mm height was found to be 158g. Henceforth, this mass of stones was poured into the auger shaft that was then raised by 50mm. This ensured that the stones were surrounded by the soil only. Consequently, the 2050g hammer was dropped 5 times from a height of 600mm. This imparted the same amount of energy as that used to compact the soil. The precast concrete plug was then added as necessary to form the full hybrid stone column.

4.8 Testing

It was necessary to select a suitable loading rate at which the load was applied on the stone columns. Ghazavi and Javad (2013) and Hong *et al*. (2015) used a displacement rate of 1mm/min. However, a penetration rate of 2mm/min was used by Dash and Bora (2013), the reason being that this rate of displacement produced an undrained response in the saturated clay bed that they used. As a result, the angle of friction of the saturated clay sample converged to zero, leading to a maximum decrease in bearing capacity of the resultant configuration. Referring to ASTM D1883 (2016), a penetration rate of 1.3mm/min is used for testing the California Bearing Ratio (CBR). Since the plunger for the CBR mould and that used for testing was the same diameter (roughly 50mm),

the same rate of penetration (1.3mm/min) was adopted so that the values obtained from the test can be related to CBR values if necessary.

After preparing the specimen, it was placed in the Zwick 1406 machine for testing, as shown in Figure 4-15. This specific machine can be used to test materials both in compression and in tension up to a maximum load of 100kN. For this study, a load in compression was applied at a rate of 1.3mm/min and its magnitude was recorded for consecutive displacements of 1µm until 50mm penetration or a cut-off load was reached. Care was taken such that the concrete plug does not fail in compression hence a cutoff load for each grade of concrete was calculated as per BS 1881-121 (1983). This ensured that the concrete plug was loaded within its elastic range.

Figure 4-15: Zwick 1406 machine used for testing stone columns.

4.9 Repeatability

To ensure the reliability of the results, a few tests having the same parameters were repeated and the results were compared with each other. Figure 4-16 shows the results obtained for D0G10S0, D0G20S0 and repeated tests of D1G10S4. The D0G10S0 and D0G20S0 represented the compacted clay only with no stone columns. Table 4-6

shows the moisture contents of the different samples. From Figure 4-16, it can be deduced that the performance of D1G10S0/D1G20S0 and D1G10S4a/b are close to each other hence, the experiment is considered repeatable. However, the small variation of the graphs can be explained by two parameters (moisture contents of the soil and arrangement of stones within the column) that cannot be controlled as precisely as possible. These parameters will be elaborated in section 5.3.

Table 4-6: Moisture content of tests carried out for repeatability tests.

Test series	<mass of container >	<mass of container + sample>	<mass of container + oven dried sample>	Moisture content
D1G10S0	19.417	51.415	46.101	19.91
D1G20S0	21.558	47.294	43.109	19.42
D0G10S4a	17.547	39.584	35.963	19.66
D0G10S4b	18.997	45.710	41.282	19.87

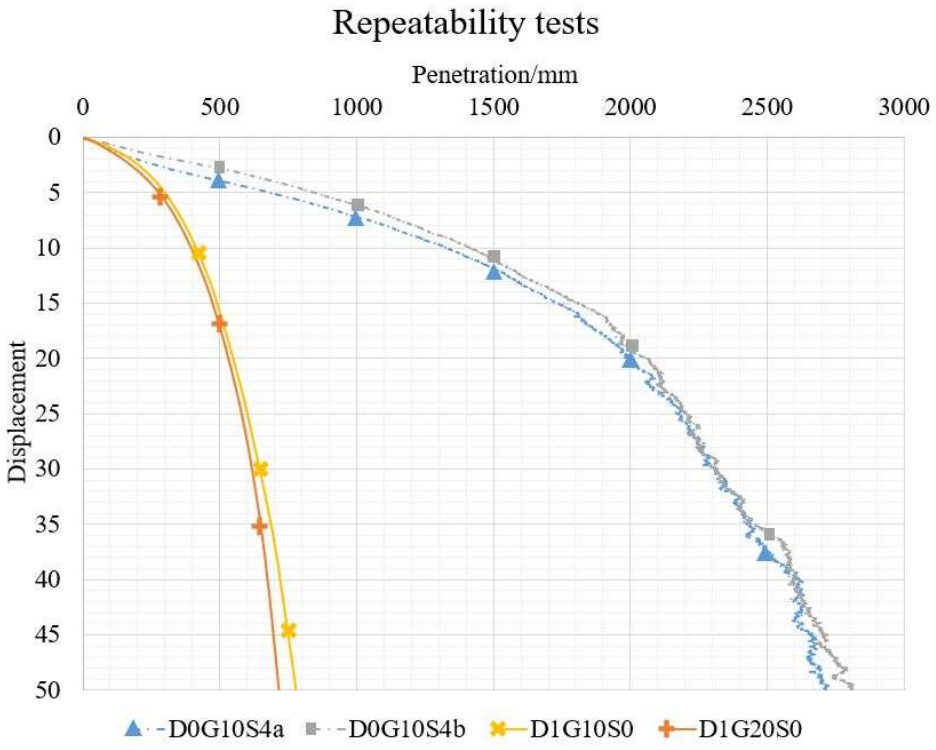

Figure 4-16: Repeatability results to ensure the reliability of results.

4.10 Modelling

After the columns were tested, a mixture of plaster of Paris and sand was prepared at a ratio of 1:1 for modelling purposes. The concrete plug and the aggregates were carefully removed so that the soil retains the deformed shape of the columns. Around 70% water by weight was added to the mix until a uniform paste with a relatively low viscosity was obtained. The slurry was then funnelled into the void created by the removal of the stone columns materials. The whole setup was left to stand for a period of around 30 minutes after which the soil surrounding the stone column was carefully removed. At this stage, the plaster of Paris was hard enough to retain the shape of the tested column but had not yet developed its full strength. Hence, care was taken to avoid a twisting motion especially while removing the extension collar of the CBR mould otherwise, this would have damaged the plaster column. Figure 4-17 shows a representation of the procedures adopted to prepare the stone column model.

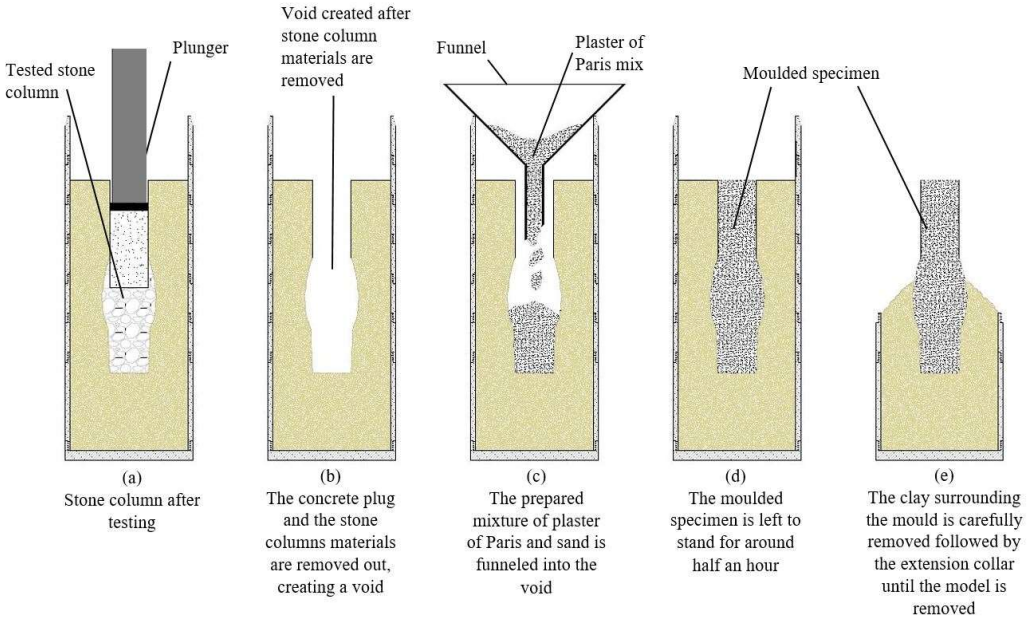

Figure 4-17: Diagrammatic representation of procedures adopted for modelling the stone columns.

After the moulds were removed, the depth of soil beneath them were measured using a Vernier calliper and recorded accordingly. This was used to determine the type of failure of each column, whether it was through bulging or punching failure. The

different models obtained from the plaster of Paris were marked at 1 cm spacing as shown in Figure 4-18 and the average diameters at each respective marking were measured. These measurements were used to accurately draw the specimens to analyse their respective behaviour in terms of deformation as elaborated later in section 5.4.

Figure 4-18: Sample of a model obtained from physical modelling.

Chapter 5: Results, analysis and discussion

5.1 Introduction

This chapter presents results obtained from the different experimental investigations carried out to address the different objectives set for this study. The aim was to investigate whether the introduction of a binder material, such as concrete, within the stone column, could be used to minimise bulging and increase its performance.

By comparing the results with each other, the stone column with the optimum performance was identified. Consequently, the influence of different concrete grades on its performance was examined and relevant conclusions were drawn. With the help of physical modelling, the response of the different hybrid stone columns to the applied load was obtained. These were compared with the experimental results obtained to explain their behaviour. Results from additional experiments, with regards to a combination of a reinforced bedding layer and the optimum stone column, were presented hereafter. The application of this research was then highlighted together with its benefits.

The findings of this research could be used to promote better construction approach for developments on soft soils. As explained in Chapter 4 (Research and Methodology), the tests have been done on a scaled model of the actual dimensions and spacing of the stone columns used on site. Moreover, the soil used for testing was prepared such that it exhibited the properties of a soft soil (having a CBR of around 4% or less) while giving the flexibility to perform the tests for different configurations. Hence, it is expected that similar improvements will be obtained if the recommended hybrid stone column is used on site.

5.2 Behaviour of the (hybrid) stone columns under applied load

The general trend was an increase in settlement/displacement as the load/pressure was increased. However, this was dependant on the type of column and the respective configuration in which it was tested. This section is divided into four different subsections and each of them presents the behaviour of the stone columns in a unique

configuration. Details about the individual configurations (D0, D1 D2, D3) and stone columns (S0, S1, S2, S3, S4, S5, SC5) can be obtained from Chapter 4, section 4.5. Enlarged graphs of each tested configuration with respect to different grades of concrete are found in Appendix G.

5.2.1 Model D0

The D0 configuration modelled a situation whereby the base of the stone column was in full contact with a hard/load bearing stratum. From Figure 5-1, it is observed that the full concrete plugs, SC5, showed the maximum performance as they were less compressible than the compacted stones. As the concrete was gradually replaced with the graded stone column material, the performance decreased. The full stone column, S5, exhibited the least load bearing capacity and could bear around 2 to 4 times more load compared to the unreinforced soil, S0.

The performance of the SC5 column in this configuration is comparable to the behaviour of a stiff encasement, as observed by (Gniel and Bouazza, 2009, Murugesan and Rajagopal, 2006, Ghazavi and Javad, 2013, Mani and Nigee, 2013, Keykhosropur *et al*., 2012). From Figure 5-1, it was noted that the performance was dependent on the length of the 'encasement' (length of concrete plug in this case), contrary to what has been reported by Murugesan and Rajagopal (2006) who stipulated that increasing the length of encasement beyond a length of 3.2D brings no additional benefits. However, the same cannot be said when the column was not in contact with a firm supporting surface.

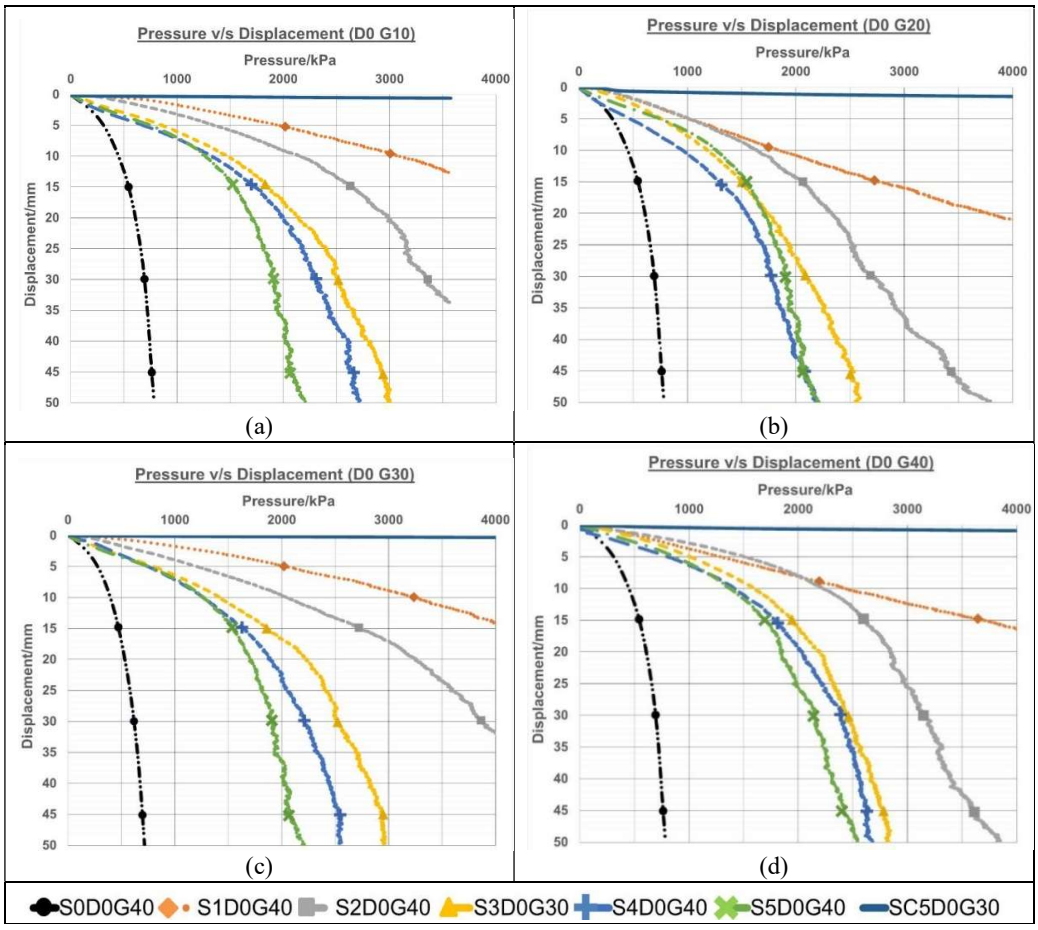

Figure 5-1: Performance of stone columns in D0 configurations for different grades of concrete.

5.2.2 Model D1

When there was a soil layer of thickness D, 50mm, in between the column and the firm surface, there was a considerable change in the behaviour of the stone columns compared to that in D0 configuration, as shown in Figure 5-2. It was found that the difference between the performances of successive stone columns was less prominent. That is, the individual lines in each graph were closer to each other compared to the D0 configuration.

Unlike for the D0 configuration, the performance of the SC5 column was poorer in this case. It was also noted that the SC5 column exhibited a different behaviour irrespective of the grade of concrete. From Figure 5-2, the line for SC5 column

'dipped' and then levelled out after about 35mm penetration of the plunger for nearly every grade of concrete tested. The difference can be explained due to the compressibility of the soil beneath the column.

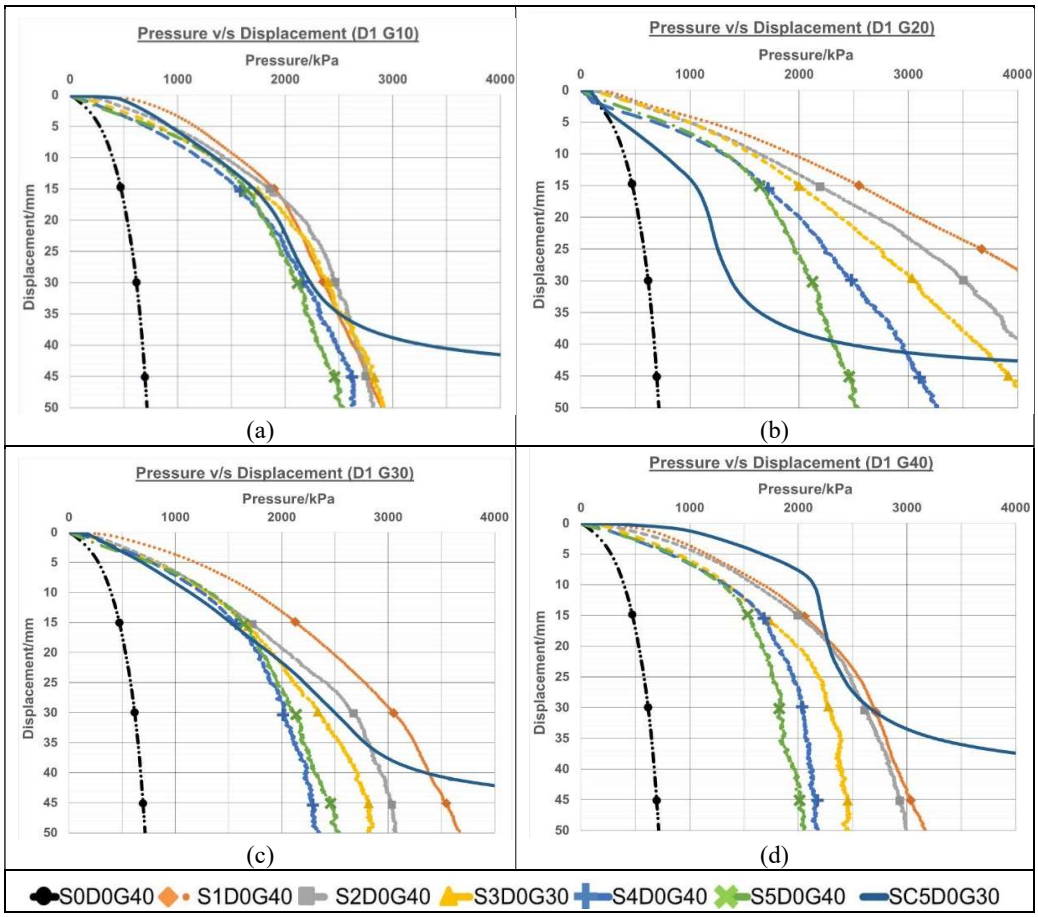

Figure 5-2: Performance of stone columns in D1 configurations for different grades of concrete.

From Figure 5-3, it is seen that the active wedge was already in contact with the base of the bespoke for that specific soil (friction angle = 27.1°) before testing. This wedge could not effectively displace the soil sideways. Therefore, as the load was applied the column compressed the soil until a point where it became dense enough to transfer the load directly to the firm mould base. This was the instant where the load carrying capacity of the column suddenly began to increase.

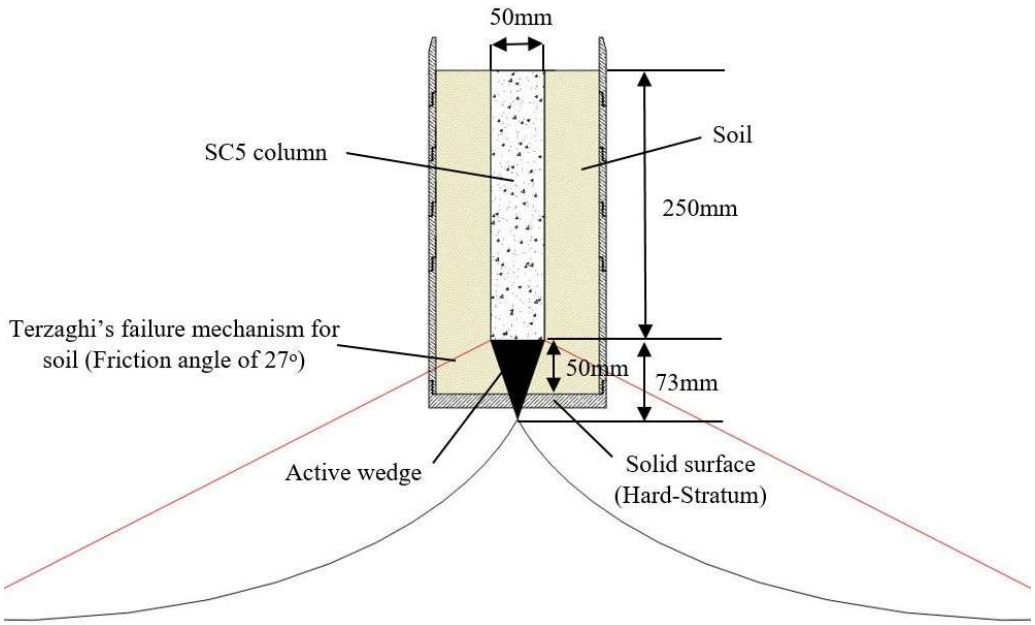

Figure 5-3: Terzaghi's failure mechanism of the soil (friction angle = 27.1°) used for testing of the columns.

5.2.3 Model D2

The performance of the columns in the D2 configuration was different compared to the D0 and D1 configuration, as shown in Figure 5-4. In this case, increasing the length of the concrete did not necessarily bring an increase in performance. The results obtained somehow related to the observations made by Murugesan and Rajagopal (2006). However, the increase in the encasement (concrete in this case) of the stone column beyond 3.2D lead to a decrease in performance rather than the constant performance predicted by Murugesan and Rajagopal (2006).

It was observed that the maximum bearing capacity obtained was between S2 and S3 column (which had a length of encasement of length 3D and 2D respectively), regardless of the grade of concrete. Interestingly, for all tested grade of concrete in this configuration, the hybrid stone columns performed better than the full concrete column, SC5.

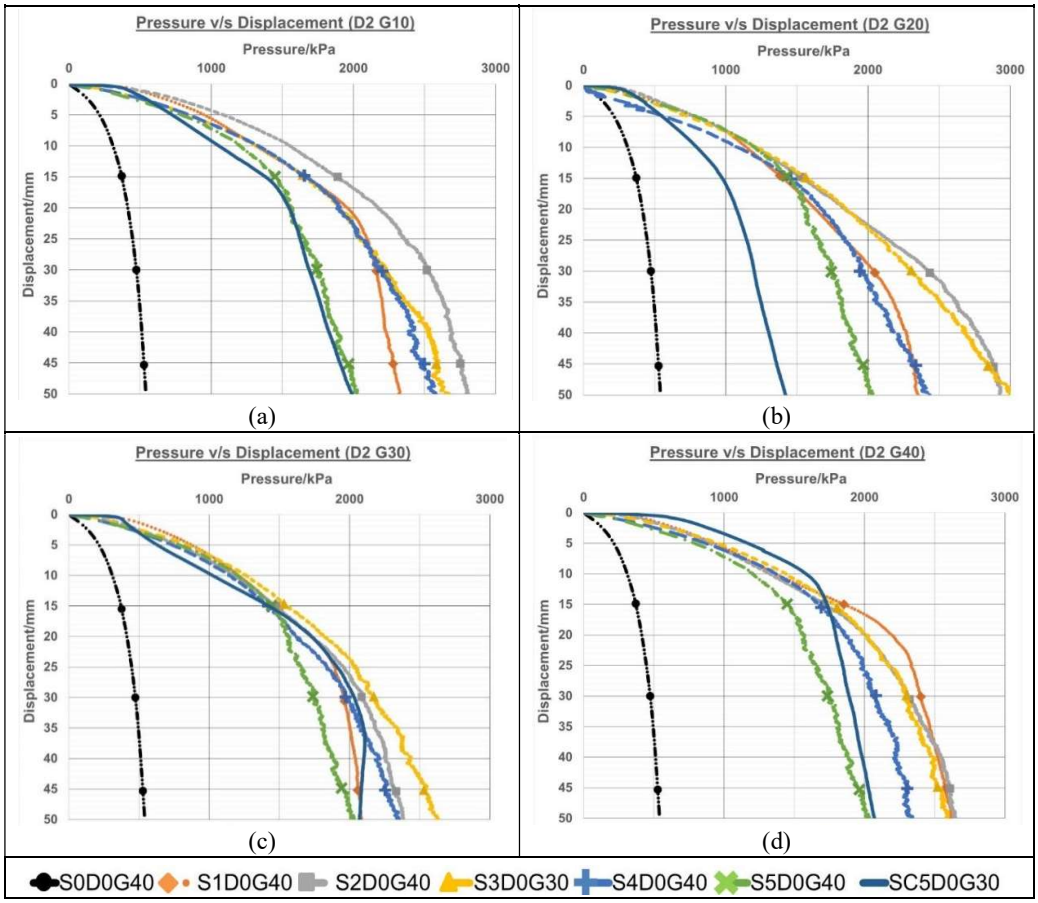

Figure 5-4: Performance of stone columns in D2 configurations for different grades of concrete.

5.2.4 Model D3

Likewise, the performance of the columns for the D3 configurations, from Figure 5-5, is comparable to that obtained from the D2 configuration. In most cases, the full concrete plug (SC5) exhibited the least bearing capacity compared to the other columns (except S5). It was observed that the optimum performance was in between S2 and S3 columns as well. Even in this case, increasing the grade of concrete did not bring any additional increase in performance.

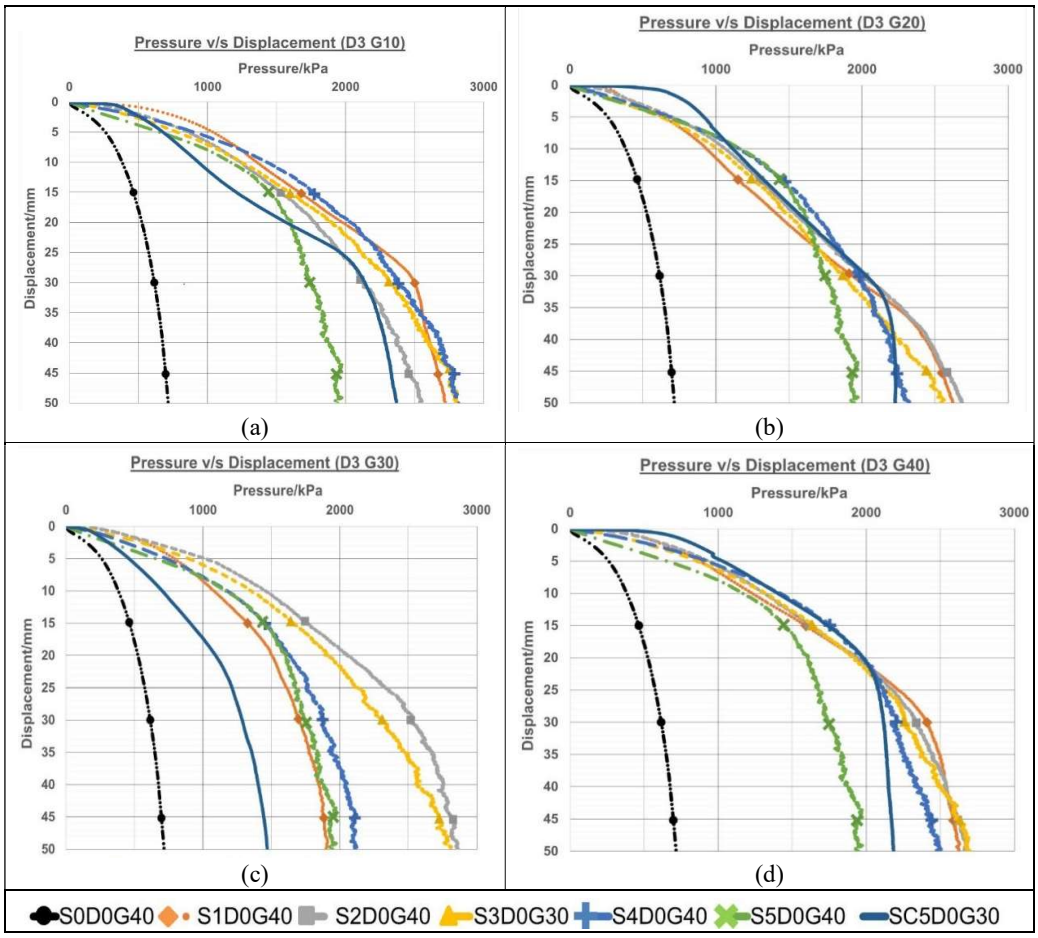

Figure 5-5 Performance of stone columns in D3 configurations for different grades of concrete.

5.3 Improvement factor brought by stone columns

The results obtained for the different configurations from Figure 5-1, Figure 5-2, Figure 5-4 and Figure 5-5 were further analysed and represented in terms of their load carrying capacity (Load improvement ratio) with respect to the unreinforced soil. The Load improvement ratio (LR) gave an estimate of the extra load that the individual column could carry with respect to the unreinforced soil. It was defined as follows:

$$Load\ improvement\ Ratio\ (LR) = \frac{load\ carried\ by\ stone\ column}{load\ carried\ by\ soft\ soil\ only}, \quad for\ same\ settlement$$

The load improvement factor depends on the behaviour of the individual columns. However, although the results were accurate, it was not precise. This means that repeated experiment yielded roughly, rather than exactly, the same result. This was because of two principal factors that could not be controlled as precisely as possible, namely:

i. The arrangement of the stone column aggregates.

The stone column aggregates were not of uniform size as they were made from a careful selection of aggregates within a specific size distribution, as elaborated in section 4.2.2. Hence, there could have been a slight difference in their packing arrangement which eventually may have had an effect on the column response to the applied load.

ii. The exact moisture content of the soil.

Necessary measures were taken in meticulously preparing the soil at a moisture content of 20%, which was determined from section 4.3. However, it was seen that the samples were not always at 20% moisture content. They rather had a standard deviation of ±0.34 and a mean of 19.68% moisture content. From the previous experiment, Figure 4-8, it has been shown that the moisture content of the soil affected its CBR value. Hence it is believed that this small fluctuation in moisture content must have had an influence on its bearing capacity as well. Details about the moisture contents for each tested specimen are attached in Appendix F.

The results of the improvement factor for the different configurations (D0, D1, D2 and D3) are shown in Table 5-1, Table 5-2, Table 5-3 and Table 5-4 respectively. It is noted from these tables that there are some load improvement factors that were undetermined. This was because the respective experiment had to be stopped at these points to prevent damage to the concrete plug, as per BS 1881-121 (1983) which has been elaborated in section 4.8. Enlarged tables of the load improvement factor are attached in Appendix E.

5.3.1 Model D0

From the load improvement factors of Model D0, as shown in Table 5-1, it is observed that the load improvement ratio (LR) increases with an increase in the length of the concrete plug. The full stone column, S5 (100% stone), yielded a maximum load improvement factor of around 3.3 while S1 (20% stone and 80% concrete) column yielded a maximum factor of around 17-folds.

Table 5-1: Load improvement ratio (LR) factor for D0 configuration.

Test series	Variable Parameter	s/D (Settlement/Diameter ratio)											Moisture Content
		2%	10%	20%	30%	40%	50%	60%	70%	80%	90%	100%	
G10D0	S1	7.1	6.3	6.9	Undetermined								19.57
	S2	4.6	4.3	4.8	4.9	4.9	4.8	4.8	Undetermined				19.68
	S3	2.0	2.8	3.3	3.4	3.5	3.6	3.6	3.7	3.8	3.8	3.8	19.76
	S4	1.3	2.2	3.0	3.2	3.3	3.3	3.3	3.4	3.5	3.5	3.5	19.66
	S5	1.7	2.4	2.8	2.8	2.8	2.7	2.8	2.7	2.7	2.7	2.8	19.52
	SC5	Undetermined											19.72
G20D0	S1	3.4	3.3	4.1	5.1	6.2	7.8	Undetermined					19.76
	S2	3.5	3.3	3.7	3.8	3.8	3.8	3.9	4.1	4.3	4.5	4.8	19.99
	S3	2.7	2.5	2.6	2.7	2.9	2.9	3.0	3.1	3.2	3.3	3.3	19.55
	S4	1.0	1.5	2.1	2.4	2.5	2.6	2.5	2.6	2.6	2.7	2.8	19.68
	S5	1.7	2.4	2.8	2.8	2.8	2.7	2.8	2.7	2.7	2.7	2.8	19.52
	SC5	Undetermined											19.42
G30D0	S1	7.5	7.4	8.2	8.8	9.5	11.2	14.4	Undetermined				19.52
	S2	3.9	4.4	5.2	5.8	6.1	6.2	6.3	6.4	6.7	6.9	7.4	18.65
	S3	2.0	2.9	3.6	3.9	4.2	4.2	4.1	4.2	4.2	4.2	4.2	19.38
	S4	2.4	2.7	3.2	3.5	3.6	3.5	3.6	3.6	3.6	3.7	3.5	19.50
	S5	1.8	2.7	3.2	3.3	3.2	3.1	3.1	3.0	3.0	2.9	3.1	19.89
	SC5	Undetermined											19.43
G40D0	S1	3.9	4.2	5.4	6.8	8.4	11.2	17.0	Undetermined				20.02
	S2	4.8	4.9	4.9	4.8	4.7	4.5	4.5	4.6	4.6	4.7	4.9	19.52
	S3	3.4	3.3	3.5	3.5	3.6	3.5	3.5	3.6	3.6	3.6	3.6	20.00
	S4	1.6	2.6	3.1	3.3	3.3	3.4	3.4	3.4	3.4	3.4	3.4	19.84
	S5	2.4	2.8	3.1	3.1	3.0	3.0	3.1	3.1	3.1	3.1	3.2	19.52
	SC5	Undetermined											19.27

5.3.2 Model D1

From Table 5-2, it was seen that the improvement factors obtained for the column S2, S1 and SC5 are very different from that obtained for the D0 configurations. The maximum LR for the S5 column, in this case, was around 3.5 while there was a considerable drop in the values for S1 column compared to the results obtained in Table 5-1. For small settlements of less than 35mm (s/D < 70%) the column S1 was among the columns having the best performance with an average load improvement ratio of 5.

For larger displacement, greater than 35mm, the performance of the SC5 column increased drastically yielding a maximum improvement ratio of 9.6. As explained in section 5.2.2, this sudden increase in performance was due to the layer of soil beneath the column being compressed up to a point where it was stiff enough to transfer the applied load directly to the load supporting layer (the base of the mould in this case).

Table 5-2: Load improvement ratio (LR) factor for D1 configuration.

Test series	Variable Parameter	s/D (Settlement/Diameter ratio)											Moisture Content
		2%	10%	20%	30%	40%	50%	60%	70%	80%	90%	100%	
G10D1	S1	5.6	4.2	3.9	4.0	3.9	3.8	3.8	3.8	3.9	4.0	4.1	19.46
	S2	3.4	3.4	3.6	3.9	4.1	4.1	4.0	4.0	4.0	3.9	3.9	18.83
	S3	2.6	3.0	3.4	3.6	3.9	3.9	3.9	3.9	4.0	4.1	4.1	19.29
	S4	2.1	2.5	3.0	3.3	3.4	3.5	3.5	3.6	3.7	3.8	3.7	19.10
	S5	1.9	2.8	3.3	3.5	3.4	3.4	3.4	3.4	3.4	3.5	3.5	19.38
	SC5	4.4	3.4	3.4	3.6	3.6	3.6	3.6	3.9	4.9	Undetermined		19.29
G20D1	S1	3.8	4.2	4.9	5.4	5.8	6.3	6.7	6.9	7.0	7.0	7.1	19.73
	S2	3.8	3.6	4.1	4.6	5.1	5.4	5.7	5.9	6.1	6.2	6.4	19.69
	S3	3.3	3.6	4.0	4.2	4.5	4.7	5.0	5.1	5.4	5.6	5.8	19.76
	S4	0.9	2.4	3.3	3.6	3.8	3.9	4.0	4.2	4.4	4.5	4.6	19.15
	S5	1.9	2.8	3.3	3.5	3.4	3.4	3.4	3.4	3.4	3.5	3.5	19.38
	SC5	1.2	1.3	1.9	2.2	2.2	2.2	2.2	2.5	3.6	Undetermined		19.45
G30D1	S1	4.8	4.3	4.4	4.5	4.7	4.8	4.9	5.0	5.0	5.1	5.1	19.93
	S2	3.1	3.0	3.3	3.6	3.9	4.2	4.3	4.3	4.3	4.3	4.3	19.36
	S3	2.7	2.9	3.3	3.5	3.6	3.6	3.8	3.9	4.0	4.0	3.9	19.69
	S4	2.6	2.8	3.2	3.3	3.3	3.3	3.3	3.3	3.3	3.3	3.3	19.90
	S5	1.9	2.8	3.3	3.5	3.4	3.4	3.4	3.4	3.4	3.5	3.5	19.56
	SC5	2.5	2.5	2.9	3.2	3.5	3.8	4.0	4.3	5.0	9.6	Undetermined	18.72
G40D1	S1	5.3	4.2	4.2	4.3	4.4	4.4	4.4	4.3	4.3	4.4	4.4	19.74
	S2	4.3	3.9	4.0	4.2	4.3	4.3	4.2	4.2	4.2	4.2	4.2	19.87
	S3	3.2	3.2	3.4	3.6	3.7	3.8	3.7	3.7	3.5	3.5	3.4	19.81
	S4	2.6	2.9	3.4	3.5	3.4	3.4	3.3	3.2	3.2	3.1	3.0	19.44
	S5	2.6	3.1	3.3	3.2	3.2	3.0	3.0	2.9	2.9	2.9	2.9	19.80
	SC5	7.9	6.0	5.4	4.7	4.3	4.2	4.3	5.0	9.3	Undetermined		19.80

5.3.3 Model D2 and D3

For the D2 configuration, the columns S2 and S3 brought the maximum load improvement ratio. At a maximum displacement of 50 mm, they both had an average load ratio 5. The full concrete column generally showed the least performance compared to the other columns (S1, S2, S3 and S4). Table 5-3 shows the load improvement ratio of the D2 configuration.

Likewise, the column S2 and S3 showed the maximum performance for configuration D3. However, their improvement ratio was slightly less compared to the D2 configuration with an average of around 3.8 for each of them. Table 5-4 shows the load improvement ratio for the D3 configuration.

Table 5-3: Load Improvement (LR) factor for D2 configuration.

Test series	Variable Parameter	s/D (Settlement/Diameter ratio)											Moisture Content
		2%	10%	20%	30%	40%	50%	60%	70%	80%	90%	100%	
G10D2	S1	5.5	4.4	4.3	4.5	4.7	4.7	4.6	4.4	4.4	4.3	4.3	19.51
	S2	6.2	5.1	5.0	5.1	5.3	5.3	5.3	5.3	5.3	5.2	5.2	19.46
	S3	3.9	3.9	4.2	4.5	4.6	4.6	4.7	4.8	4.9	4.9	4.9	19.20
	S4	4.0	3.9	4.3	4.5	4.6	4.6	4.6	4.7	4.7	4.7	4.8	19.01
	S5	3.4	3.7	3.9	3.9	3.8	3.7	3.7	3.7	3.7	3.7	3.8	19.66
	SC5	4.5	3.4	3.4	3.7	3.7	3.6	3.6	3.6	3.6	3.6	3.7	19.49
G20D2	S1	3.9	3.7	3.7	3.8	3.9	4.1	4.3	4.4	4.4	4.4	4.3	19.88
	S2	4.2	3.6	3.9	4.2	4.4	4.8	5.1	5.3	5.4	5.5	5.4	19.85
	S3	3.2	3.4	3.9	4.2	4.5	4.7	4.9	5.1	5.3	5.4	5.6	19.72
	S4	1.6	2.6	3.5	3.9	4.1	4.1	4.1	4.2	4.3	4.4	4.5	19.45
	S5	3.4	3.7	3.9	3.9	3.8	3.7	3.7	3.7	3.7	3.7	3.8	19.66
	SC5	3.4	2.6	2.6	2.6	2.6	2.6	2.5	2.5	2.8	2.6	2.6	20.55
G30D2	S1	5.2	4.1	3.9	4.0	4.2	4.2	4.1	4.0	4.0	3.9	3.9	20.52
	S2	3.9	3.6	3.8	4.0	4.2	4.4	4.4	4.4	4.4	4.4	4.4	19.96
	S3	3.8	3.9	4.1	4.2	4.4	4.6	4.6	4.7	4.7	4.8	4.9	19.93
	S4	3.4	3.4	3.7	3.8	3.9	4.1	4.2	4.2	4.3	4.3	4.4	20.17
	S5	3.4	3.7	3.9	3.9	3.8	3.7	3.7	3.7	3.7	3.7	3.8	19.91
	SC5	3.9	2.9	3.3	3.8	4.2	4.3	4.3	4.2	4.1	4.0	3.8	20.08
G40D2	S1	5.3	4.3	4.4	5.0	5.3	5.2	5.1	5.0	4.9	4.9	4.8	19.90
	S2	5.0	4.2	4.3	4.6	4.9	4.9	4.9	4.9	5.0	4.9	4.9	19.76
	S3	4.8	4.5	4.7	4.8	4.9	4.9	4.8	4.8	4.9	4.8	4.8	19.97
	S4	3.9	4.0	4.4	4.5	4.5	4.5	4.4	4.4	4.3	4.4	4.3	19.99
	S5	3.4	3.7	3.9	3.9	3.8	3.7	3.7	3.7	3.7	3.7	3.8	20.12
	SC5	7.4	5.4	5.1	4.7	4.3	4.1	4.0	3.9	3.9	3.8	3.8	19.54

Table 5-4: Load Improvement (LR) factor for D3 configuration.

Test series	Variable Parameter	s/D (Settlement/Diameter ratio)											Moisture Content
		2%	10%	20%	30%	40%	50%	60%	70%	80%	90%	100%	
G10D3	S1	6.1	4.0	3.6	3.6	3.8	4.0	4.1	3.9	3.9	3.8	3.8	19.30
	S2	4.3	3.3	3.3	3.3	3.4	3.4	3.5	3.5	3.5	3.5	3.6	19.93
	S3	3.4	3.0	3.3	3.4	3.6	3.7	3.8	3.8	3.8	4.0	3.9	19.45
	S4	3.7	3.5	3.8	3.8	3.9	3.9	3.8	3.9	4.0	4.0	3.9	19.70
	S5	2.1	2.5	3.1	3.1	3.0	2.9	2.8	2.8	2.8	2.8	2.7	19.79
	SC5	4.1	2.6	2.4	2.6	3.0	3.4	3.5	3.4	3.4	3.3	3.3	19.68
G20D3	S1	3.2	2.5	2.4	2.5	2.7	2.9	3.1	3.4	3.6	3.7	3.7	19.67
	S2	3.2	2.7	2.8	2.8	2.9	3.1	3.3	3.5	3.6	3.7	3.8	19.48
	S3	2.3	2.4	2.6	2.7	2.8	2.9	3.0	3.2	3.3	3.5	3.5	19.51
	S4	2.5	2.7	3.0	3.2	3.2	3.2	3.2	3.2	3.2	3.2	3.3	19.38
	S5	2.1	2.5	3.0	3.1	3.1	2.9	2.8	2.8	2.8	2.8	2.7	19.79
	SC5	6.4	3.5	2.9	2.9	3.0	3.1	3.3	3.4	3.3	3.2	3.1	19.99
G30D3	S1	4.4	3.0	2.8	2.9	2.9	2.8	2.8	2.7	2.7	2.7	2.7	19.96
	S2	4.7	3.9	3.8	3.8	3.9	4.1	4.1	4.1	4.1	4.0	4.0	19.67
	S3	3.9	3.4	3.5	3.6	3.6	3.7	3.8	3.8	3.8	3.9	3.9	19.71
	S4	3.1	2.8	3.1	3.1	3.1	3.0	3.1	3.0	3.0	3.0	2.9	20.25
	S5	2.1	2.5	3.1	3.1	3.0	2.9	2.8	2.8	2.8	2.8	2.7	19.81
	SC5	2.3	1.8	1.8	2.0	2.1	2.1	2.1	2.1	2.1	2.1	2.1	20.31
G40D3	S1	4.9	3.4	3.2	3.4	3.7	3.9	3.9	3.8	3.8	3.7	3.7	20.09
	S2	5.0	3.6	3.4	3.5	3.7	3.8	3.8	3.8	3.7	3.8	3.7	19.75
	S3	4.0	3.3	3.5	3.6	3.6	3.7	3.7	3.7	3.7	3.7	3.8	20.25
	S4	4.0	3.5	3.7	3.8	3.8	3.7	3.6	3.5	3.5	3.5	3.5	20.13
	S5	2.1	2.5	3.0	3.1	3.0	2.9	2.8	2.8	2.8	2.8	2.7	19.60
	SC5	6.8	4.0	3.7	3.7	3.8	3.6	3.4	3.3	3.2	3.1	3.1	19.30

5.4 Bulging

The performance of these hybrid stone columns can be related to the way they behaved under the applied loading. This was determined through physical modelling as explained in section 4.10. Bulging is the main load transfer mechanism of a stone column unless it is very short (Mani and Nigee, 2013). However, if there is excessive bulging, unwanted/differential settlement may arise which may lead to cracking or instability of a structure. Henceforth, they are normally confined by geogrid/geotextile to control bulging. Gniel and Bouazza (2009) and Hong *et al.* (2015) observed that increasing the stiffness of a geotextile encasement forces the bulging to occur at a deeper depth within the stone column. Comparable results were obtained in this study when part of the stone column was replaced with concrete as shown in Figure 5-6.

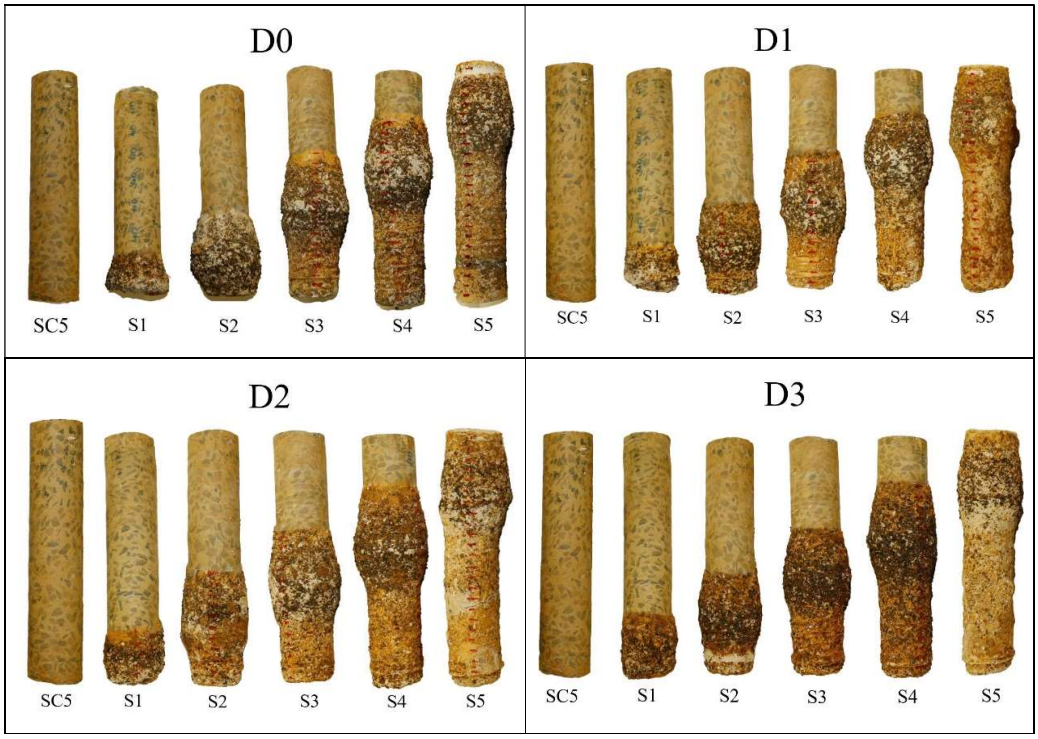

Figure 5-6: Position of bulging for the different tested column in different configurations.

From physical modelling using plaster of Paris, shown in Figure 5-6, it was seen that full bulging occurred for S2 to S5 column only. From the results, summarised in Table 5-5, it was observed that full bulging ranged from 2 to 2.4D. It was also noted that as

the bulging is forced into a deeper level of the soil, there was a slight decrease in its length.

Table 5-5: Bulging length with respected to different stone column arrangements in terms of its diameter (D).

	D0	D1	D2	D3	Average Bulging length
SC5	0	0	0	0	0.00
S1	1	1	1	1	1.00
S2	2	2	2	2	2.00
S3	2.06	2.12	2.18	2	2.09
S4	2.2	2	2.34	2.2	2.19
S5	2.16	2.4	2.16	2.2	2.23

Changing the configuration, from D0 to D3, in which a specific column was tested did not have a definite trend on the length of bulging, as shown in Table 5-5 and Figure 5-6. For example, the bulging length for the S2 column was constant whereas that of the S3 column showed slight variation throughout. The concrete plug behaved as a reinforcement, it replaced the region where the stone column was to bulge and it transferred the loading to a deeper level within the column. As a result, when the length of the concrete plug was increased, bulging occurred further away from the surface of the soil.

An element deeper into the ground will experience a greater confining force. This may explain why the column S2 and S3 had a higher performance than the S4 and S5 column despite having roughly the same bulging length. Moreover, when the length of concrete was increased, less side friction was developed by the hybrid stone column due to the concrete's smoother surface compared to the stone aggregates. Hence, the column with increasing length of the concrete plug had a higher penetration into the ground, as shown in Figure 5-7, and the mode of failure gradually changed from bulging to punching failure. The diameters of the columns and their relative displacement were measured as described in section 4.10.

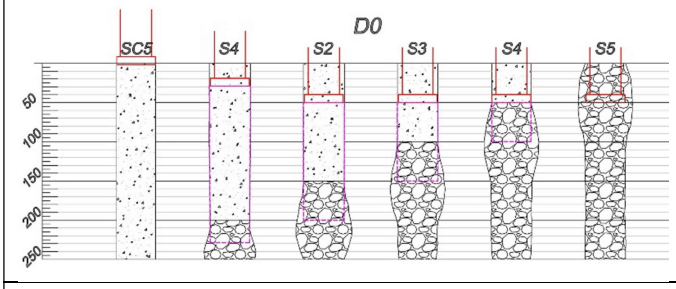

D0:

The columns were in full contact with the base of the mould prior to testing

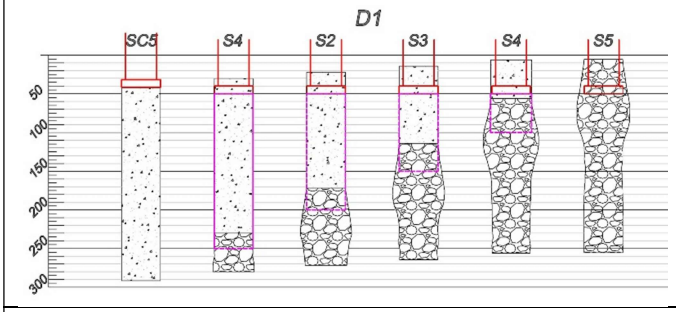

D1:

The columns were at a distance of D (50mm) from the base of the mould prior to testing

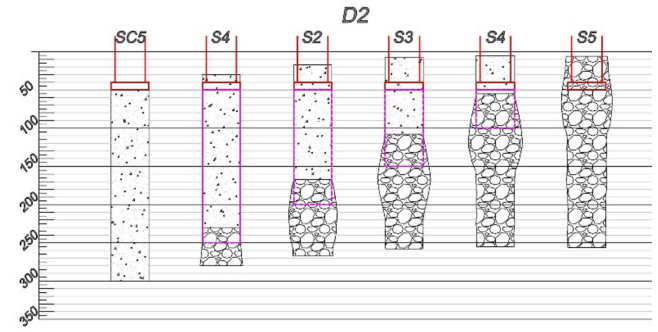

D2:

The columns were at a distance of 2 x D (100mm) from the base of the mould prior to testing

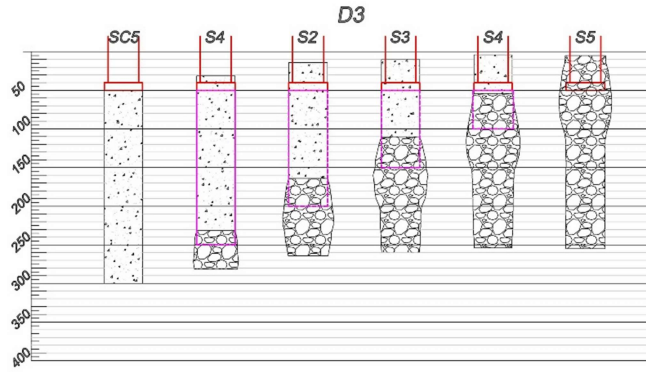

D3:

The columns were at a distance of 3 x D (150mm) from the base of the mould prior to testing

Figure 5-7: Diagrammatic representation of stone column after testing and modelling.

5.5 The optimum stone column

When the stone column was in contact with a hard stratum or within 50mm (50mm is the diameter, D, of the stone column) from the base of the mould (for D1 configuration), increasing the length of the concrete increased the bearing capacity of the column. However, for the D1 configuration, the behaviour of the full concrete column (SC5) changed drastically compared to that in the D0 configuration. It suffered from considerable settlements when subjected to loading condition but this improved substantially after around 35mm penetration as seen from Figure 5-7. Hence, using a full concrete column is only suitable when the load is transferred directly onto a load-bearing stratum. Otherwise, it is advisable to use a combination of stone and concrete column for better performance.

It was noted that when there was a soil layer having a thickness greater than D (D: Diameter of the stone column) beneath the columns, their performance was different to previously tested conditions (D0 and D1). For the D2 and D3 configuration, it was observed that the hybrid stone columns S2 and S3 brought the maximum increase in the load improvement factor. However, it can be argued that the optimum hybrid stone column was a combination that consisted of 40% concrete and 60% stone column (namely S3 column, as shown in Figure 5-8).

Figure 5-8: S3 column.

In addition, it is economically better to construct the S3 column rather than the S2 column because it uses 20% less concrete. From the results elaborated in Table 5-3 and Table 5-4, it was found that an improvement factor ranging from 3.5 to 5.6 can be achieved by the S3 column in such case.

5.6 Grade of concrete

When the effects of the different grades of concrete (for S2 and S3 column) were compared to each other, it was found that there is no distinctive correlation between the strength of the concrete and the improvement factor of the column as shown in Table 5-6.

Table 5-6: Improvement factor of S2 and S3 column in D3 configuration for different grades of concrete.

Grade of concrete	Stone column	s/D (Settlement/Diameter ratio)											Moisture content
		2%	10%	20%	30%	40%	50%	60%	70%	80%	90%	100%	
10	**S3**	3.4	3.0	3.3	3.4	3.6	3.7	3.8	3.8	3.8	4.0	3.9	19.45
20	**S3**	2.3	2.4	2.6	2.7	2.8	2.9	3.0	3.2	3.3	3.5	3.5	19.51
30	**S3**	3.9	3.4	3.5	3.6	3.6	3.7	3.8	3.8	3.8	3.9	3.9	19.71
40	**S3**	4.0	3.3	3.5	3.6	3.6	3.7	3.7	3.7	3.7	3.7	3.8	20.25
10	**S2**	4.3	3.3	3.3	3.3	3.4	3.4	3.5	3.5	3.5	3.5	3.6	19.93
20	**S2**	3.2	2.7	2.8	2.8	2.9	3.1	3.3	3.5	3.6	3.7	3.8	19.48
30	**S2**	4.7	3.9	3.8	3.8	3.9	4.1	4.1	4.1	4.1	4.0	4.0	19.67
40	**S2**	5.0	3.6	3.4	3.5	3.7	3.8	3.8	3.8	3.7	3.8	3.7	19.75

Figure 5-9 and Figure 5-10 shows a graphical representation of the improvement factor for S2 and S3 column respectively with respect to the different settlements and grades of concrete. It was observed that increasing the grade of concrete did not necessarily bring an additional increase in bearing capacity. The details of the compressive tests on the different grades of concrete are attached in Appendix A.1.7. The Grade 10 (compressive strength of 17.29MPa) can be said to be having the same performance as Grade 40 (compressive strength of 52,15Mpa).

Taking the above observation into consideration, it can be deducted that low strength concrete may be promoted for use in such hybrid stone column because of its better economic advantages. In addition, the concrete mix may be combined with other waste materials to promote sustainable development provided that the resulting concrete plug maintains its integrity.

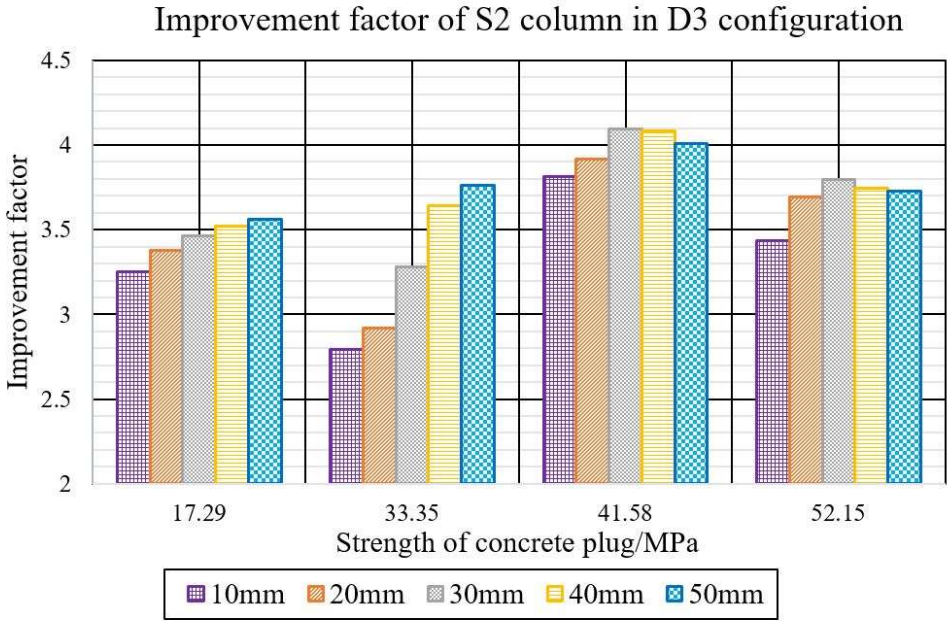

Figure 5-9: Improvement factor for different settlements of the S2 column with regards to various grades of concrete.

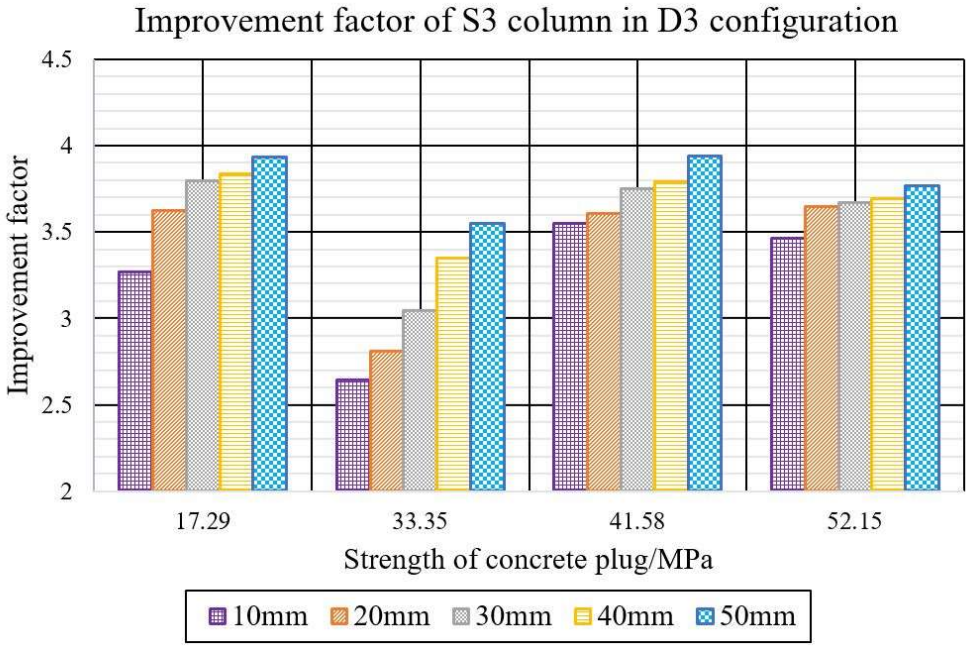

Figure 5-10: Improvement factor for different to settlements of the S3 column with regards to various grades of concrete.

5.7 Geosynthetic- reinforced bedding layer

This section compares the behaviour of an unreinforced/reinforced bedding layer over the compacted soil S0 (with no additional reinforcement), the S5 (100% stone) column and the S3 (40% concrete, 60% stone) column respectively. The results have been divided into three different subsections to address the findings.

5.7.1 Soil layer, S0

It was observed from Figure 5-11 that the performance of the soil, S0, increased when an unreinforced bedding layer was placed on top. This was further improved when the layer was reinforced with a geocomposite. It was noted that after 25mm settlement, its performance outweighed that brought by the S5 column.

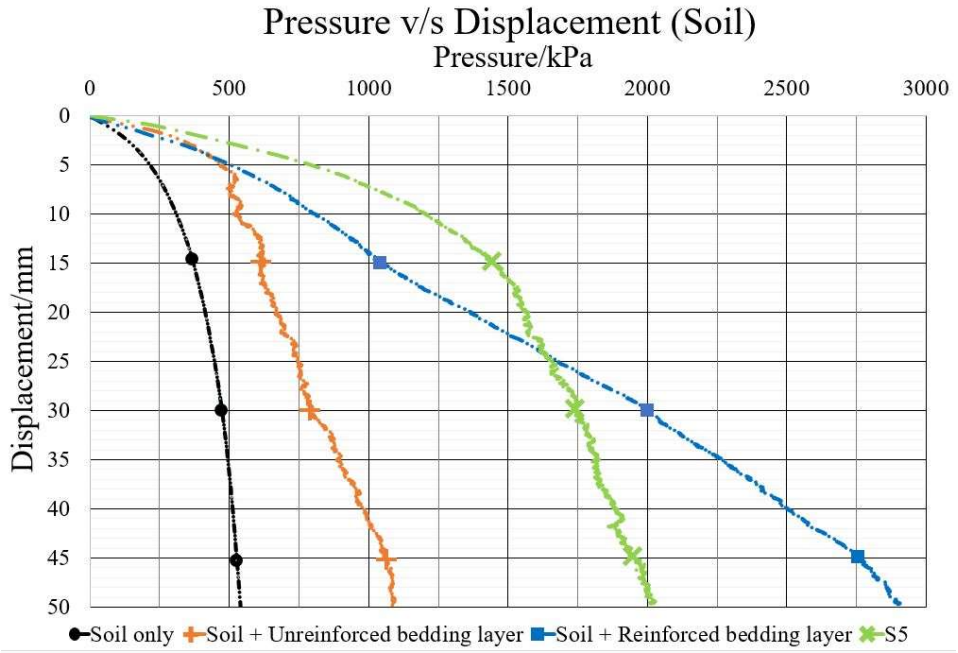

Figure 5-11: Performance of Soil with bedding layer and geocomposite.

5.7.2 S5 Column

Figure 5-12 shows the results obtained when the S5 column was tested with a reinforced/unreinforced bedding layer. It was observed that the performance obtained by the overlying unreinforced bedding layer was not in accordance to that reported in the literature review. The unreinforced bedding layer led to a decrease in performance

rather than the predicted increase when compared to results obtained from the compacted soil only (Figure 5-11). Since the material of the bedding layer was not confined (such as in case of a geocell), they could easily move sideways due to the loose interactions between the particles (as shown in Figure 5-13). This sliding may have led to the abnormalities in the graph as shown in Figure 5-12.

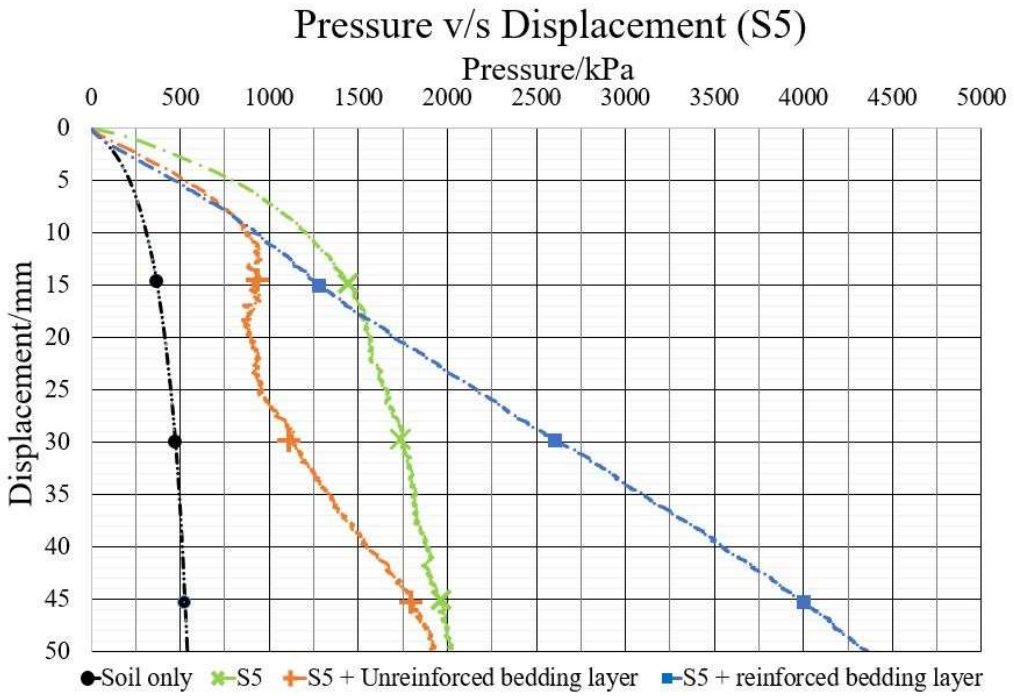

Figure 5-12: Performance of S5 stone column with bedding layer and geocomposites.

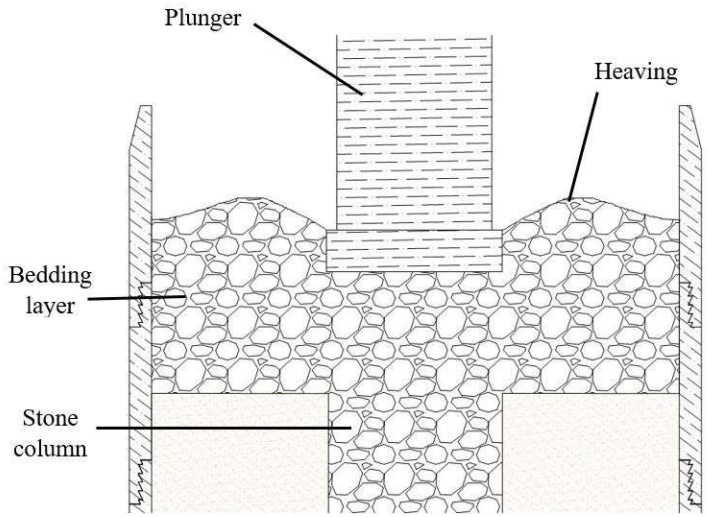

Figure 5-13: Behaviour of material within un-reinforced bedding layer during testing.

When the bedding layer was reinforced with the geocomposite, a change in behaviour was obtained. It can be seen from Figure 5-12, for the tested load range, the resulting graph was obeying Hooke's law (the force is proportional to the extension/ displacement). After around 17mm displacement, the performance of the S5 column with a reinforced bedding layer exceeded that of the S5 stone column only.

The geocomposite assisted to spread the applied load over an extended area compared to the plunger. Consequently, this led to a reduction in heaving and an increase in bearing pressure, as shown in Figure 5-14. At 50mm displacement, it was noted that the S5 column with the reinforced bedding layer carried more than twice the load of the S5 column only, (accounting to more than 700% increase in load carrying capacity compared to that of the soil layer without any reinforcement)

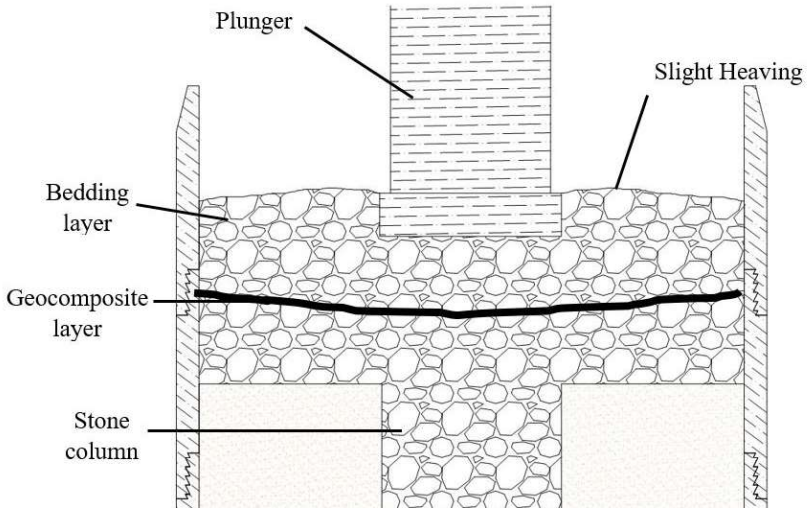

Figure 5-14: Behaviour of material within reinforced bedding layer during testing.

5.7.3 S3 Column

A similar relationship, compared to the S5 column, was obtained for the S3 stone column as shown in Figure 5-15. The bedding layer reinforced with the geocomposite brought an improvement factor of 2 folds compared to the S3 column only. With comparison to the soil layer S0 (without any reinforcement/stone column), the load improvement factor brought by the S3 column with a reinforced bedding layer was 9.9 times (nearly 900% increase) as shown in Figure 5-15.

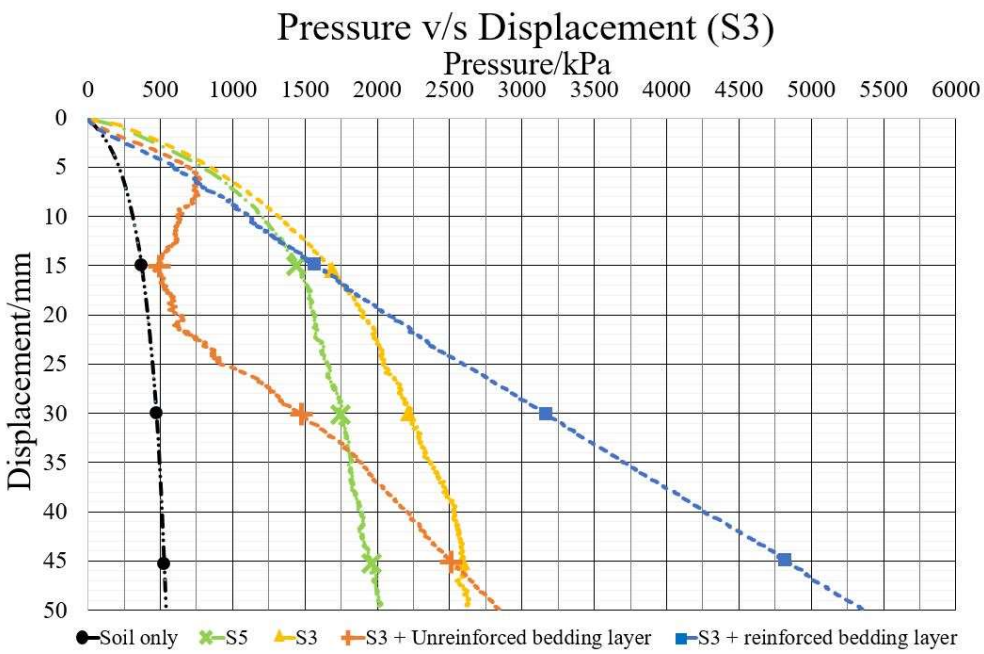

Figure 5-15: Performance of S3 column with and without reinforced/unreinforced bedding layer.

It is noted, from Figure 5-15 and Figure 5-14, that the 'S3 + Unreinforced bedding layer' graph showed a greater dip than the 'S5 + Unreinforced bedding layer' graph. As experiment proceeded, the plunger gradually penetrated the bedding layer. Consequently, the bedding's layer material (constituting of compacted stones) was gradually forced downward and sideways. It is believed that it was easier for the stones to slide over the smooth concrete surface of the S3 column rather than the rough stone surface of the S5 column. Hence, since less resistance was experienced for the S3 column, a greater reduction in performance was observed for the dip.

In this study, a single layer of geocomposite was used to reinforce the bedding layer. This brought an improvement of more than 900% (Load Improvement factor of 9.9) compared to the unreinforced soil layer. There is still a possibility to further improve the bearing capacity, if needed, by using additional layers of geosynthetic materials. Moreover, the material used for the bedding layer did not behave as expected and was not in conformity with previous studies, which stated that a bedding layer reinforces the soil. Hence, a better engineering fill material should be used for optimum performance.

Chapter 6: Application and conclusions

The findings of this research have diverse applications. For example, in problematic situations where roads may suffer from settlement due to a soft soil foundation layer (as shown in Figure 6-1), stone columns with a combination of other ground improvement techniques may be used as an engineering approach.

Figure 6-1: Possible settlement failure of Terre-Rouge-Verdun Road, Mauritius (L'express, 2015, Defimedia.info, 2016).

Stone columns and geosynthetics can be used together to increase the bearing capacity of a foundation layer. Installation of vertical drains may assist the stone column for water dissipation if it is used with a concrete plug (as shown in Figure 6-3). Otherwise, if some settlement is allowed during the construction phase, the S5 columns may be used instead of S3 columns. In such case, there will be no need to install the vertical drains. However, if these drains are installed, it will help to consolidate deeper soil layers and mitigate problems that may arise due to groundwater fluctuations.

6.1 Construction approach

The same construction approach as described in section 2.10 for Vibro concrete column and section 3.2.3 for compacted aggregate piers can be used to install the

proposed column, S3. The graded stone column aggregates can be poured and compacted until it occupies around 60% of the area of the column after which fresh concrete can be poured to fill the remaining area. The concrete should be left to cure so that the column can mobilise its required strength. Figure 6-2 shows a proposed installation technique that can be used on site.

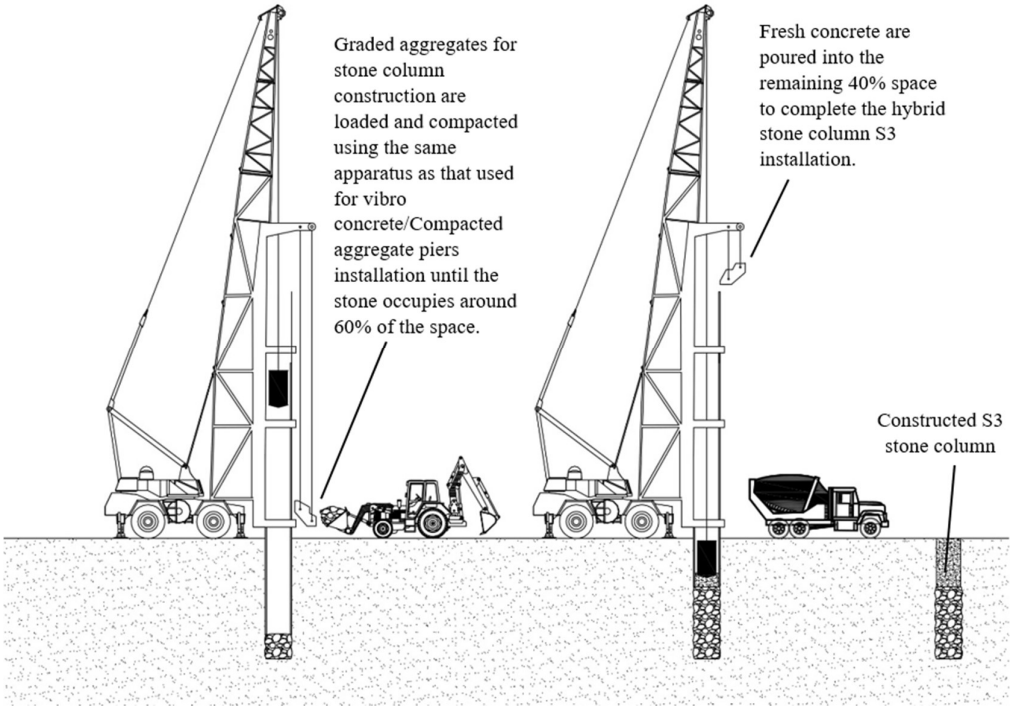

Figure 6-2: Proposed construction method for installation of S3 columns on site.

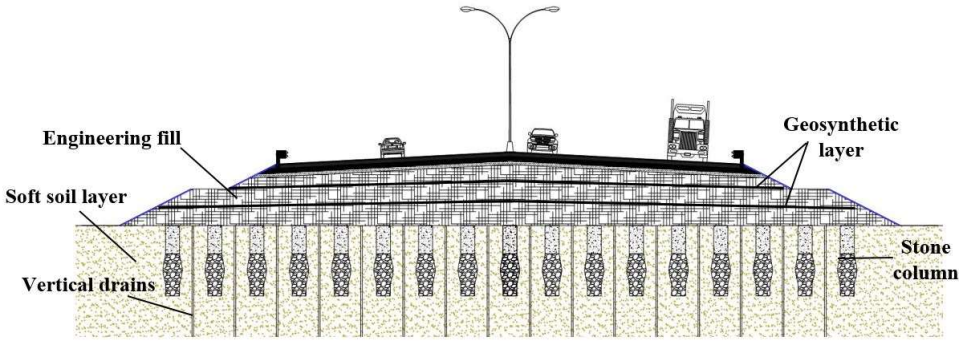

Figure 6-3: Proposal for the construction of an embankment on a soft soil foundation.

6.2 Conclusion

The specific aim and objectives set out have been met through the lab scale experiments that were done on the stone columns. The main conclusions that can be drawn from the findings elaborated in Chapter 5 and 6 are as follows:

1. Increasing the strength of the concrete plug did not have any significant improvement in the bearing capacity of the stone column. Hence, low strength concrete may be promoted for use in such applications. These concrete plugs may also be combined with other waste materials to promote sustainability if they maintain their integrity.
2. The behaviour of the stone columns was dependent on whether they were in contact with a load-bearing stratum (D0 configuration) or if there was a layer of soil beneath them (D1, D2 and D3 configuration). For applications, if the columns are in contact with a hard stratum, increasing the length of the concrete plug/section will be advantageous. If the soil layer, beneath the columns, is of considerate thickness (greater than the diameter of the columns) then it will be better to use a hybrid stone column. However, it is emphasized that field testing should be done before using them on site.
3. S3 stone column provided the optimum performance (around 200% to 500% increase in bearing capacity) when the thickness of soil beneath it was more than the dimension of its diameter.
4. The inclusion of a reinforced bedding layer on top of a stone column can increase its performance by more than 2 folds. The maximum increase in performance (around 900% increase in bearing capacity) was obtained when the optimum stone column, S3, was used in conjunction with a reinforced bedding layer.

6.3 Recommendation for further studies

This study involved experiments on a lab scale model, additional tests should be done on the field using the findings to have a comparison with regards to the results of this study. Moreover, the stone column used for testing has been scaled down accordingly but no scaling could be done for the geosynthetic layer. Although the optimum hybrid

stone column, S3, combined with a reinforced bedding layer yielded to a maximum increase of 9.9 folds in bearing compared to the soil alone for the lab testing, the final improvement should be verified on site before application.

There are several other issues that can be addressed through extended investigations to either update existing literature or to provide new data for analysis. These are:

1. Investigating how the grading of the stone columns affects its performance.
2. Studying how the optimum thickness of a bedding layer varies with materials having different properties.
3. Analysing how the length and diameter of bulging for the stone column are affected by the properties of materials by which it is surrounded.
4. Examining how the type/position of geosynthetics (Geomembrane/ Geogrid/Geocell) affects the optimum thickness of the bedding layer.
5. Using numerical modelling software to predict the behaviour of the stone column in a view for it to be used for design purposes.

A : Appendices

A.1 Concrete design

Concrete plugs to be used for the stone columns had to be designed accordingly to obtain 4 different concrete classes to be used for testing. Currently, grade C8 - C30 concrete are normally used for premix Vibro-concrete column Franki (2010). However, the approach of this research was to reinforce the stone column in the region where it normally bulges. For this scenario, different concrete grades (10, 20, 30 and 40Mpa) were used as the concrete plug and their improvement with respect to each other was studied in this case. The concrete was batch and cast in 100 × 100 × 100mm square mould to be used for assessing the strength of the respective grade and in cylindrical (300mm × 150 mm Diameter) mould to be used to extract 50 mm concrete cores.

A.1.1 Preliminary investigations on aggregates

Preliminary investigations were carried out on aggregates to determine certain factors that were necessary for developing a suitable mix design. These elements were principally the relative densities, water absorption and sieve size distributions of the aggregates.

A.1.2 Relative density

The relative density of a sample is the ratio of its density to that of water. It is a key factor for the determination of the wet density of the concrete to be used for proportioning the aggregates in a mix design. The test procedures were carried to determine the relative density of the fine aggregate (Dune sand) and the coarse crushed aggregates (Greywacke) were carried out as per ASTM C128 (2015) and ASTM C127 (2015) respectively. The average value for the relative density of the materials is shown in Table A-1.

A.1.3 Determination of water absorption

The water absorption of the sample is the ratio of an increase in mass of a Saturated Surface Dried (SSD) sample compared to its oven-dry basis. It is important to determine the water absorption of the aggregates to calculate the exact amount of water to be added to an oven dried sample for it to be to the Saturated Surface dried condition best prior to the batching process. The test procedures were carried to determine the water absorption of the fine aggregate (Dune sand) and the coarse aggregates (Greywacke) were carried out as per ASTM C128 (2015) and ASTM C127 (2015) respectively. The average value for the water absorption and relative density of the materials are shown in Table A-1 and Table A-2.

Table A-1: Shows relative density and absorbed water of the Dune sand.

Specific gravity- Dune sand			
Specimen Description		**Standard:**	ASTM C 128
Dune sand		**Method:**	-
Mass of container + SSD sample	752.7	917.7	897.9
Mass of container	256.2	324.6	452.8
Mass of SSD aggregates	496.5	593.1	445.1
Pyknometer + aggregates + water	2101.4	2160.4	2070.1
Pyknometer + water	1799.3	1797.1	1797.3
Mass of Oven dried sample	486	577.8	435.6
Relative density	2.55	2.58	2.58
Absorbed water	2.16	2.65	2.18
<Relative density>	2.57		
<Absorbed water>	2.33		

Table A-2: Relative density and absorbed water of greywacke.

Specific gravity- Greywacke (9.5mm)			
Specimen Description		**Standard:**	ASTM C 127
Greywacke		**Method:**	-
Mass of container + SSD sample	1445.1	1580.7	1464.9
Mass of container	324.6	450.9	534.6
Mass of SSD aggregates	1120.5	1129.8	930.3
Pyknometer + aggregates + water	2510.5	2520.4	2392.3
Pyknometer + water	1797.5	1797.5	1797.5
Mass of Oven dried sample	1116.4	1126.4	927.1
Relative density	2.75	2.78	2.77
Absorbed water	0.37	0.30	0.35
<Relative density>	2.77		
<Absorbed water>	0.34		

A.1.4 Calculating free water

The free water content is the amount of water added to a concrete mix with its aggregates are at the saturated surface-dry (SSD) condition. On the other hand, the absorbed water is the amount of water added to the oven dried aggregates so that they attain SSD conditions. Figure A-1 shows a diagrammatic representation of an aggregate at saturated surface dry conditions. Tests to determine the amount of water needed to attain an SSD condition from an oven dried basis was determined in accordance to ASTM C128 (2015) and ASTM C127 (2015) for fine and coarse aggregates respectively.

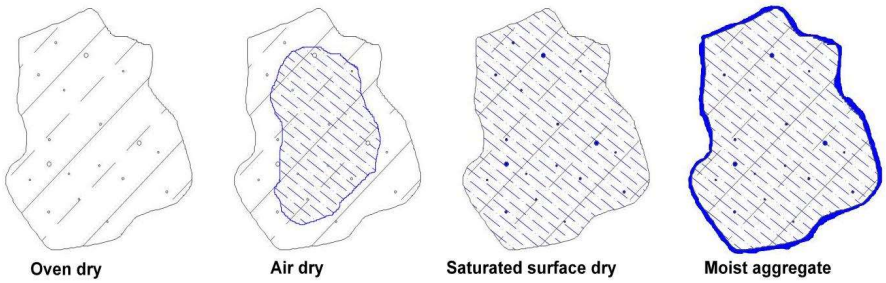

Figure A-1: Different conditions arising when aggregates are exposed to water and different drying conditions.

A.1.5 Calculating mass of cement

The grade of concrete to be designed are 10, 20, 30 and 40 MPa with a slump of 60 to 180mm. The cement was used was a CEM II cement (with fly ash) of 42.5N/mm^2 class strength. The greywacke aggregates to be used was a maximum size of 9.5mm and the sand was classified as being of good quality. Table A-3 was used to obtain the free water content of the mix and adjusted accordingly using data from Table A-4.

$$\text{Free water content} = 205 + 20 = 225\ L/m^3$$

Table A-3: Water content (L/m^3) of concrete mixes (stone 19mm, slump 75mm) (Owens, 2009).

Sand quality	Water content, ℓ/m^3	
	Natural	Crusher
Very poor	240	235
Poor	225	225
Average	210	215
Good	195	205
Excellent	180	195

Table A-4: Water content adjustment of concrete mixes for aggregates other than 19mm.(Owens, 2009).

Maximum size of stone, mm	9,5	13,2	19,0	26,5	37,5
Correction, ℓ/m^3	+20	+10	0	-10	-20

Due to the variability of concrete, it is important to design the concrete mix above the desired value (Marsh B K, 1997).

$$F_m = F_c + k(sd)$$

F_m - Target mean strength

F_s - Specified characteristic strength

sd - Standard deviation, taken as 8 for less than 20 results (Marsh B K, 1997)

k - Constant, taken as 1.64 for 5 % defective samples

Since Figure A-2 was not sufficient to determine the water/cement ratio at 53 N/mm^2, it was compared with Figure A-3. A curve at 42.5 N/mm^2 was drawn in Figure A-3 and the free water to cement ratio was estimated for each concrete grade. The values for 33 N/mm^2 and 43 N/mm^2 from Figure A-2 corresponded with a parallel curve drawn at 42.5 N/mm^2 on Figure A-3. Hence, the line drawn in Figure A-3 was used to estimate the water to cement ratio of the targeted mean strength of the different grades. Table A-5 shows the water to cement ratio and cement content for each grade.

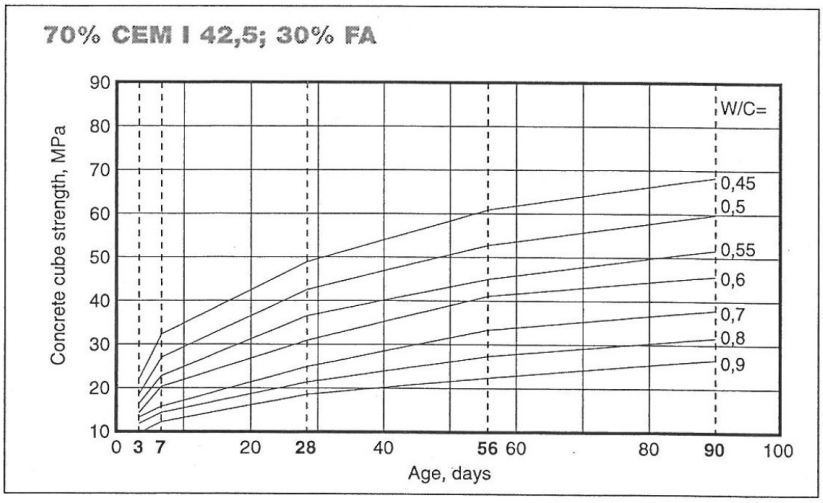

Figure A-2: Compressive strength development of CEM I 42.5; 30% FA (Cement & Concrete Institute, 1999).

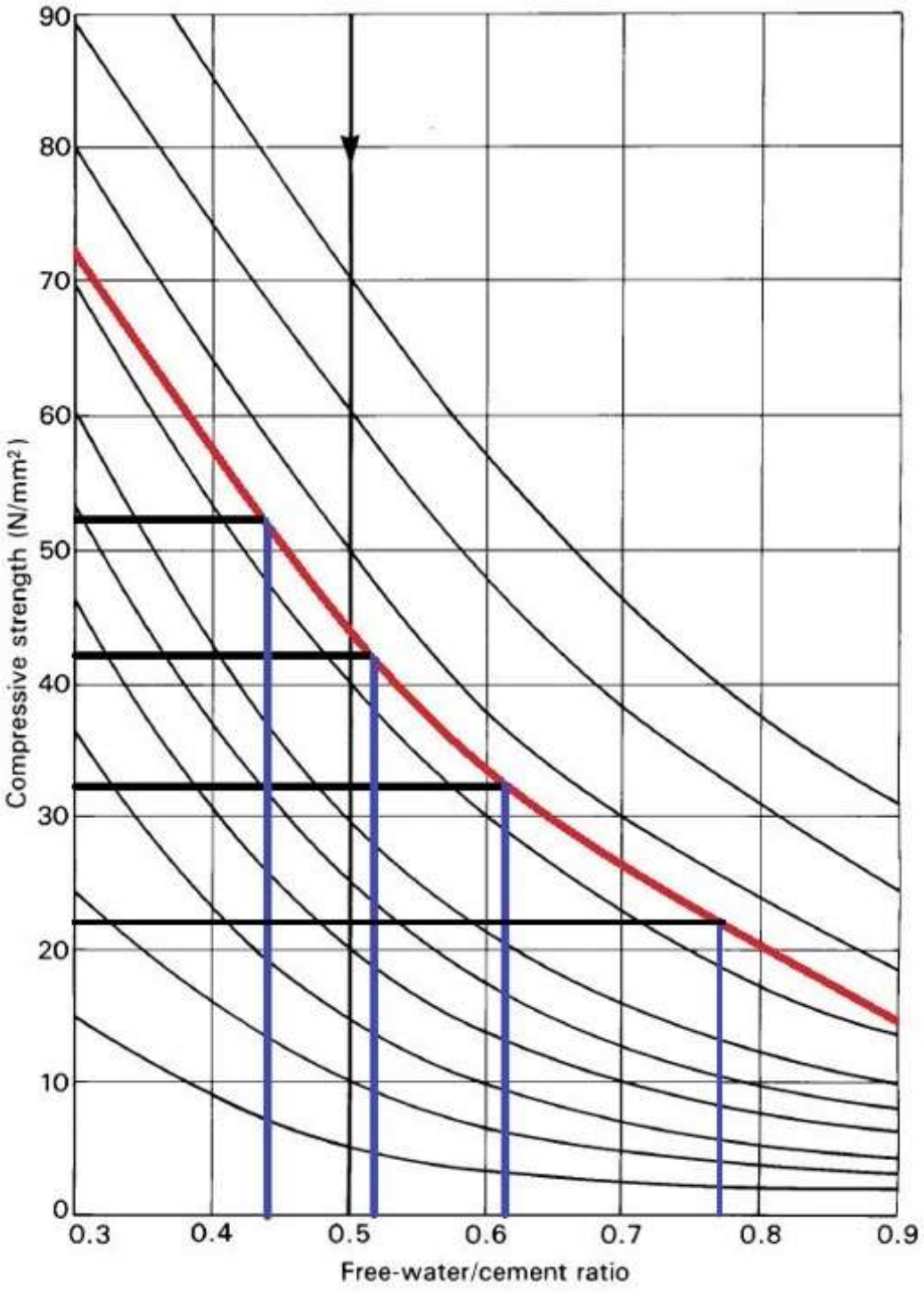

Figure A-3: Compressive strength based on the free water-cement ratio for different class strength (Adapted from Marsh B K (1997)).

Table A-5: F_m value for F_c value of 20,30 and 40N/mm^2.

F_c	k	s	F_m	W/C	Cement content (kg/m3)
10	1.64	8	23.12	0.78	288
20	1.64	8	33.12	0.61	369
30	1.64	8	43.12	0.51	441
40	1.64	8	53.12	0.44	511

A.1.6 Calculating mass of aggregates needed

The first step to determine the mass of the aggregates is to determine the wet density of the mix. The specific gravity of the coarse aggregates was determined according to ASTM C127 (2015) and was found to be 2.77 Since the free water content was 225 l/m^3, the wet density of the mix was estimated to be 2425 kg/m^3 from Figure A-4.

$$\rho_{wet} = M_{agg} + M_{water} + M_{cement}$$

ρ_{wet} - Density of concrete mix (kg/m^3)

M $_{agg}$ - Mass of aggregate in concrete mix per m^3

M $_{water}$ - Mass of water in concrete mix per m^3

M $_{cement}$ - Mass of cement in concrete mix per m^3

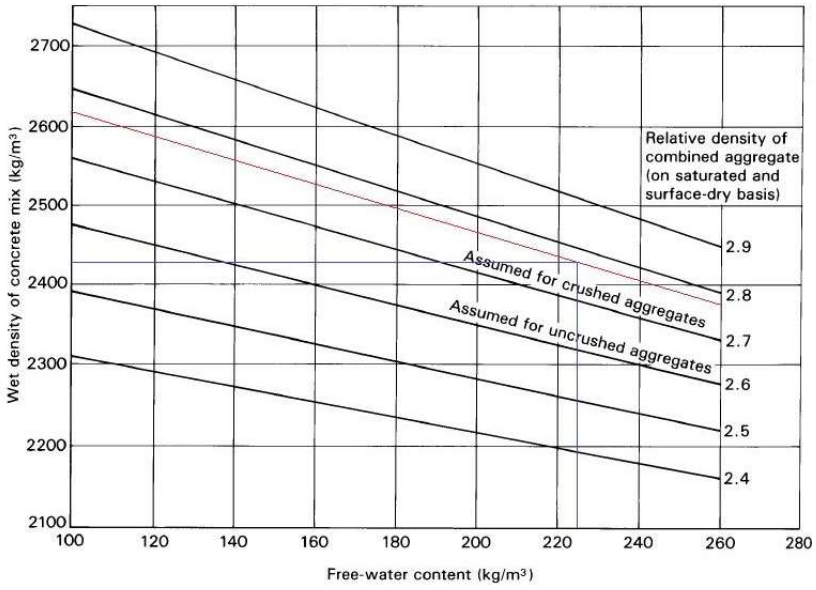

Figure A-4: Wet density of concrete mix with respect to the relative density of crushed aggregate and free water content (Adapted from Marsh B K (1997)).

Having obtained the total mass of aggregates, the next step is to find the proportion of fine aggregates of each respective mix. This was determined using Figure A-5. The proportions of the materials used for the grades have been summarised in Table A-6.

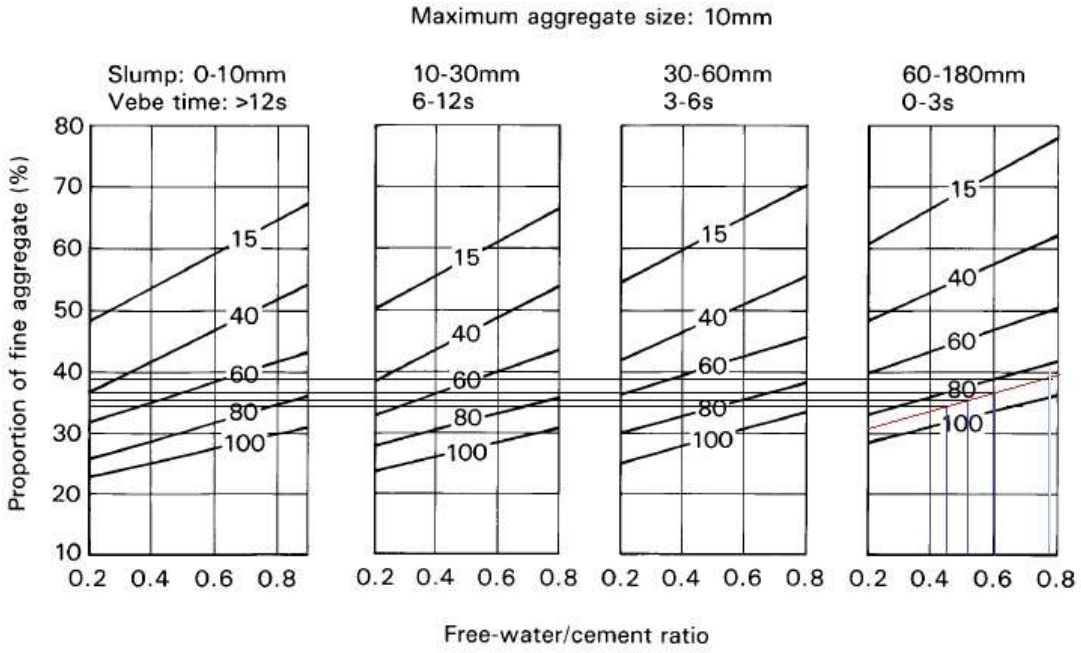

Figure A-5: Proportion of fine aggregates of the concrete mix w.r.t free water/cement ratio (Marsh B K, 1997).

Table A-6: Summary of concrete mix for different grades of concrete.

Grade of concrete	C10	C20	C30	C40
Cement	288	369	441	511
Total mass of aggregate	1912	1831	1750	1689
% of fine aggregate	39	37	35	34
Mass of fine aggregate	746	678	613	574
Mass of coarse aggregate	1166	1154	1138	1115
Absorbed water (L)	21.3462	19.721	18.1521	17.1652
Free water	224.64	228.78	229.32	224.84

A.1.7 Compressive strength

Compressive strength test, conforming to BS EN 12390-3 (2001) been performed at 28 days samples after samples were cured following BS EN 12390-2 (2000). The average dimensions and weight of each cube were measured and recorded. Excess

moisture was wiped off from the surface of the test specimens and any loose foreign materials were freed from them. The specimens were placed and centred in position with their surfaces of casting perpendicular to the direction of testing. The samples were loaded at an approximate rate of 0.5 N/mm^2 and the maximum load sustained by the samples were noted and recorded accordingly. It was observed that each cube had a normal failure, as shown in Figure A-6. The results of the tests are shown in Table A-7.

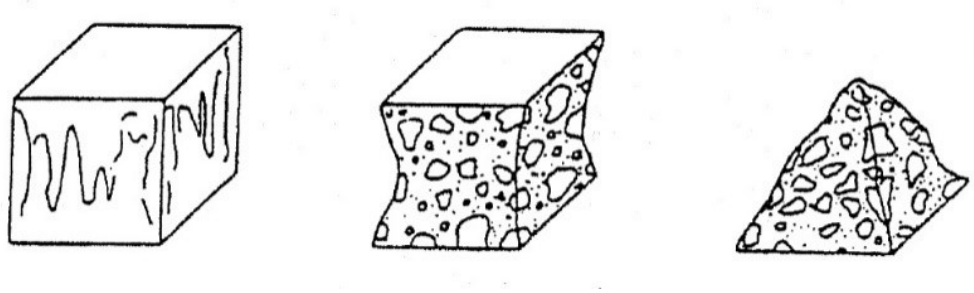

Figure A-6: Normal failure mechanisms expected for cubes in compression (BS EN 12390-3, 2001).

Table A-7: Results obtained from compression tests.

Identification	Weight of cube	Dimension of cube			Area of cube	Failure Load	Compressive strength (N/mm²)	Remarks
	(g)	(mm×	mm	×mm)	(mm²)	(kN)		
C10-A	2380	100	100	100	10000	155.00	15.50	28 days
C10-B	2367	100	100	100	10000	170.00	17.00	28 days
C10-C	2405	100	100	100	10000	163.00	16.30	28 days
C10-D	2353	100	100	100	10000	173.00	17.30	28 days
C10-E	2359	100	100	100	10000	190.00	19.00	28 days
C10-F	2385	100	100	100	10000	182.00	18.20	28 days
C10-G	2390	100	100	100	10000	165.00	16.50	28 days
C10-H	2345	100	100	100	10000	185.00	18.50	28 days
Average compressive strength							17.3	

Identification	Weight of cube	Dimension of cube			Area of cube	Failure Load	Compressive strength (N/mm²)	Remarks
	(g)	(mm×	mm	×mm)	(mm²)	(kN)		
C20-A	2376.7	100	100	100	10000	390.00	34.66	28 days
C20-B	2404.6	100	100	100	10000	370.00	32.66	28 days
C20-C	2404.1	100	100	100	10000	380.00	33.66	28 days
C20-D	2421.3	100	100	102	10000	399.00	35.56	28 days
C20-E	2382.5	100	100	98	10000	374.00	33.06	28 days
C20-F	2388.3	100	100	99	10000	392.00	34.86	28 days
C20-G	2408.8	100	100	101	10000	380.00	33.66	28 days
C20-H	2398.9	100	100	100	10000	358.00	31.46	28 days
C20-I	2380.0	100	100	100	10000	378.00	33.46	28 days
C20-J	2363.6	100	100	98	10000	348.00	30.46	28 days
Average compressive strength							33.4	

Identification	Weight of cube	Dimension of cube			Area of cube	Failure Load	Compressive strength (N/mm²)	Remarks
	(g)	(mm×	mm	×mm)	(mm²)	(kN)		
C30-A	2393.9	100	100	98	10000	470.00	42.66	28 days
C30-B	2437.1	100	100	99	10000	446.00	40.26	28 days
C30-C	2408.4	100	100	100	10000	470.00	42.66	28 days
C30-D	2420.8	100	100	101	10000	452.00	40.86	28 days
C30-E	2416.6	100	101	102	10100	442.00	39.42	28 days
C30-F	2435.7	100	101	101	10100	450.00	40.21	28 days
C30-G	2412.4	100	100	101	10000	458.00	41.46	28 days
C30-H	2439.8	100	100	101	10000	480.00	43.66	28 days
C30-I	2440.3	100	101	101	10100	470.00	42.19	28 days
C30-J	2428.9	100	101	101	10100	472.00	42.39	28 days
					Average compressive strength		41.6	

Identification	Weight of cube	Dimension of cube			Area of cube	Failure Load	Compressive strength (N/mm²)	Remarks
	(g)	(mm×	mm	×mm)	(mm²)	(kN)		
C40-A	2424.1	100	100	101	10000	540.00	49.66	28 days
C40-B	2465.1	101	101	103	10201	574.00	51.93	28 days
C40-C	2412.2	100	100	101	10000	576.00	53.26	28 days
C40-D	2434.8	100	101	101	10100	584.00	53.48	28 days
C40-E	2465.0	101	101	102	10201	582.00	52.71	28 days
C40-F	2421.3	100	100	103	10000	578.00	53.46	28 days
C40-G	2435.0	101	101	101	10201	568.00	51.34	28 days
C40-H	2431.1	101	101	102	10201	580.00	52.52	28 days
C40-I	2428.1	100	101	100	10100	582.00	53.28	28 days
C40-J	2443.3	100	100	102	10000	542.00	49.86	28 days
					Average compressive strength		52.2	

B : Compaction of clay and stone columns

B.1 Calculations- Compaction of clay

Number of joules per drop= $\frac{305}{1000} \times 24.5 = 7.47\,J$

Total number of Joules per layer= $7.47 \times 56 = 418\,J$

Volume of 1 layer = 7.26×10^{-4} m^3

Total Energy input for 1m^3 $\frac{418}{7.26 \times 10^{-4}} = 575758\,J/m^3 \sim 600kN/m^3$

A modification to the procedure was brought forward in view to minimise the preparation time while keeping the same compaction effort.

Weight of new hammer = 4532 g = 44.5 N

Height of drop = 510 mm

Number of joules per drop= $\frac{510}{1000} \times 44.5 = 22.7\,J$

Total number of Joules per layer= $22.7n\,J$

The soil would be compacted to a thickness of 50 mm per layer.

Hence, Volume of 1 layer = 9.07×10^{-4} m^3

Total Energy input for 1m^3 = $\frac{22.7\,N}{9.07 \times 10^{-4}} = 25027n\,J/m^3 \sim 25.027n\,kN/m^3$

n - Total number of drops per layer

Equating 25.027 kN/m^3 with 600 kN/m^3 gives a total of 24 drops per layer.

B.2 Calculations- Compaction of stone column materials

Mass of hammer = 2050g = 20.11 N

Height of drop = H

Drop per layer = $\boldsymbol{n}$

Diameter of stone column= 50 mm

Number of joules per drop= $\frac{H}{1000} \times 20.11 = 0.02H\ J$

Total number of Joules per layer= $0.02Hn\ J$

The stone column material would be compacted to the same thickness as the soil material, which is to a thickness of 50 mm per layer.

Hence, Volume of 1 layer = 9.82×10^{-5} m^3

Total Energy input for 1m^3 = $\frac{0.02\ Hn}{9.82 \times 10^{-5}} = 204Hn\ J/m^3 \sim 0.2\ Hn\ kN/m^3$

We have two variables (H and n), equating the total energy input for 1 m^3 to 600 kN/m^3 the following values as shown in Table B-1 is obtained.

Table B-1: Variation of the number of blows for the compaction of a stone column with respect to the height of fall.

H /mm	n (Number of blows per layer)
100	30
200	15
300	10
600	5

C : Sieve analysis of stone column materials

Table C-1: Sieve analysis of stone column materials

Sieve Analysis: Stone column materials

Sample:	Stone column aggregates
mass of sample + plate/g	1223
mass of plate/g	257
Mass of sample/ g	966

Test No:	1
Date:	19 June 2016
Tested by:	Pudaruth. Y
Standard:	ASTM D 6913
Method:	B
Oven dried sample	

Sieve size/mm	Mass of sieve/g	Mass of sieve sample/g	Mass of sample/g	% Retained	Cum % retained	Cum % passing
6.700	703.3	703.3	0.00	0.00	0.00	100.00
5.600	609.4	609.8	0.40	0.15	0.15	99.85
4.750	437.5	438.8	1.30	0.49	0.64	99.36
3.350	599.8	620.8	21.00	7.93	8.57	91.43
2.360	402.6	493.5	90.90	34.31	42.88	57.12
2.000	400.3	445.6	45.30	17.10	59.98	40.02
1.180	440.0	537.7	97.70	36.88	96.87	3.13
0.850	513.9	521.8	7.90	2.98	99.85	0.15
0.600	536.7	536.9	0.20	0.08	99.92	0.08
Pan	460.1	460.3	0.20	0.08	100.00	0.00
		Total mass	264.90	100.00		

Remarks: _____

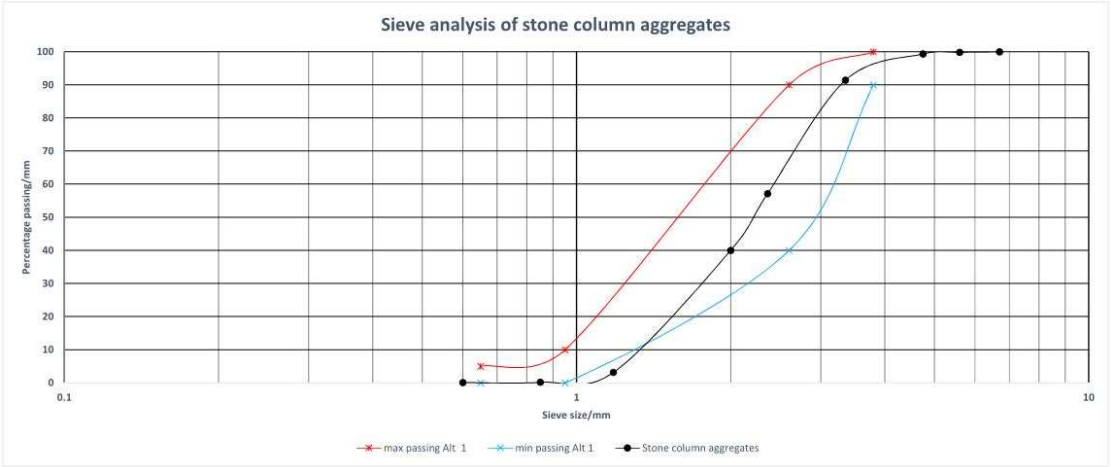

D10 passing	1.30
D30 passing	1.80
D60 Passing	2.50

Cu value	1.92
Cc value	1.00

D : Tests carried out on soil material used for testing

This section presents all the tests that were carried out to obtain the properties/characteristics of the soil that was used for testing

D.1 Atterberg limit test

Soil consists of a mixture of air, water and the soil particles themselves. The most important characteristic of clay particles is their plasticity, therefore their ability to be moulded into various shapes. This property is normally governed by the particle size of the clay particles and the water content of the soil. At a low water content, the clay particles develop a strong internal attractive force due to their charged nature. This force is termed as cohesion. The point at which there is not enough water to hold the particles together (the particles crumbles) is termed as the plastic limit. As the water content increases, more lubrication is brought in between the soil particles and the lesser will be the cohesion force. Therefore, the soil mass will tend to be more like a liquid. At this point, the soil will no longer have cohesion and will flow under its own weight and it is said that the soil has reached its liquid limit. The Atterberg limit test is used to identify the plastic and liquid limit of a specified soil. It is used to identify the nature of the particular soil with respect to its plasticity index (PI) which, is used for precise classification of the soil particles. The Atterberg limit test was performed in accordance to ASTM D4318 (2010). shows data for the liquid limit and the plastic limit.

D.2 Calibration of apparatus.

The Casagrande's apparatus can be easily knocked off calibration and hence should be regularly checked prior to any test. It must be ensured that the height of drop is between 10 ± 2 mm. Figure D-1 shows the process of calibrating the Casagrande's apparatus. The metal gauge is placed in contact at the point where the cup made contact with the surface. The top adjustment screw is untightened and the side adjustment screw is adjusted until the cup just touches the metal gauge. Once the necessary adjustment is done, the top adjustment screw is then tightened to secure the setup into place.

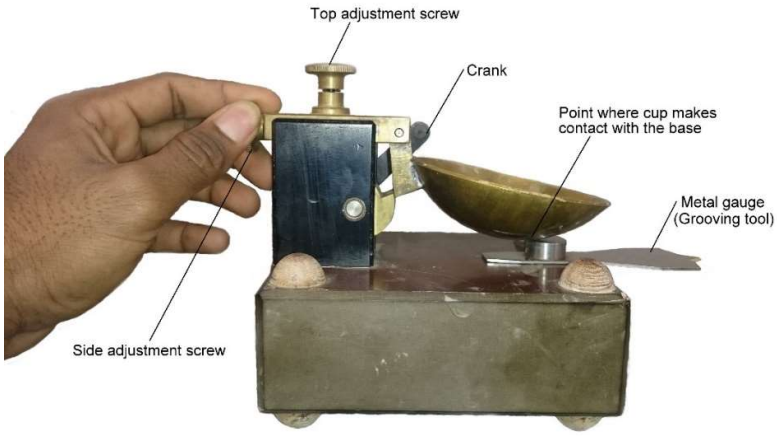

Figure D-1: Calibration of Casagrande's apparatus.

D.2.1 Liquid limit test

Method A (multipoint test) was used to obtain the liquid limit of the soil passing 425µm sieve. Water was added to about 500g of the sample until it produced a blow account between 30 and 35. The sample was then left to cure for a minimum of 16 hours. The following day, the sample was remixed and a portion of it was spread horizontally on the cup as shown in Figure D-2a. It must be ensured that no air bubble is entrapped by the soil as the spreading is done. With a downward movement, a groove was made into the soil sample with the help of the grooving tool. The former should be held perpendicular to the cup surface throughout its motion. The soil scraped off is collected for determination of water content.

The crank is turned such that two drops are produced per second. The process is maintained until the grove closes by about 13mm as shown in Figure 3-11b and the number of blows is recorded. The grooving tool is then used to extract soil sample, perpendicular to the initial depression made, for determination of water content as well. The moisture content of the soil is varied until four different blow counts (15-20, 20-25, 25-30 and 30-35) are obtained. Figure D-3 illustrates the summary of results for the liquid limit test. From the graph, it can be shown that the liquid limit for 25 blows is 37% water content.

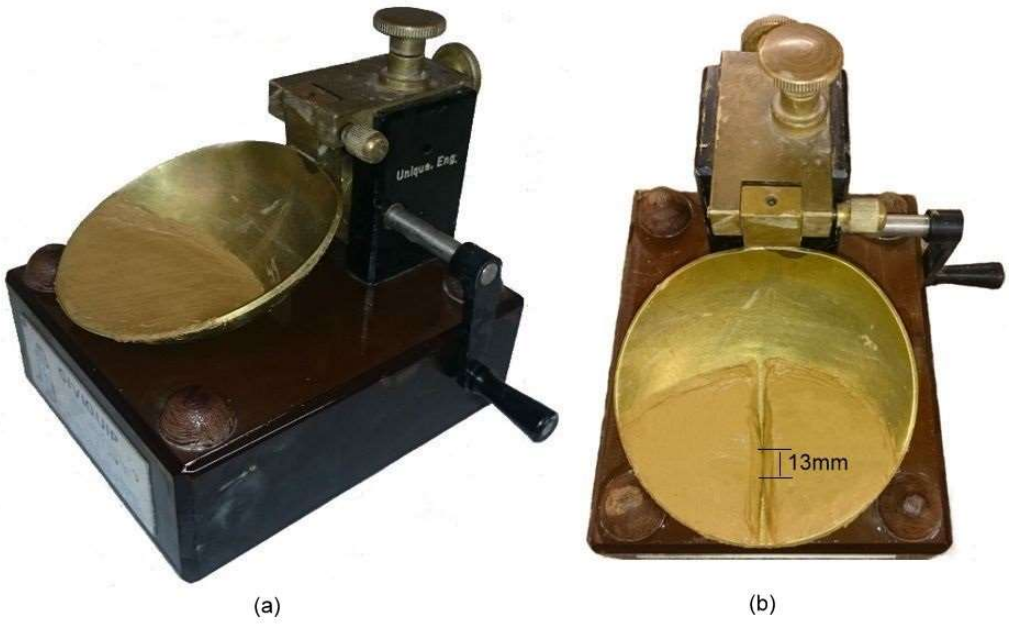

Figure D-2: Soil sample before and after testing for the liquid limit.

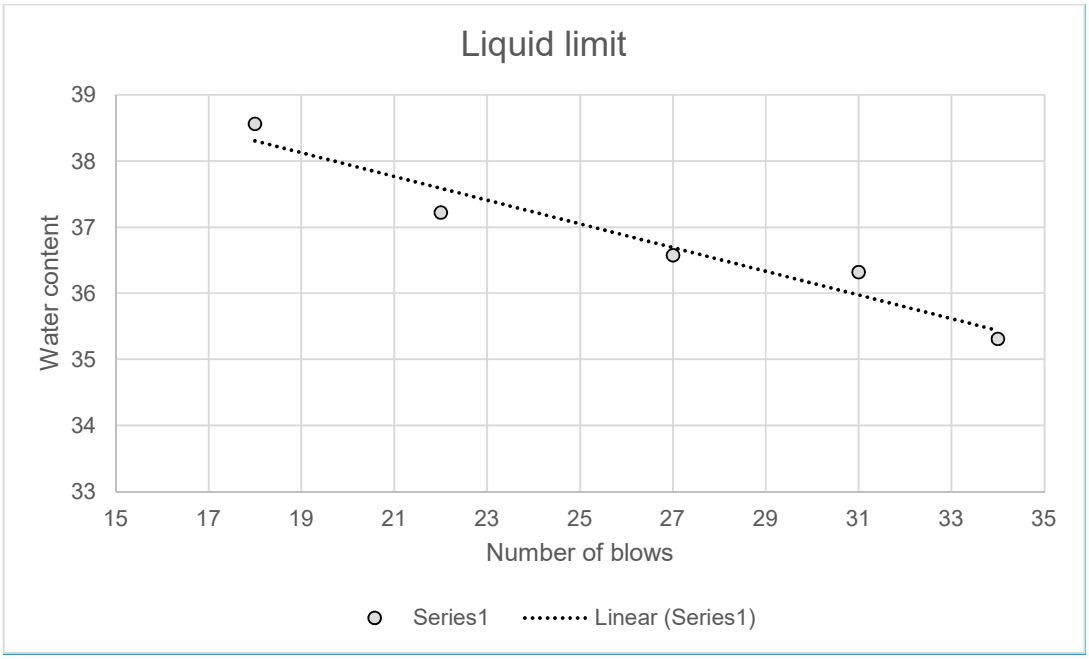

Figure D-3: Summary of result for liquid limit test

D.2.2 Plastic limit

Around 20g of the sample used for the liquid limit test was selected. The sample was rolled into a spherical mass then carefully rolled into about 3.2 mm thread. Once the thread was formed, the sample was spread onto a glass plate and then rolled back into a 3.2 mm thread. The process was repeated until the soil mass crumbles, as shown in Figure D-4, and thus can no longer be formed into the desired thread. The soil mass was then collected for determination of moisture content. From results illustrated in, it was noted that the plastic limit occurs at 18% water content.

Figure D-4: Clay sample ready for determination of moisture content at the plastic limit.

D.2.3 Plasticity index

The Plasticity index of the soil is the difference between the liquid limit and the plastic limit. It is the range of water content for which the soil behaves like a plastic material.

$$\boldsymbol{Plasticity\ index = Liquid\ limit\ - Plastic\ limit}$$

$$\boldsymbol{= 37 - 18}$$

$$\boldsymbol{= 19}$$

Using the plasticity chart from ASTM 2487, as shown in Figure D-5, the soil can be classified as CL (clay with a low plasticity).

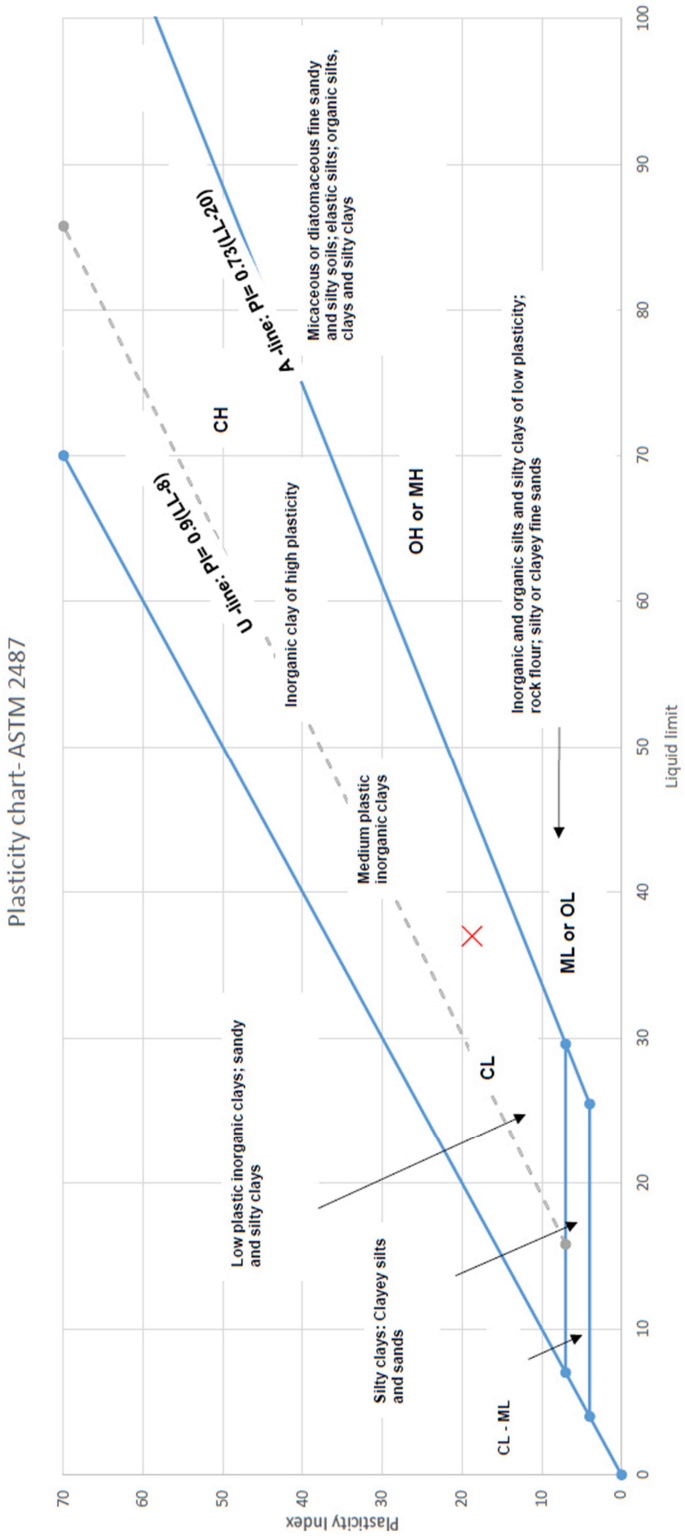

Figure D-5: Plasticity chart used to classify material according to the Unified Soil Classification System (ASTM D2487, 2011).

Table D-1: Atterberg limit tests results

Atterberg Limit test

Specimen Description	
Air dried reddish brown silty-clay, passing 425µm sieve	
Specimen preparation:	Wet

Standard:	ASTM D4318 2010
Method:	A

Liquid limit

Sample Num.	Num. of blows	<Mass of mould> <MM>/g	Mass of soil + mould <MMS>/g	Average mass of dry soil + mould <MS>/g	Average Moisture content <Mc>/%
1	34	2.103	9.510	7.577	35.31
2	31	2.093	10.852	8.520	36.32
3	27	2.095	10.321	8.118	36.57
4	22	2.118	11.003	8.593	37.22
5	18	2.117	9.064	7.131	38.56
				MC at LL(25 blows)	37

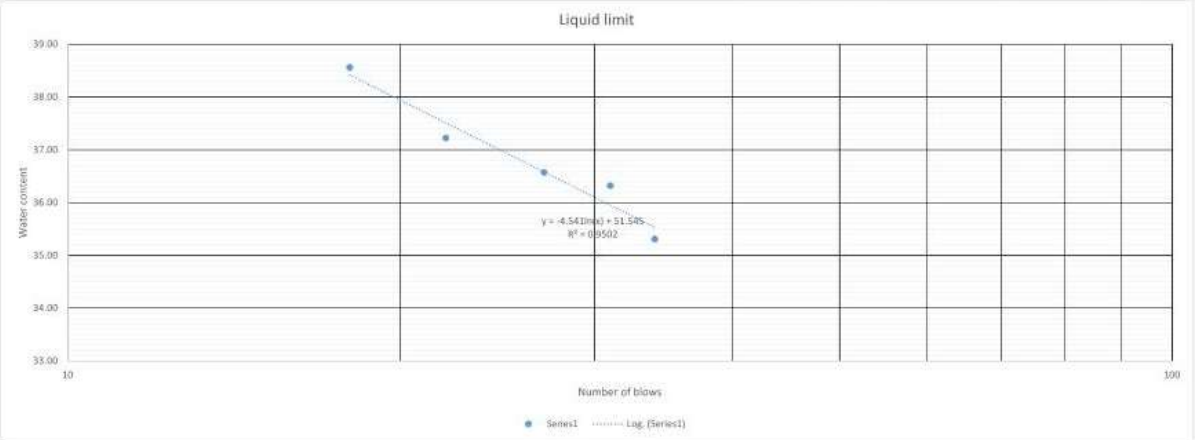

Plastic limit

Sample Num.	<Mass of mould> <MC>/g	Mass of soil + mould <MCS>/g	Mass of ovendried soil + mould <MS>/g	Average Moisture content <Mc>/%
1	2.120	8.423	7.452	18
2	2.143	6.473	5.803	18
			Average PL	18

Plasticity index: Liquid limit - Plastic limit
19

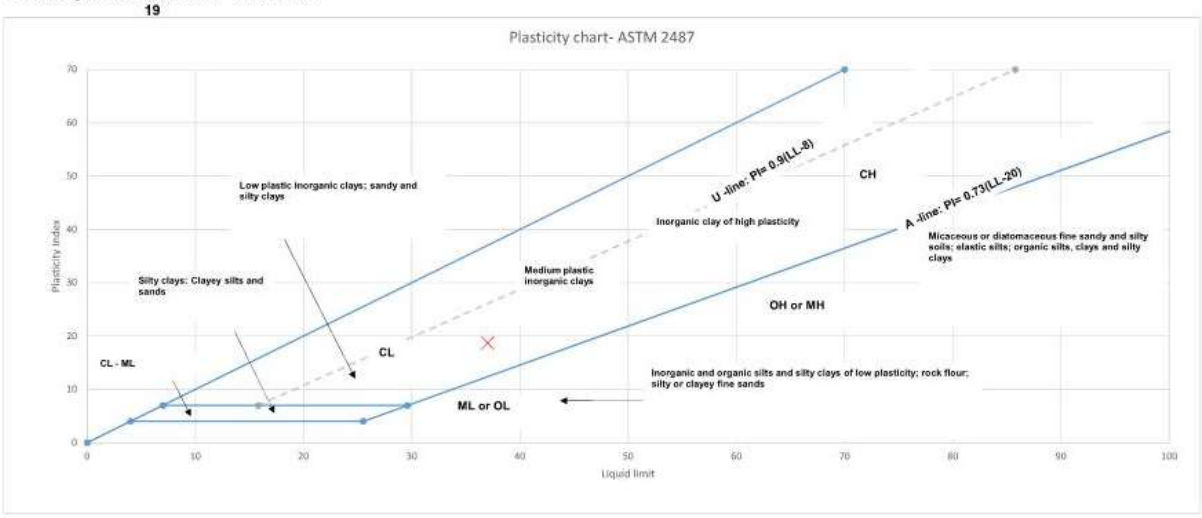

D.3 California bearing ratio (CBR) test

The California bearing ratio (CBR) test was developed by the California Division of Highways in the 1930s for the assessment of subgrade stability for road construction purposes. It was mainly used to assess the bearing capacity of road pavements, airport runways and earth-dams. The CBR value of a specific material is dependent on the type material, its moisture content, compacted density and by the method of sample preparation. The test is still widely used for the construction of pavement, however, ironically, it has replaced by Hveem Stabilometer test in California (Carter and Bentley, 1991). Having obtained the CBR value of a soil, its classification can be estimated using Figure D-6.

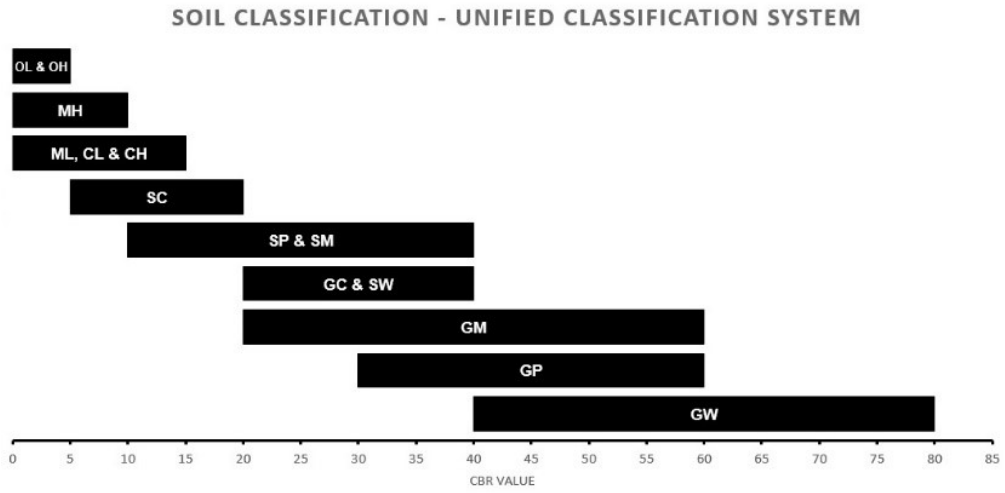

Figure D-6: Relationship between CBR values and soil classification (Carter and Bentley, 1991).

The CBR value is basically the ratio of pressure applied by a specific plunger at a predetermined penetration to that of the standard pressure required at this same point. The stronger the material, the higher will be the CBR value. According to ASTM D1883 (2016), the CBR is expressed as the ratio of the unit load on the piston required to penetrate 0.1 in. (2.5 mm) and 0.2 in (5.1 mm) of the test material to the unit load required to penetrate a standard material of well-graded crushed stone. Agarwal and Ghanekar (1970) found a relationship between the liquid limit and the optimum moisture content of the soil for the CBR value of a soaked sample, which is as follows:

$$CBR = 21 - 16\,log(OMC) + .0.07\,LL$$

OMC: Optimum moisture content

LL: Liquid limit

There are also several relationships that can be interpolated from a given CBR value. Table D-2 shows the estimated plasticity index of a soil at different formation level from the CBR value.

Table D-2: Estimated Laboratory CBR values for British soils compacted at natural moisture content (Carter and Bentley, 1991).

Type of soil	**CBR**		
	Plasticity Index (%)	**Depth of water table below formation level**	
		More than 600mm	**600mm or less**
Heavy Clay	70	2	1
	60	2	1.5
	50	2.5	2
	40	3	2
Silty clay	30	5	3
Sandy clay	20	6	4
	10	7	5
Silty	-	2	1
Sand (poorly graded)	Non- plastic	20	10
Sand (well graded)	Non- plastic	40	15
Well- graded sandy gravel	Non- plastic	60	20

Overseas Road Note 31 (1993) classifies the soil according to different traffic classes, that is, the suitable soil with respect to the total equivalent axle loading throughout the design lifetime of the road pavement. Table D-3 shows the relationship between the traffic classes and subgrade strength class. Table D-4 can also be used to obtain an estimate for the plasticity index of the soil based on the CBR value.

Table D-3: Key to the structural catalogue of Traffic class and respective CBR class strength.

Traffic classes (10^6 esa)	**Subgrade strength class (CBR)**
T1 = <0.3	
T2 = 0.3 - 0.7	S1 = 2
T3 = 0.7 - 1.5	S2 = 3,4
T4 = 1.5 - 3.0	S3 = 5-6
T5 = 3.0 - 6.0	S4 = 8-14
T6 = 6.0 -10	S5 = 15 - 29
T7 = 10 - 17	S6 = >30
T8 = 17 - 30	

Table D-4: Subgrade strength class for different Plasticity Index and depth of water table (Overseas Road Note 31, 1993).

	Subgrade strength classes				
***Depth of water table**	**Non-plastic sand**	**Sandy clay**	**Sandy clay**	**Silty clay**	**Heavy clay**
from formation level (m)		**PI=10**	**PI=20**	**PI=30**	**PI=40**
0.5	S4	S4	S2	S2	S1
1	S5	S4	S3	S2	S1
2	S5	S5	S4	S3	S2
3	S6	S5	S4	S3	S2
*Highest seasonal level attained by water should be used					

The CBR test was carried out according to ASTM D1883 (2016) and compaction was done in accordance to ASTM D1557 (2012). Method C was chosen with respect to ASTM D1557 (2012) for compaction. The material was compacted in five layers with 56 blows in each layer with a standard hammer of 44.48N dropped from a height of 457.2mm. Figure D-7, illustrates the compaction pattern using the standard hammer.

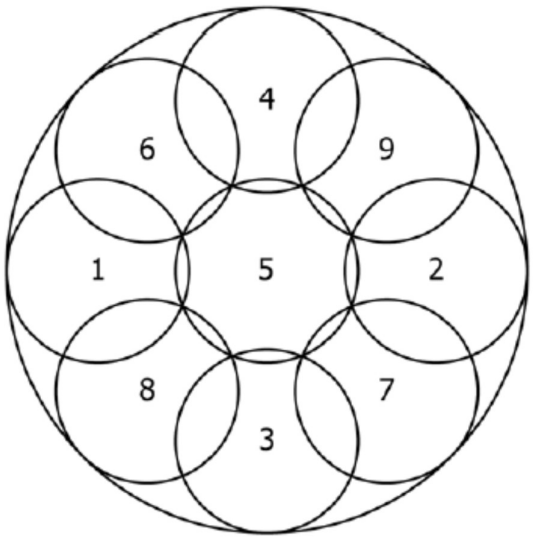

Figure D-7: Compaction pattern of 152.4mm (6in) mould (ASTM D1557, 2012).

After compacting the soil to the desired density, its surface was trimmed off as shown in Figure D-8. A representative portion of the material was taken for determination of the moisture content. Having assembled the different components of the mould together, it was placed in a water bath for 96 ± 2 hours.

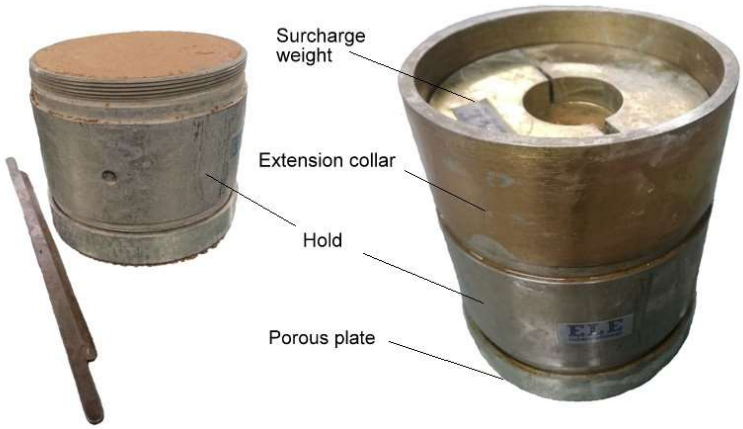

Figure D-8: Assembly of CBR mould prior to soaking/testing.

After 96 ± 2 hrs, the sample was taken out of the water and allowed to drain for around 15 minutes after which the mould was placed in the testing machine as shown in Figure D-9. Table D-5 shows the summary of results obtained from the set of CBR test carried out on the sample. Figure D-10 shows the CBR graphs obtained for the tested samples.

Table D-6, Table D-7 and Table D-8 shows the raw data obtained from the tests.

Figure D-9: Setup of the mould prior to testing.

Table D-5: Summary of results for CBR value of soil.

	Test number			
Penetration/mm	Test 1 CBR %	Test 2 CBR %	Test 3 CBR %	Average CBR
2.5	4.85	4.16	3.01	4.01
5	6.07	5.31	3.9	5.1

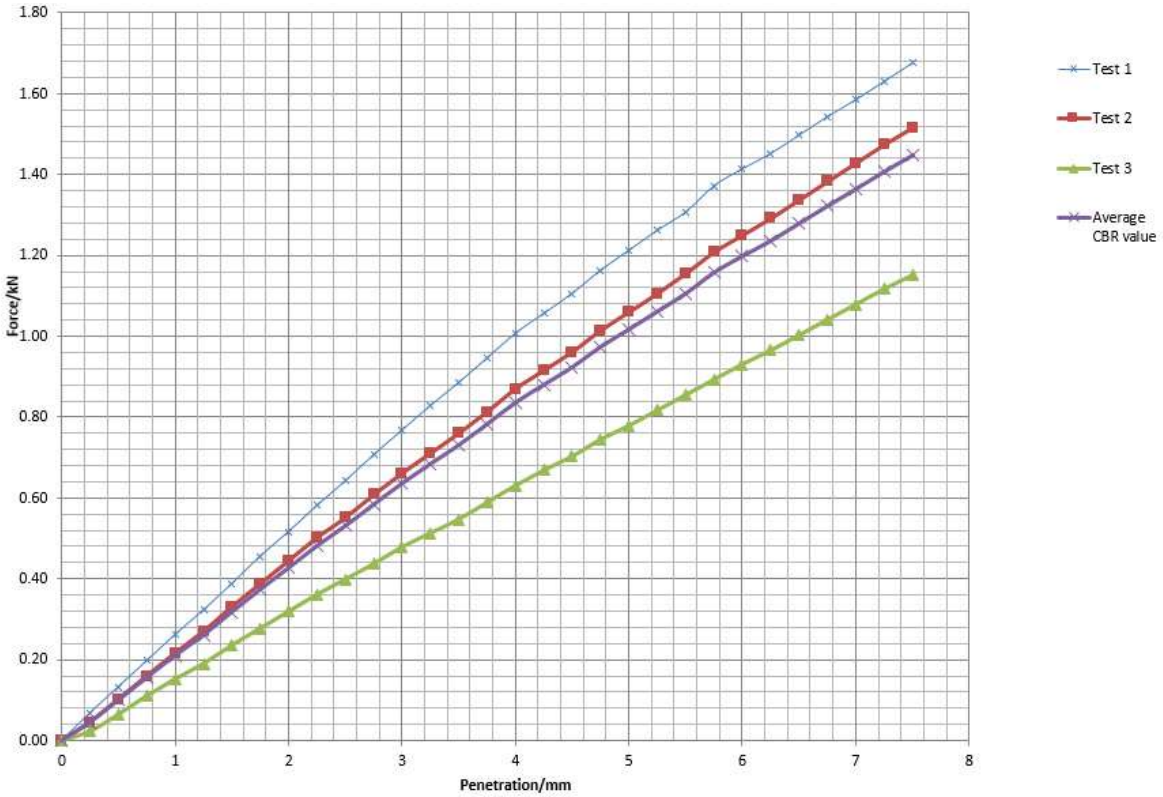

Figure D-10: CBR test data.

Table D-6: CBR Data for Test 1

CBR TEST 1

Max dry unit weight	1855 kg/m³
Test method	ASTM 1883 and ASTM 1557
Hammer	44.48N
Drop	457.2 mm
Blows	56
Layers	5

Soaked CBR	Unsoaked CBR
x	

Dimension of CBR mould		
Diameter	Length	Volume(m3)
151.87	126.99	2.30E-03
151.81	126.85	2.30E-03
151.73	126.79	2.29E-03
151.80	126.88	**2.30E-03**

Top of mould

Penetration/mm	Load/kN	Standard load/kN	CBR %
2.5	0.6	13.24	4.85
5	1.2	19.96	6.07

	Sample Num.	<Mass of mould> <MM>/g	Mass of soil + mould <MMS>/g	Oven dried soil + mould <MS>/g	Average Moisture content <Mc>/%
Before test	1	25.915	131.307	117.526	15.04
	2	18.403	98.729	88.272	14.97

Mass CBR mould + sample before soaking/g	10715
Mass CBR mould + sample after soaking/g	10757
Mass CBR mould/g	5715
Density of sample before soaking (kg/m3)	2177
Density of sample after soaking (kg/m3)	2196

Penetration/ mm	Force Device/ unit Top	Force on plunger (kN) Top	Penetration/ mm	Force Device/ unit Top	Force on plunger (kN) Top
0	0	0.00	**4**	265	1.01
0.25	18	0.07	**4.25**	278	1.06
0.5	35	0.13	**4.5**	291	1.11
0.75	52	0.20	**4.75**	306	1.16
1	69	0.26	**5**	319	1.21
1.25	85	0.32	**5.25**	332	1.26
1.5	102	0.39	**5.5**	344	1.31
1.75	120	0.46	**5.75**	361	1.37
2	136	0.52	**6**	372	1.41
2.25	153	0.58	**6.25**	382	1.45
2.5	169	0.64	**6.5**	394	1.50
2.75	186	0.71	**6.75**	406	1.54
3	202	0.77	**7**	417	1.58
3.25	218	0.83	**7.25**	429	1.63
3.5	233	0.89	**7.5**	441	1.68
3.75	249	0.95			

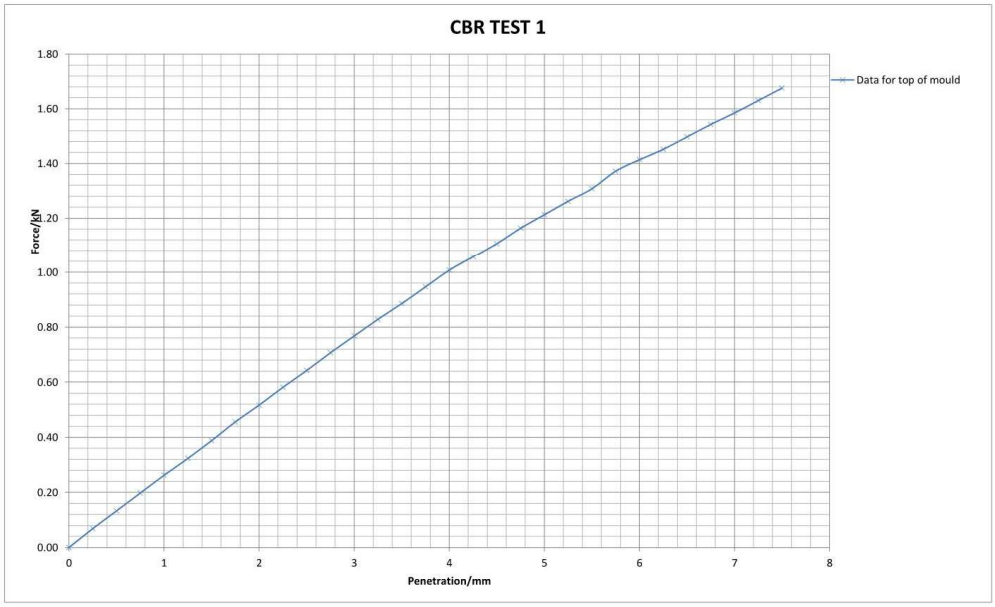

Table D-7: CBR data for test 2

CBR TEST 2

Max dry unit weight	1855 kg/m³
Test method	ASTM 1883 and ASTM 1557
Hammer	44.48N
Drop	457.2 mm
Blows	56
Layers	5

Soaked CBR	Unsoaked CBR
x	

Dimension of CBR mould		
Diameter	Length	Volume(m3)
151.87	126.99	2.30E-03
151.81	126.85	2.30E-03
151.73	126.79	2.29E-03
151.80	126.88	**2.30E-03**

Top of mould

Penetration/mm	Load/kN	Standard load/kN	CBR %
2.5	0.6	13.24	4.16
5	1.1	19.96	5.31

	Sample Num.	<Mass of mould> <MM>/g	Mass of soil + mould <MMS>/g	Oven dried soil + mould <MS>/g	Average Moisture content <Mc>/%
Before test	1	25.92	167.276	148.632	15.19
	2	25.919	163.883	145.765	15.12

Mass CBR mould + sample before soaking	10642
Mass CBR mould + sample after soaking	10681
Mass CBR mould	5715
Density of sample before soaking (kg/m3)	2146
Density of sample after soaking (kg/m3)	2163

Penetration/ mm	Force Device/ unit Top	Force on plunger (kN) Top	Penetration/ mm	Force Device/ unit Top	Force on plunger (kN) Top
0	0	0.00	**4**	229	0.87
0.25	12	0.05	**4.25**	241	0.92
0.5	27	0.10	**4.5**	253	0.96
0.75	42	0.16	**4.75**	267	1.01
1	57	0.22	**5**	279	1.06
1.25	71	0.27	**5.25**	291	1.11
1.5	87	0.33	**5.5**	304	1.16
1.75	102	0.39	**5.75**	318	1.21
2	117	0.44	**6**	329	1.25
2.25	132	0.50	**6.25**	340	1.29
2.5	145	0.55	**6.5**	352	1.34
2.75	160	0.61	**6.75**	364	1.38
3	174	0.66	**7**	376	1.43
3.25	187	0.71	**7.25**	388	1.47
3.5	200	0.76	**7.5**	399	1.52
3.75	214	0.81			

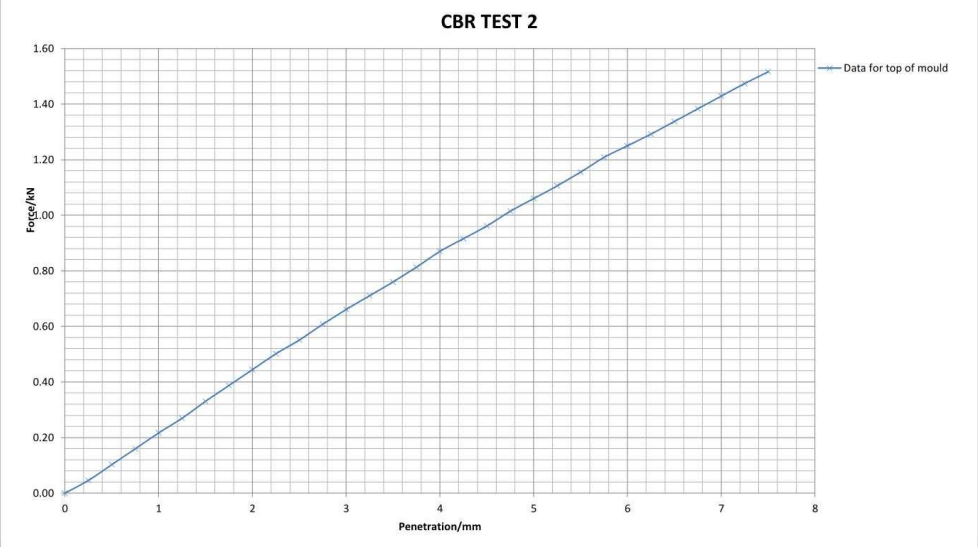

Table D-8: CBR data for test 3

CBR TEST 3

Max dry unit weight	1855 kg/m³
Test method	ASTM 1883 and ASTM 1557
Hammer	44.48N
Drop	457.2 mm
Blows	56
Layers	5

Soaked CBR	Unsoaked CBR
x	

Dimension of CBR mould		
Diameter	Length	Volume(m3)
151.87	126.99	2.30E-03
151.81	126.85	2.30E-03
151.73	126.79	2.29E-03
151.80	126.88	**2.30E-03**

Top of mould

Penetration/mm	Load/kN	Standard load/kN	CBR %
2.5	0.4	13.24	3.01
5	0.8	19.96	3.90

	Sample Num.	<Mass of mould> <MM>/g	Mass of soil + mould <MMS>/g	Oven dried soil + mould <MS>/g	Average Moisture content <Mc>/%
Before test	1	17.671	114.999	101.972	15.45
	6	18.400	95.338	85.076	15.39

Mass CBR mould + sample before soaking/g	10569
Mass CBR mould + sample after soaking/g	10612
Mass CBR mould/g	5715
Density of sample before soaking (kg/m3)	2114
Density of sample after soaking (kg/m3)	2133

Penetration/ mm	Force Device/ unit Top	Force on plunger (kN) Top	Penetration/ mm	Force Device/ unit Top	Force on plunger (kN) Top
0	0	0.00	4	166	0.63
0.25	6	0.02	4.25	176	0.67
0.5	17	0.06	4.5	185	0.70
0.75	29	0.11	4.75	196	0.74
1	40	0.15	5	205	0.78
1.25	50	0.19	5.25	215	0.82
1.5	62	0.24	5.5	225	0.86
1.75	73	0.28	5.75	235	0.89
2	84	0.32	6	245	0.93
2.25	95	0.36	6.25	254	0.97
2.5	105	0.40	6.5	264	1.00
2.75	115	0.44	6.75	274	1.04
3	126	0.48	7	284	1.08
3.25	135	0.51	7.25	294	1.12
3.5	144	0.55	7.5	303	1.15
3.75	155	0.59			

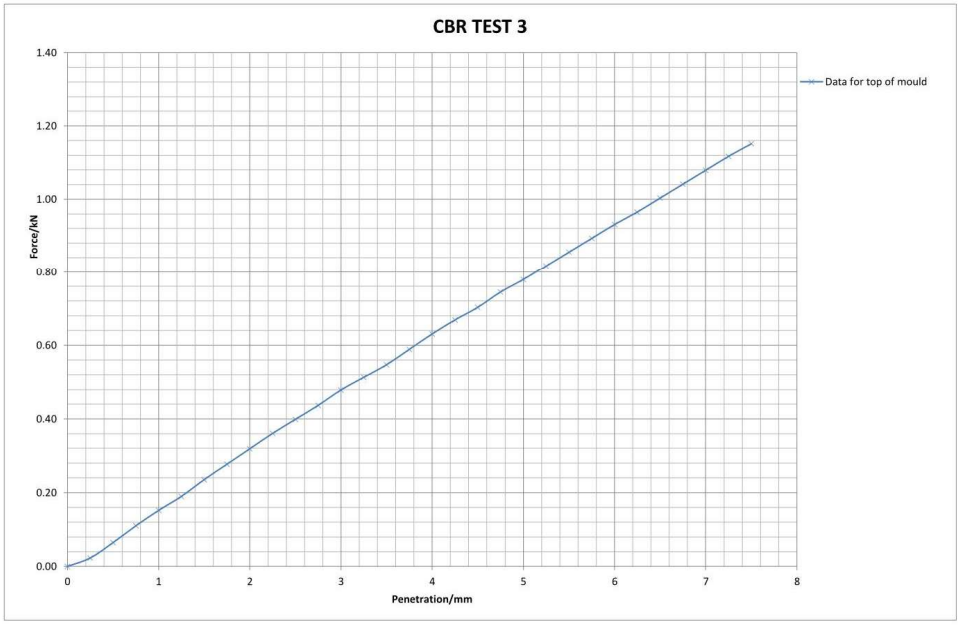

D.4 Proctor compaction test

The degree of compaction of a soil varies with its water content. The compaction effort will reduce the air void content of the soil without affecting its water content. To attain the highest possible compaction density, the soil should be compacted at its optimum moisture content. This water content is the point at which the water present within the soil provides sufficient lubrication to the soil particles for them to be easily packed in the best possible way. Increasing the water content beyond this point will lead to a decrease in the density of the soil because the water will tend to replace the soil particles. Since the density of water is less than that of soil, a gradual decrease in density will be observed after the optimum moisture content has been reached. The application of this test is of relevance in engineering fill for construction of roads and foundations. A soil compacted at its optimum moisture content will have a maximum shear strength, therefore, an increase in bearing capacity and will be less susceptible to volume changes ASTM D698 (2012) was adopted to obtain the maximum dry density of the soil sample at its optimum moisture content.

The material to be tested was a suspected to be a clay sample which was mechanically pulverised. Since the sample was below 4.75mm, Method A was adopted for the test. The aim of the experiment was to produce different samples of varying water content and determining the density of each one to finally plot a required graph to identify the optimum moisture content. About 2.3 kg of the soil sample was weighed and mixed with a predetermined quantity of water. The soil was compacted into 3 different layers, each having a thickness of about 1/3rd of the 4-inch mould height. A standard rammer having a mass of 2.495 ± 0.009 kg was allowed to free fall on each layer from a height of 304.8 ± 1 mm. Each layer was compacted uniformly using 25 blows, following the pattern in Figure D-11.

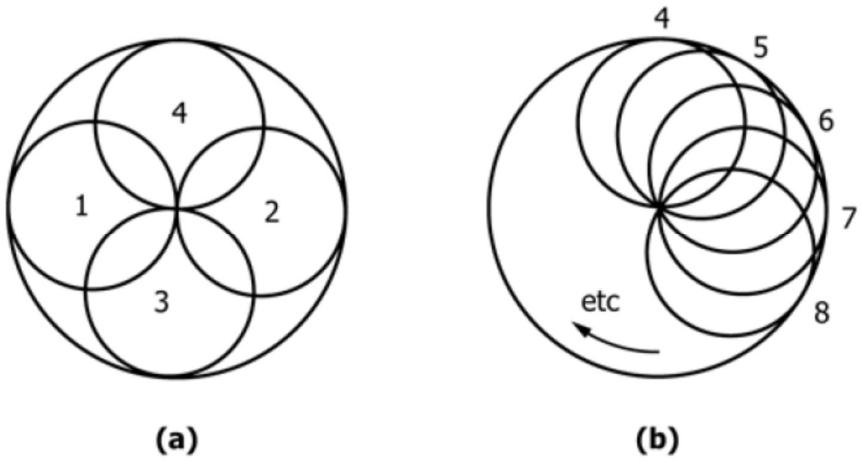

Figure D-11: Rammer pattern for compaction in the 4-inch mould (ASTM D698, 2012).

The sample was carefully trimmed across the top of the mould and its mass was determined to the nearest gram. A representative sample of the soil was taken out to assess its moisture content. The experiment was repeated until sufficient set of values are obtained to plot the compaction curve. Figure D-12 shows the results obtained following the Proctor compaction test. From the graph, it can be shown that the maximum dry density of 1850kg/m^3 was obtained at around the optimum moisture content of 14.2%. Table D-9 shows the raw data for the proctor test.

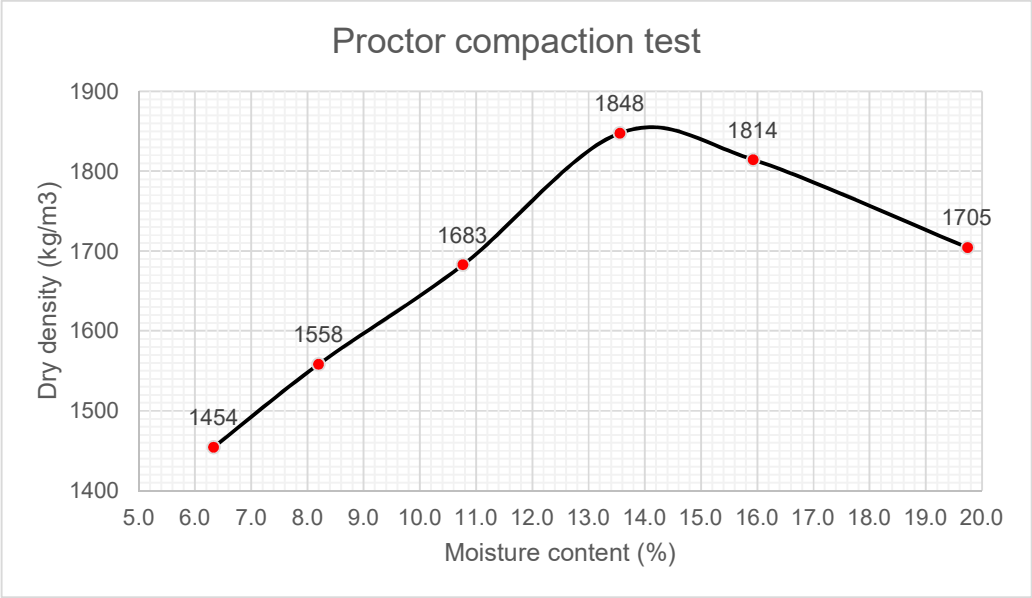

Figure D-12: Proctor compaction test result.

Table D-9: Raw data for proctor test.

Proctor compaction test

Standard:	ASTM D 698
Method:	A

Mould

D1	D2	D3	<D>/mm
102.7	102.45	102.36	102.5033333
L1	L2	L3	<L>/mm
116.4	116.42	116.31	116.37
		Volume/m^3	0.0009603

Soil- Description

Air dried reddish brown silty-clay, passing 425µm sieve

Density

Sample Num.	<Mass of mould> <MM>/g	Mass of soil + mould <MMS>/g	Average mass of soil <MS>/g	Average moist Density <ρm>/ kg/m^3	Average dry Density <ρd>/ kg/m^3
1	4435	5920	1485	1546	1454
2	4435	6054	1619	1686	1558
3	4435	6225	1790	1864	1683
4	4435	6450	2015	2098	1848
5	4435	6455	2020	2104	1814
6	4435	6395	1960	2041	1705

Moisture content

Sample Num.	<Mass of mould> <MC>/g	Mass of soil + mould <MCS>/g	Mass of ovendried soil + mould <MS>/g	Average Moisture content <Mc>/%
1	2.1	21	19.75	6.33
2	2.1	19.8	18.3	8.20
3	2.1	19.55	17.65	10.76
4	2.1	23.45	20.65	13.56
5	2.1	19.65	16.95	15.93
6	2.1	27.6	23.05	19.74

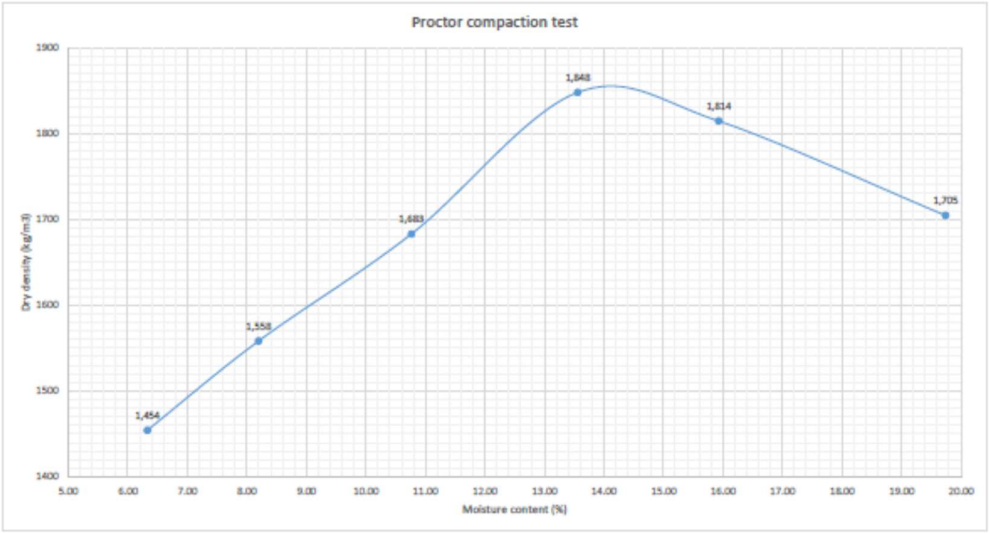

D.5 Specific gravity

The specific gravity, G_s, is the ratio of the mass of a unit volume of the soil particles to the mass of a gas-free distilled water displaced by the soil at 20°C. The specific gravity is used to determine phase relationship of soil particles such as the degree of saturation, void ratio. ASTM D854 (2014) was adopted to obtain the specific gravity of the soil particles. Table D-10 shows the lab results obtained for the determination of the specific gravity.

Table D-10: Specific gravity test results

Specific gravity					
Specimen Description				Standard:	ASTM D4318 2010
Air dried reddish brown silty-clay, passing 425µm sieve				Method:	A
Specimen preparation:	Wet				
Sl. No.	**Observations an Calculations**	**Determination No.**			
		1	**2**	**3**	**4**
Observation					
	Density bottle No.	58	6	24	1
	Mass of empty density bottle (M_1)	33.806	35.357	33.871	34.995
	Mass of bottle + dry soil (M_2)	41.668	42.938	41.668	42.752
	Mass of bottle, soil and water (M_3)	89.463	88.642	88.292	92.334
	Mass of bottle filled with water (M_4)	84.526	83.891	83.408	87.477
Calculations					
	Mass of soil ($M_2 - M_1$)	7.862	7.581	7.797	7.757
	Mass of water displaced by soil ($(M_4+M_2-M_1-M_3)$)	2.925	2.830	2.913	2.900
	Calculate G using formula	2.688	2.679	2.677	2.675
				Average G	**2.68**

D.6 Sieve analysis

Soil contains particles of various shapes and sizes. The sieve analysis is done in view to classify a soil into its respective category. The sieve analysis was performed in accordance to ASTM D6913 (2009) and method B was adopted (the mass should be recorded to at least 4 significant figures). The test is only applicable to the fraction of soil having grain sizes greater than 75µm. A hydrometer test was carried out for the particles that pass 75µm sieve. ASTM D422 (2007) was followed to carry out the hydrometer test.

ASTM D2487 (2011) was used to categorise the material used for testing. A series of sieves are stacked all together, starting from the highest down to the lowest aperture size. A known mass of oven dried soil is placed on top of the sieve and the whole stack

is placed on a mechanical shaker and vibrated until satisfactory sieving is obtained (between 10 to 20 minutes). The mass of soil retained by each sieve size is recorded and the cumulative percentage retained on each sieve is calculated. According to ASTM D6913 (2009), the sample mass should not exceed the minimum dry mass suggested by 50 % to prevent overloading of the sieve (Table D-11). Table D-12 shows the raw data from the sieve and hydrometer analysis. Figure D-13 shows the grading of the soil sample.

Table D-11: Minimum mass requirement for the specimen (ASTM D6913, 2009).

Maximum Particle Size of Material (99 % or more passes)		Minimum Dry Mass of Specimen, g or kg[A]	
Alternative Sieve Designation	Maximum Particle Size, mm	Method A Results Reported to Nearest 1 %	Method B Results Reported to Nearest 0.1 %
No. 40	0.425	50 g	75 g
No. 10	2.00	50 g	100 g
No. 4	4.75	75 g	200 g[B]
⅜ in.	9.5	165 g[C]	[D]
¾ in.	19.0	1.3 kg[C]	[D]
1 in.	25.4	3 kg[C]	[D]
1-½ in.	38.1	10 kg[C]	[D]
2 in.	50.8	25 kg[C]	[D]
3 in.	76.2	70 kg[E]	[D]

Table D-12: Sieve and Hydrometer analysis data

Sieve Analysis: Soil

Sample:	Lean clay
mass of sample + plate/g	385.816
mass of plate/g	276.232
Mass of sample/ g	109.584

Test No:	1
Tested by:	Pudaruth. Y
Standard	ASTM D6913 (2009)
Method	B

Sieve size/mm	Mass of sieve/g	Mass of sieve sample/g	Mass of sample/g	% Retained	Cum % retained	Cum % passing
1.180	552.536	552.551	0.015	0.014	0.014	99.986
0.600	536.532	536.583	0.051	0.047	0.060	99.940
0.425	505.824	508.557	2.733	2.494	2.554	97.446
0.300	513.24	521.912	8.672	7.914	10.468	89.532
0.250	506.198	509.678	3.48	3.176	13.643	86.357
0.150	469.687	477.78	8.093	7.385	21.029	78.971
0.075	463.3	492.972	29.672	27.077	48.106	51.894

Hydrometer Analysis: Soil

Temperature	20
Ft	0.15
fz	-0.5
fm	0.5
Rcp	
Gs	2.68
a	0.993261456
Ws	63.905

Oven dried	
Mass of container	182.592
Mass of container + sample	246.497
Mass of sample	63.905

Time (min)	Actual hydrometer reading,R	Rcp	% finer	Rcl	L	A	D
2	35	34.65	53.8557381	35.5	10.5	0.00135	0.0031
4	34	33.65	52.30145995	34.5	10.65		0.00221
8	31	30.65	47.63862548	31.5	11.15		0.0016
16	27.5	27.15	42.19865193	28	11.7		0.00116
30	26	25.65	39.8672347	26.5	11.95		0.00085
60	23	22.65	35.20440023	23.5	12.45		0.00062
120	20.5	20.15	31.31870484	21	12.9		0.00044
240	19.5	19.15	29.76442669	20	13		0.00031
480	18.5	18.15	28.21014853	19	13.2		0.00022
1440	16	15.65	24.32445314	16.5	13.6		0.00013

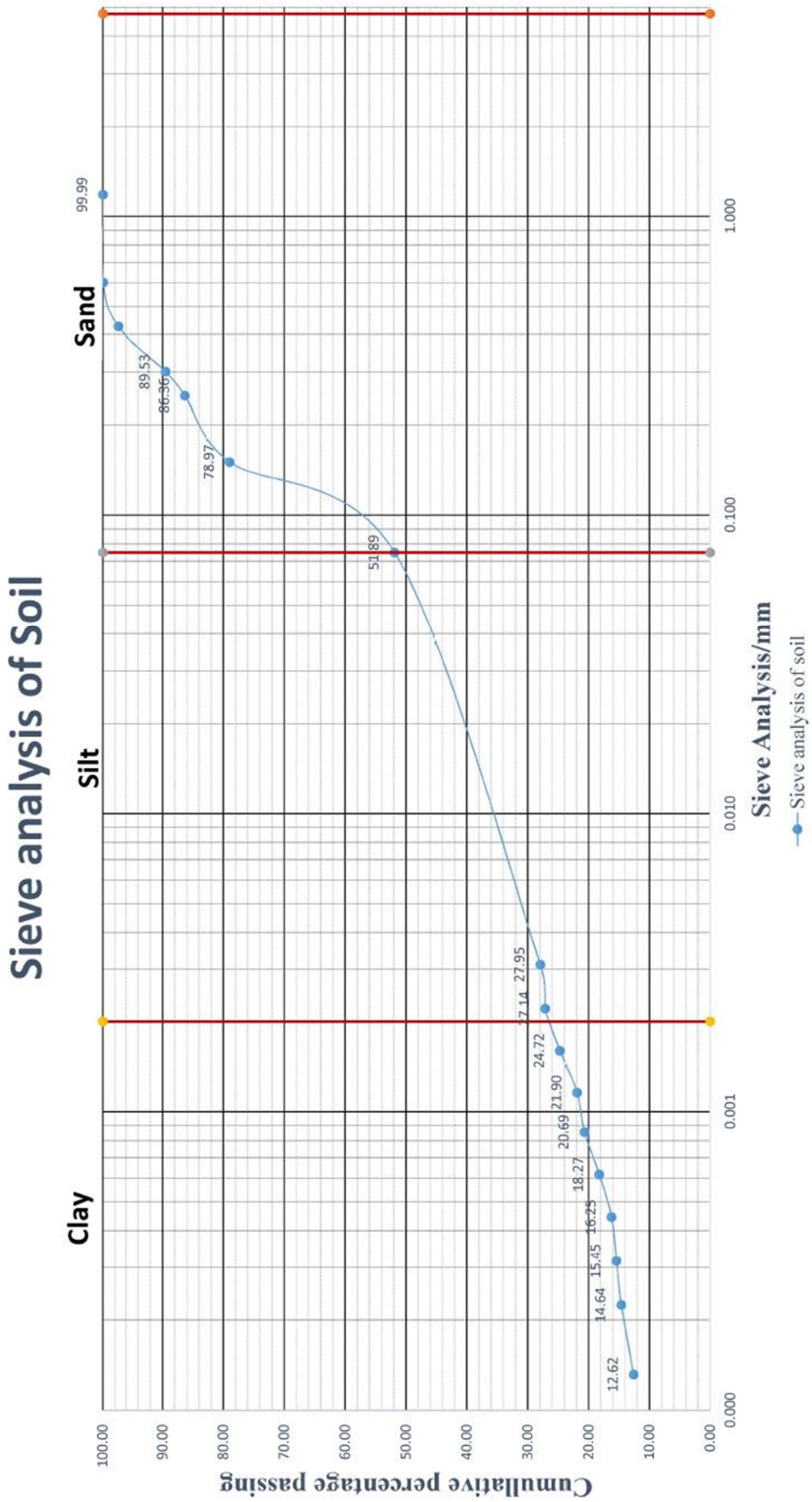

Figure D-13: Sieve size distribution of soil particles according to their different grain sizes.

D.7 Shear strength

The shear strength is a measure of the maximum stress that a soil can sustain before undergoing failure. It is the maximum stress that is experienced by a soil before it yields. In brittle soil, yielding can induce a slip surface along which sliding may occur. The shear strength of a soil is developed due to frictional forces between the soil particles. The Mohr-Coulomb's equation relating the shear stress, apparent cohesion and friction angle is shown below.

$$T_f = c' + \sigma_n \tan \emptyset'_p$$

T_f- Limiting shear stress

c' - Apparent drained cohesion

σ_n- Normal stress on slip surface

$\emptyset'_p$- Angle of friction

A direct shear test under consolidated drained conditions was performed as per performed as per ASTM D3080 (2011). The sample was prepared at its maximum dry density and loaded in the ShearTrac-II Direct Shear Apparatus for testing. The normal load applied to the sample was varied for different samples prepared to the same density and thickness and the maximum shear forces for each of them was noted. An appropriate graph of Shear force against Normal force was plotted to determine the friction angle and the drained cohesion strength of the sample. Figure D-14 shows the apparatus used to determine shear strength parameters. Table D-13 shows the data obtained from the direct shear test.

Figure D-14: ShearTrac-II Direct Shear Apparatus used to determine shear strength parameters.

It was determined that:

1: friction angle, $\emptyset'_p = 27.1^o$

2: Drained cohesion strength, c'= 13.1 kPa

Table D-13; Data obtained from the direct shear test.

Shear analysis

Test No:	1
Tested by:	Pudaruth. Y
Standard	ASTM D3080 (2011)

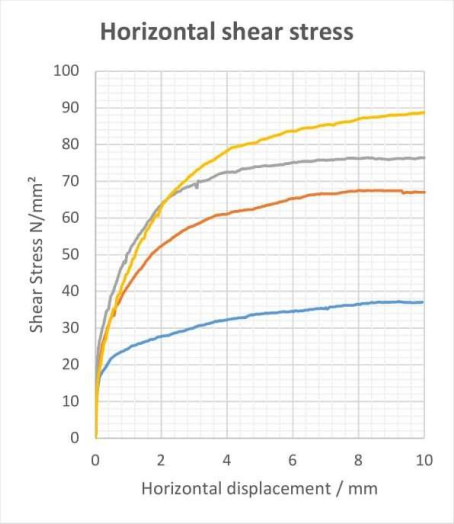

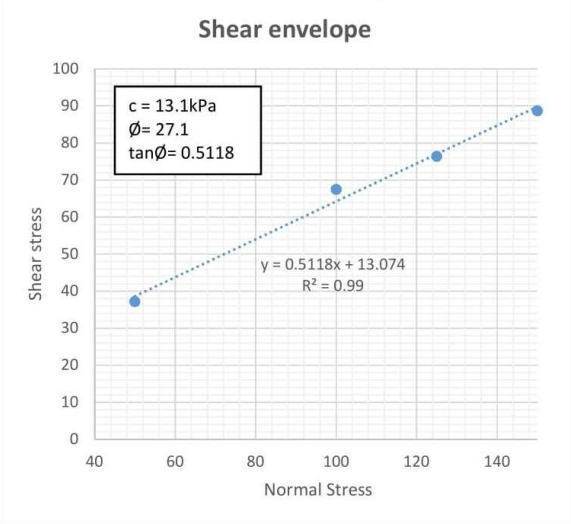

Test No.		1	2	3	4
Sample No		1	2	3	4
Shape		Square	Square	Square	Square
Initial	Dimension,mm	101.6	101.6	101.6	101.6
	Area, mm^2	10323	10323	10323	10323
	Height, mm	30	30	30	30
	Water Content, %	20.27	18.75	18.21	18.4
	Dry Density, kN/m^3	17.12	17.33	17.41	17.39
	Saturation,%	100.03	95.96	94.44	95.0
	Void ratio	0.54705	0.52751	0.52056	0.52302
Consol. Heigth,mm		29.955	29.955	27.202	26.978
Consol. Void Ratio		0.54471	0.52724	0.37873	0.37
Normal Stress,kPa		50	100	125.01	150
Max. Shear Stress,kPa		37.2	67.5	76.4	88.7
Ult. Shear Stress,kPa		37.1	67.5	76.4	88.7
Time to Failure, min		187.0	174.0	203.0	203.0
Disp. Rate,mm/min		0.05	0.05	0.05	0.05
Assumed Specific Gravity		2.7	2.7	2.7	2.7
Liquid Limit		37	37	37	37
Plastic Limit		18	18	18	18
Plasticity Index		19	19	19	19

Remarks:

E : Load improvement factor of stone column

Table E-1: Load improvement ratio of columns in the D0 configuration.

Test series	Variable Parameter	s/D (Settlement/Diameter ratio) 2%	10%	20%	30%	40%	50%	60%	70%	80%	90%	100%	Moisture Content
G10D0	S1	7.1	6.3	6.9	Undetermined								19.57
	S2	4.6	4.3	4.8	4.9	4.9	4.8	4.8	Undetermined				19.68
	S3	2.0	2.8	3.3	3.4	3.5	3.6	3.6	3.7	3.8	3.8	3.8	19.76
	S4	1.3	2.2	3.0	3.2	3.3	3.3	3.3	3.4	3.5	3.5	3.5	19.66
	S5	1.7	2.4	2.8	2.8	2.8	2.7	2.8	2.7	2.7	2.7	2.8	19.52
	SC5	Undetermined											19.72
G20D0	S1	3.4	3.3	4.1	5.1	6.2	7.8	Undetermined					19.76
	S2	3.5	3.3	3.7	3.8	3.8	3.8	3.9	4.1	4.3	4.5	4.8	19.99
	S3	2.7	2.5	2.6	2.7	2.9	2.9	3.0	3.1	3.2	3.3	3.3	19.55
	S4	1.0	1.5	2.1	2.4	2.5	2.6	2.5	2.6	2.6	2.7	2.8	19.68
	S5	1.7	2.4	2.8	2.8	2.8	2.7	2.8	2.7	2.7	2.7	2.8	19.52
	SC5	Undetermined											19.42
G30D0	S1	7.5	7.4	8.2	8.8	9.5	11.2	14.4	Undetermined				19.52
	S2	3.9	4.4	5.2	5.8	6.1	6.2	6.3	6.4	6.7	6.9	7.4	18.65
	S3	2.0	2.9	3.6	3.9	4.2	4.2	4.1	4.2	4.2	4.2	4.2	19.38
	S4	2.4	2.7	3.2	3.5	3.6	3.5	3.6	3.6	3.6	3.7	3.5	19.50
	S5	1.8	2.7	3.2	3.3	3.2	3.1	3.1	3.0	3.0	2.9	3.1	19.89
	SC5	Undetermined											19.43
G40D0	S1	3.9	4.2	5.4	6.8	8.4	11.2	17.0	Undetermined				20.02
	S2	4.8	4.9	4.9	4.8	4.7	4.5	4.5	4.6	4.6	4.7	4.9	19.52
	S3	3.4	3.3	3.5	3.5	3.6	3.5	3.5	3.6	3.6	3.6	3.6	20.00
	S4	1.6	2.6	3.1	3.3	3.3	3.4	3.4	3.4	3.4	3.4	3.4	19.84
	S5	2.4	2.8	3.1	3.1	3.0	3.0	3.1	3.1	3.1	3.1	3.2	19.52
	SC5	Undetermined											19.27

Table E-2: Load improvement ratio of columns in the D1 configuration.

Test series	Variable Parameter	s/D (Settlement/Diameter ratio) 2%	10%	20%	30%	40%	50%	60%	70%	80%	90%	100%	Moisture Content
G10D1	S1	5.6	4.2	3.9	4.0	3.9	3.8	3.8	3.8	3.9	4.0	4.1	19.46
	S2	3.4	3.4	3.6	3.9	4.1	4.1	4.0	4.0	4.0	3.9	3.9	18.83
	S3	2.6	3.0	3.4	3.6	3.9	3.9	3.9	3.9	4.0	4.1	4.1	19.29
	S4	2.1	2.5	3.0	3.3	3.4	3.5	3.5	3.6	3.7	3.8	3.7	19.10
	S5	1.9	2.8	3.3	3.5	3.4	3.4	3.4	3.4	3.4	3.5	3.5	19.38
	SC5	4.4	3.4	3.4	3.6	3.6	3.6	3.6	3.9	4.9	Undetermined		19.29
G20D1	S1	3.8	4.2	4.9	5.4	5.8	6.3	6.7	6.9	7.0	7.0	7.1	19.73
	S2	3.8	3.6	4.1	4.6	5.1	5.4	5.7	5.9	6.1	6.2	6.4	19.69
	S3	3.3	3.6	4.0	4.2	4.5	4.7	5.0	5.1	5.4	5.6	5.8	19.76
	S4	0.9	2.4	3.3	3.6	3.8	3.9	4.0	4.2	4.4	4.5	4.6	19.15
	S5	1.9	2.8	3.3	3.5	3.4	3.4	3.4	3.4	3.4	3.5	3.5	19.38
	SC5	1.2	1.3	1.9	2.2	2.2	2.2	2.2	2.5	3.6	Undetermined		19.45
G30D1	S1	4.8	4.3	4.4	4.5	4.7	4.8	4.9	5.0	5.0	5.1	5.1	19.93
	S2	3.1	3.0	3.3	3.6	3.9	4.2	4.3	4.3	4.3	4.3	4.3	19.36
	S3	2.7	2.9	3.3	3.5	3.6	3.6	3.8	3.9	4.0	4.0	3.9	19.69
	S4	2.6	2.8	3.2	3.3	3.3	3.3	3.3	3.3	3.3	3.3	3.3	19.90
	S5	1.9	2.8	3.3	3.5	3.4	3.4	3.4	3.4	3.4	3.5	3.5	19.56
	SC5	2.5	2.5	2.9	3.2	3.5	3.8	4.0	4.3	5.0	9.6	Undetermined	18.72
G40D1	S1	5.3	4.2	4.2	4.3	4.4	4.4	4.4	4.3	4.3	4.4	4.4	19.74
	S2	4.3	3.9	4.0	4.2	4.3	4.3	4.2	4.2	4.2	4.2	4.2	19.87
	S3	3.2	3.2	3.4	3.6	3.7	3.8	3.7	3.7	3.5	3.5	3.4	19.81
	S4	2.6	2.9	3.4	3.5	3.4	3.4	3.3	3.2	3.2	3.1	3.0	19.44
	S5	2.6	3.1	3.3	3.2	3.2	3.0	3.0	2.9	2.9	2.9	2.9	19.80
	SC5	7.9	6.0	5.4	4.7	4.3	4.2	4.3	5.0	9.3	Undetermined		19.80

Table E-3: Load improvement ratio of columns in the D2 configuration.

Test series	Variable Parameter	s/D (Settlement/Diameter ratio) 2%	10%	20%	30%	40%	50%	60%	70%	80%	90%	100%	Moisture Content
G10D2	S1	5.5	4.4	4.3	4.5	4.7	4.7	4.6	4.4	4.4	4.3	4.3	19.51
	S2	6.2	5.1	5.0	5.1	5.3	5.3	5.3	5.3	5.3	5.2	5.2	19.46
	S3	3.9	3.9	4.2	4.5	4.6	4.6	4.7	4.8	4.9	4.9	4.9	19.20
	S4	4.0	3.9	4.3	4.5	4.6	4.6	4.6	4.7	4.7	4.7	4.8	19.01
	S5	3.4	3.7	3.9	3.9	3.8	3.7	3.7	3.7	3.7	3.7	3.8	19.66
	SC5	4.5	3.4	3.4	3.7	3.7	3.6	3.6	3.6	3.6	3.6	3.7	19.49
G20D2	S1	3.9	3.7	3.7	3.8	3.9	4.1	4.3	4.4	4.4	4.4	4.3	19.88
	S2	4.2	3.6	3.9	4.2	4.4	4.8	5.1	5.3	5.4	5.5	5.4	19.85
	S3	3.2	3.4	3.9	4.2	4.5	4.7	4.9	5.1	5.3	5.4	5.6	19.72
	S4	1.6	2.6	3.5	3.9	4.1	4.1	4.1	4.2	4.3	4.4	4.5	19.45
	S5	3.4	3.7	3.9	3.9	3.8	3.7	3.7	3.7	3.7	3.7	3.8	19.66
	SC5	3.4	2.6	2.6	2.6	2.6	2.6	2.5	2.5	2.8	2.6	2.6	20.55
G30D2	S1	5.2	4.1	3.9	4.0	4.2	4.2	4.1	4.0	4.0	3.9	3.9	20.52
	S2	3.9	3.6	3.8	4.0	4.2	4.4	4.4	4.4	4.4	4.4	4.4	19.96
	S3	3.8	3.9	4.1	4.2	4.4	4.6	4.6	4.7	4.7	4.8	4.9	19.93
	S4	3.4	3.4	3.7	3.8	3.9	4.1	4.2	4.2	4.3	4.3	4.4	20.17
	S5	3.4	3.7	3.9	3.9	3.8	3.7	3.7	3.7	3.7	3.7	3.8	19.91
	SC5	3.9	2.9	3.3	3.8	4.2	4.3	4.3	4.2	4.1	4.0	3.8	20.08
G40D2	S1	5.3	4.3	4.4	5.0	5.3	5.2	5.1	5.0	4.9	4.9	4.8	19.90
	S2	5.0	4.2	4.3	4.6	4.9	4.9	4.9	4.9	5.0	4.9	4.9	19.76
	S3	4.8	4.5	4.7	4.8	4.9	4.9	4.8	4.8	4.9	4.8	4.8	19.97
	S4	3.9	4.0	4.4	4.5	4.5	4.5	4.4	4.4	4.3	4.4	4.3	19.99
	S5	3.4	3.7	3.9	3.9	3.8	3.7	3.7	3.7	3.7	3.7	3.8	20.12
	SC5	7.4	5.4	5.1	4.7	4.3	4.1	4.0	3.9	3.9	3.8	3.8	19.54

Table E-4 Load improvement ratio of columns in the D3 configuration.

Test series	Variable Parameter	s/D (Settlement/Diameter ratio) 2%	10%	20%	30%	40%	50%	60%	70%	80%	90%	100%	Moisture Content
G10D3	S1	6.1	4.0	3.6	3.6	3.8	4.0	4.1	3.9	3.9	3.8	3.8	19.30
	S2	4.3	3.3	3.3	3.3	3.4	3.4	3.5	3.5	3.5	3.5	3.6	19.93
	S3	3.4	3.0	3.3	3.4	3.6	3.7	3.8	3.8	3.8	4.0	3.9	19.45
	S4	3.7	3.5	3.8	3.8	3.9	3.9	3.8	3.9	4.0	4.0	3.9	19.70
	S5	2.1	2.5	3.1	3.1	3.0	2.9	2.8	2.8	2.8	2.8	2.7	19.79
	SC5	4.1	2.6	2.4	2.6	3.0	3.4	3.5	3.4	3.4	3.3	3.3	19.68
G20D3	S1	3.2	2.5	2.4	2.5	2.7	2.9	3.1	3.4	3.6	3.7	3.7	19.67
	S2	3.2	2.7	2.8	2.8	2.9	3.1	3.3	3.5	3.6	3.7	3.8	19.48
	S3	2.3	2.4	2.6	2.7	2.8	2.9	3.0	3.2	3.3	3.5	3.5	19.51
	S4	2.5	2.7	3.0	3.2	3.2	3.2	3.2	3.2	3.2	3.2	3.3	19.38
	S5	2.1	2.5	3.0	3.1	3.1	2.9	2.8	2.8	2.8	2.8	2.7	19.79
	SC5	6.4	3.5	2.9	2.9	3.0	3.1	3.3	3.4	3.3	3.2	3.1	19.99
G30D3	S1	4.4	3.0	2.8	2.9	2.9	2.8	2.8	2.7	2.7	2.7	2.7	19.96
	S2	4.7	3.9	3.8	3.8	3.9	4.1	4.1	4.1	4.1	4.0	4.0	19.67
	S3	3.9	3.4	3.5	3.6	3.6	3.7	3.8	3.8	3.8	3.9	3.9	19.71
	S4	3.1	2.8	3.1	3.1	3.1	3.0	3.1	3.0	3.0	3.0	2.9	20.25
	S5	2.1	2.5	3.1	3.1	3.0	2.9	2.8	2.8	2.8	2.8	2.7	19.81
	SC5	2.3	1.8	1.8	2.0	2.1	2.1	2.1	2.1	2.1	2.1	2.1	20.31
G40D3	S1	4.9	3.4	3.2	3.4	3.7	3.9	3.9	3.8	3.8	3.7	3.7	20.09
	S2	5.0	3.6	3.4	3.5	3.7	3.8	3.8	3.8	3.7	3.8	3.7	19.75
	S3	4.0	3.3	3.5	3.6	3.6	3.7	3.7	3.7	3.7	3.7	3.8	20.25
	S4	4.0	3.5	3.7	3.8	3.8	3.7	3.6	3.5	3.5	3.5	3.5	20.13
	S5	2.1	2.5	3.0	3.1	3.0	2.9	2.8	2.8	2.8	2.8	2.7	19.60
	SC5	6.8	4.0	3.7	3.7	3.8	3.6	3.4	3.3	3.2	3.1	3.1	19.30

Table E-5: Load improvement ratio of S3 and S5 columns in the D2 configuration with a reinforced/unreinforced bedding layer.

Test series	s/D= 2%	s/D=10%	s/D=20%	s/D=30%	s/D=40%	s/D=50%	s/D=60%	s/D=70%	s/D=80%	s/D=90%	s/D=100%	Moisture content
Clay + bedding layer	2.5	2.2	1.7	1.7	1.6	1.6	1.7	1.8	1.9	2.0	2.0	20.11
Clay + reinforced bedding layer	1.9	2.3	2.6	2.8	3.3	3.8	4.2	4.6	4.9	5.3	5.4	19.38
S5	3.4	3.7	3.9	3.9	3.8	3.7	3.7	3.7	3.7	3.7	3.8	19.66
S5 + unreinforced bedding layer	1.9	2.4	2.8	2.5	2.2	2.2	2.4	2.7	3.0	3.4	3.6	20.10
S5 + reinforced bedding layer	1.3	2.2	3.0	3.4	4.1	4.8	5.5	6.3	6.9	7.6	8.1	19.32
S3	3.9	3.9	4.2	4.5	4.6	4.6	4.7	4.8	4.9	4.9	4.9	19.20
S3 + unreinforced bedding layer	2.2	3.3	2.0	1.3	1.6	2.1	3.1	3.8	4.3	4.8	5.3	19.66
S3 + reinforced bedding layer	1.6	2.7	3.6	4.2	5.0	5.8	6.7	7.5	8.3	9.2	9.9	19.93

F : Moisture content

Table F-1: Moisture contents of soils tested with different columns in the D0 configuration.

Test series	Variable parameter	<mass of container>	<mass of container + sample>	<mass of container + oven dried sample>	Moisture content
D0G10	S0	18.417	50.017	44.831	19.63
	SC5	8.146	34.133	29.852	19.72
	S1	8.073	28.122	24.840	19.57
	S2	25.921	48.881	45.105	19.68
	S3	22.531	42.987	39.612	19.76
	S4	17.547	39.584	35.963	19.66
	S5	17.698	63.611	56.114	19.52
D0G20	SC5	22.528	51.013	46.380	19.42
	S1	25.916	73.530	65.675	19.76
	S2	18.997	41.115	37.430	19.99
	S3	19.045	30.142	28.327	19.55
	S4	20.587	44.244	40.354	19.68
	S5	17.698	63.611	56.114	19.52
D0G30	SC5	8.189	33.044	29.000	19.43
	S1	17.696	45.337	40.823	19.52
	S2	17.554	64.880	57.441	18.65
	S3	22.528	41.614	38.516	19.38
	S4	8.180	31.854	27.991	19.50
	S5	8.457	24.755	22.051	19.89
D0G40	SC5	18.415	39.054	35.720	19.27
	S1	17.698	45.840	41.145	20.02
	S2	18.997	34.032	31.577	19.52
	S3	22.529	49.636	45.118	20.00
	S4	17.657	42.228	38.161	19.84
	S5	25.920	46.719	43.322	19.52

Table F-2: Moisture contents of soils tested with different columns in the D1 configuration.

Test series	Variable parameter	<mass of container>	<mass of container + sample>	<mass of container + oven dried sample>	Moisture content
D1G10	S0	19.417	51.415	46.101	19.91
	SC5	18.840	40.840	37.282	19.29
	S1	18.457	35.453	32.684	19.46
	S2	17.705	35.504	32.684	18.83
	S3	18.999	43.453	39.499	19.29
	S4	17.657	38.315	35.002	19.10
	S5	17.659	40.122	36.476	19.38
D1G20	S0	21.558	47.294	43.109	19.42
	SC5	18.762	53.282	47.661	19.45
	S1	18.999	48.239	43.421	19.73
	S2	18.841	54.871	48.944	19.69
	S3	19.564	38.579	35.441	19.76
	S4	8.118	30.664	27.040	19.15
	S5	17.659	40.122	36.476	19.38
D1G30	SC5	17.696	64.880	57.441	18.72
	S1	9.718	37.246	32.671	19.93
	S2	8.116	26.582	23.587	19.36
	S3	8.131	28.588	25.223	19.69
	S4	7.992	47.687	41.098	19.90
	S5	18.417	40.700	37.054	19.56
D1G40	SC5	17.568	32.571	30.091	19.80
	S1	18.996	33.934	31.471	19.74
	S2	9.658	24.859	22.339	19.87
	S3	17.557	40.783	36.942	19.81
	S4	18.836	37.851	34.756	19.44
	S5	17.660	34.490	31.708	19.80

Table F-3: Moisture contents of soils tested with different columns in the D2 configuration.

Test series	Variable parameter	<mass of container>	<mass of container + sample>	<mass of container + oven dried sample>	Moisture content
D2G10	S0	17.560	62.867	55.213	20.33
	SC5	8.079	25.046	22.278	19.49
	S1	8.072	24.968	22.210	19.51
	S2	22.533	47.523	43.452	19.46
	S3	17.545	33.096	30.591	19.20
	S4	25.927	48.994	45.309	19.01
	S5	22.530	55.171	49.808	19.66
D2G20	SC5	25.919	102.608	89.536	20.55
	S1	25.920	61.049	55.223	19.88
	S2	21.873	28.188	27.142	19.85
	S3	18.418	73.818	64.693	19.72
	S4	17.705	52.244	46.621	19.45
	S5	22.530	55.171	49.808	19.66
D2G30	SC5	18.999	47.022	42.335	20.08
	S1	18.842	51.844	46.226	20.52
	S2	17.553	56.886	50.342	19.96
	S3	22.529	60.219	53.955	19.93
	S4	17.656	52.352	46.529	20.17
	S5	18.442	45.287	40.830	19.91
D2G40	SC5	25.921	49.702	45.815	19.54
	S1	18.838	37.803	34.655	19.90
	S2	18.416	44.089	39.853	19.76
	S3	18.996	37.359	34.302	19.97
	S4	17.698	35.919	32.884	19.99
	S5	17.552	46.612	41.745	20.12

Table F-4: Moisture contents of soils tested with different columns in the D0 configuration.

Test series	Variable parameter	<mass of container>	<mass of container + sample>	<mass of container + oven dried sample>	Moisture content
D3G10	S0	22.521	40.552	37.613	19.47
	SC5	18.456	44.720	40.401	19.68
	S1	18.839	36.528	33.666	19.30
	S2	19.002	43.045	39.049	19.93
	S3	17.703	45.420	40.906	19.45
	S4	17.656	45.171	40.642	19.70
	S5	18.996	49.604	44.548	19.79
D3G20	SC5	17.555	57.336	50.708	19.99
	S1	7.953	27.973	24.683	19.67
	S2	18.841	55.739	49.722	19.48
	S3	25.918	87.518	77.461	19.51
	S4	17.656	60.239	53.327	19.38
	S5	18.996	49.604	44.548	19.79
D3G30	SC5	22.315	45.829	41.859	20.31
	S1	22.527	54.517	49.194	19.96
	S2	18.997	45.812	41.404	19.67
	S3	17.699	36.825	33.676	19.71
	S4	18.416	47.872	42.912	20.25
	S5	17.657	35.805	32.804	19.81
D3G40	SC5	17.658	39.140	35.665	19.30
	S1	17.704	46.943	42.052	20.09
	S2	18.999	38.473	35.261	19.75
	S3	22.530	52.143	47.156	20.25
	S4	7.991	38.938	33.753	20.13
	S5	9.666	30.826	27.358	19.60

Table F-5: Moisture contents of soils when S3 and S5 columns were tested in the D2 configuration with a reinforced/unreinforced bedding layer.

Test series	<mass of container>	<mass of container + sample>	<mass of container + oven dried sample>	Moisture content
Clay only	17.560	62.867	55.213	20.33
Clay with stone bed only	17.907	36.123	33.073	20.11
Clay with reinforced clay bed	18.457	37.205	34.162	19.38
S5	22.530	55.171	49.808	19.66
S5 + unreinforced bedding layer	22.531	46.607	42.577	20.10
S5 + reinforcedstone bed	19.001	51.384	46.140	19.32
S3	17.545	33.096	30.591	19.20
S3 + unreinforced bedding layer	18.455	37.927	34.728	19.66
S3 + reinforced stone bed	18.840	70.906	62.255	19.93

G : Performance of stone columns

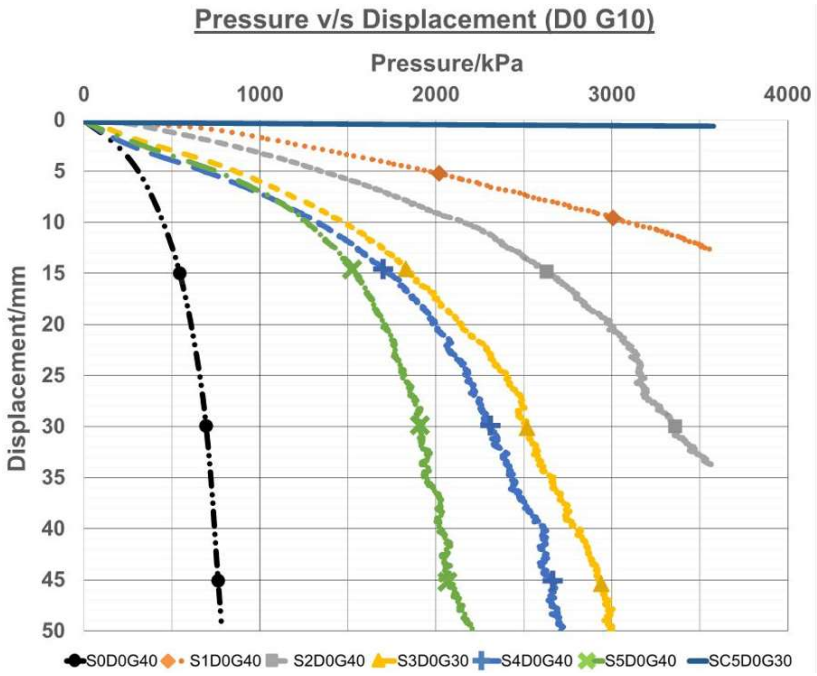

Figure G-1: Performance of stone columns in D0 configuration for G10 concrete.

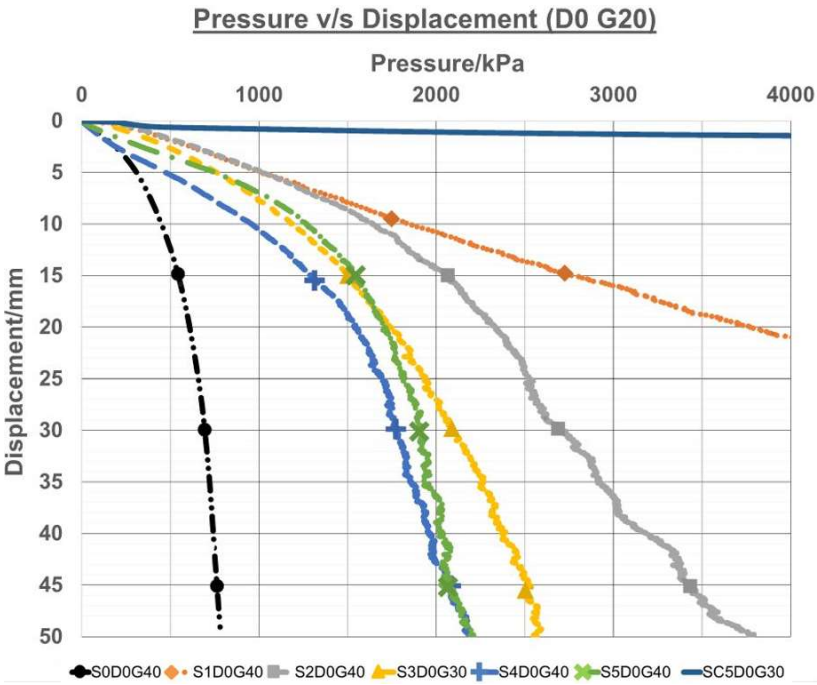

Figure G-2: Performance of stone columns in D0 configuration for G20 concrete.

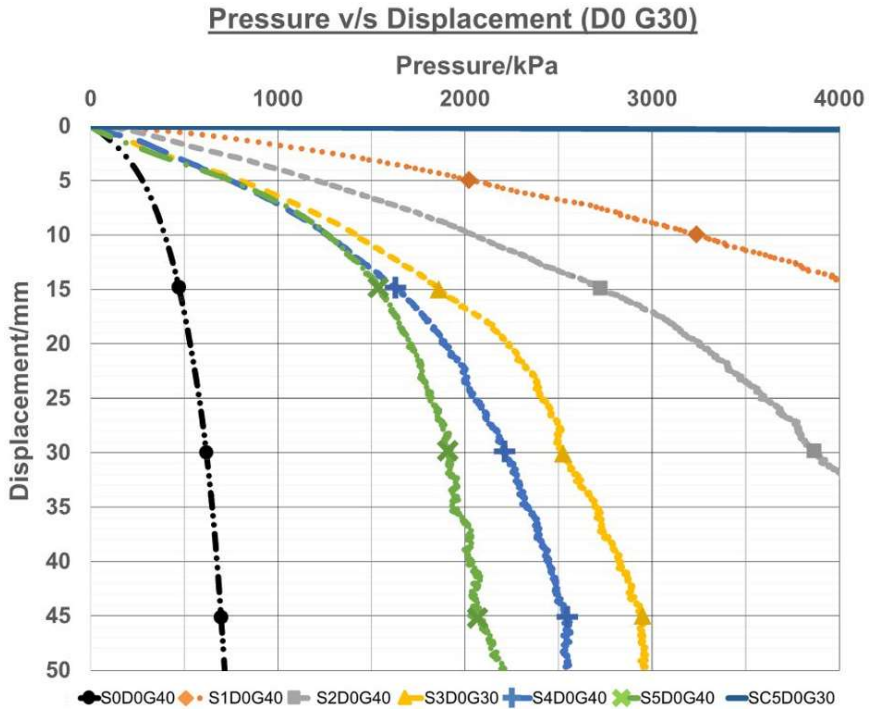

Figure G-3: Performance of stone columns in D0 configuration for G30 concrete.

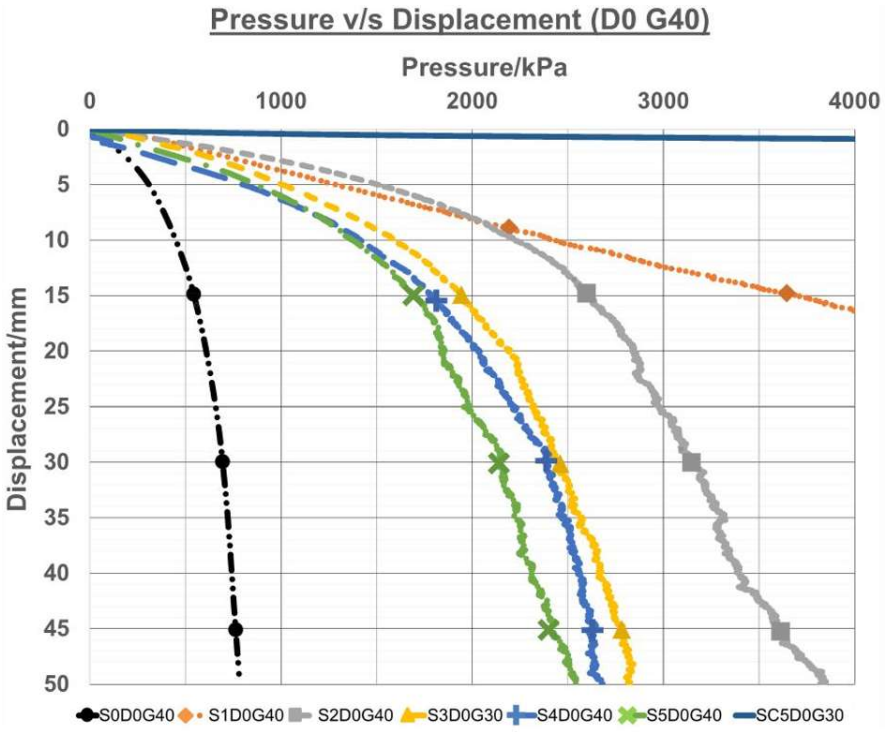

Figure G-4: Performance of stone columns in D0 configuration for G40 concrete.

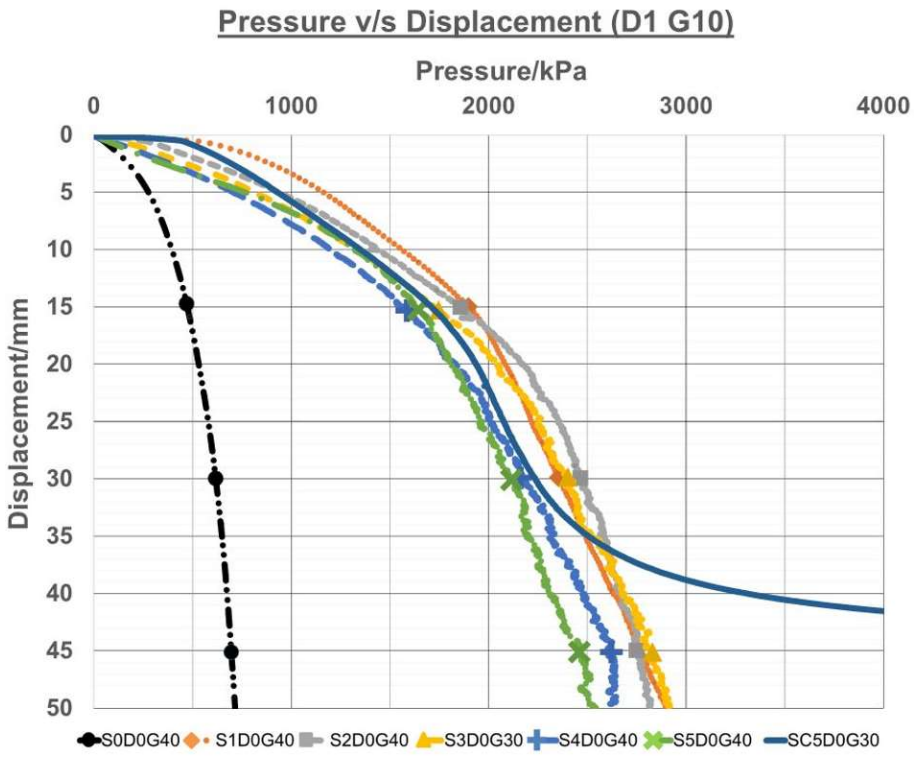

Figure G-5: Performance of stone columns in D1 configuration for G10 concrete.

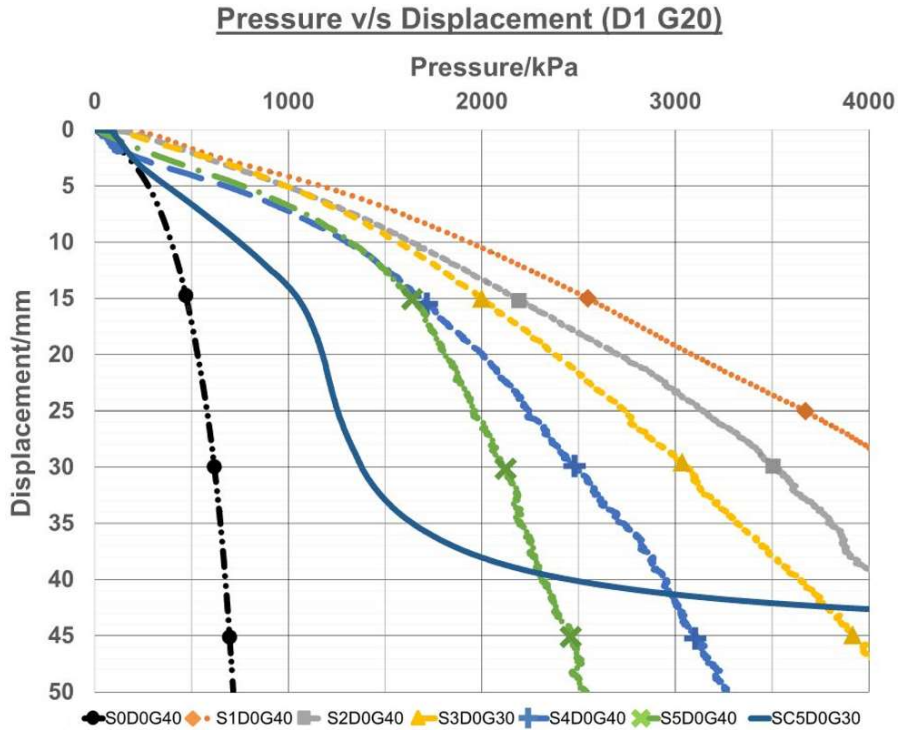

Figure G-6: Performance of stone columns in D1 configuration for G20 concrete.

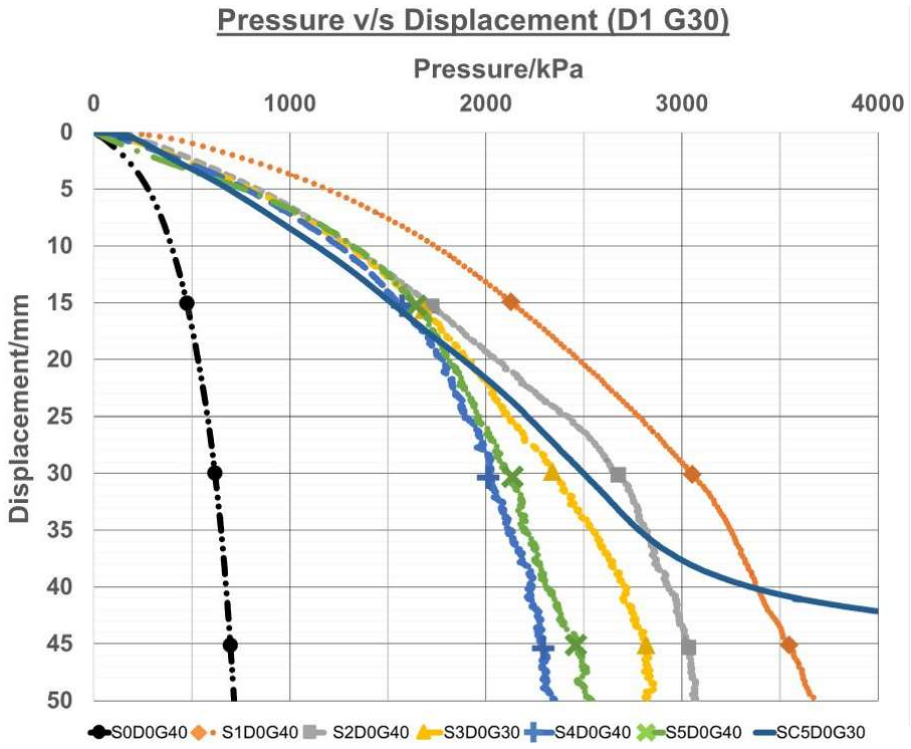

Figure G-7: Performance of stone columns in D1 configuration for G30 concrete.

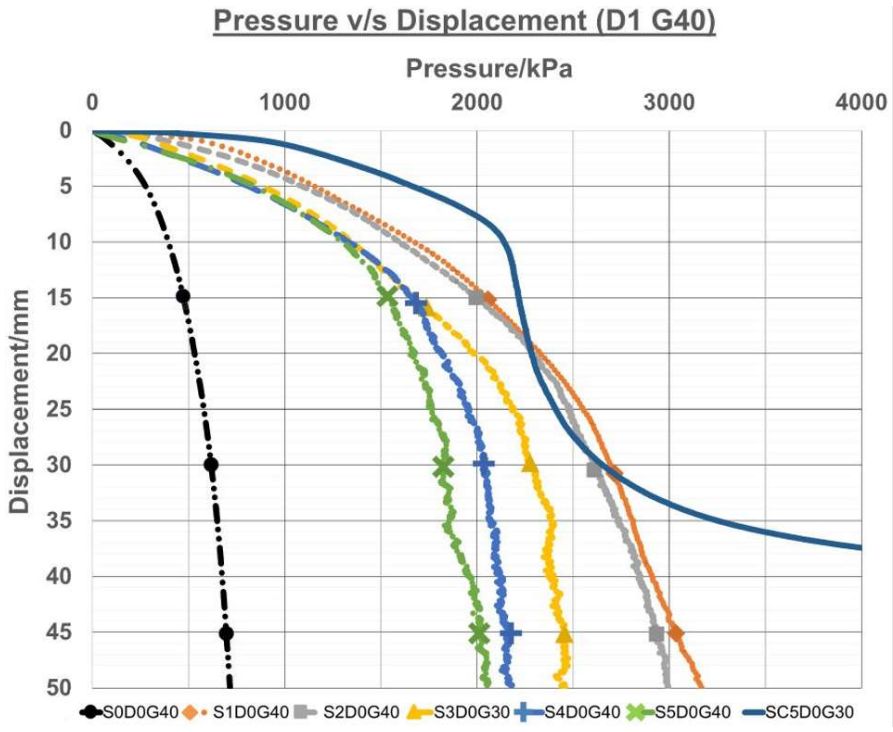

Figure G-8: Performance of stone columns in D1 configuration for G40 concrete.

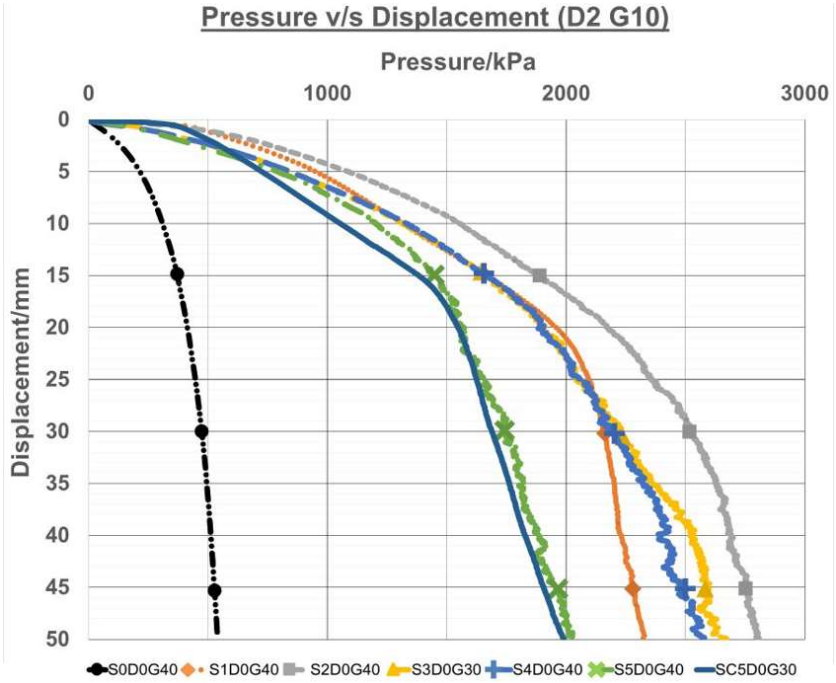

Figure G-9: Performance of stone columns in D2 configurations for G10 concrete.

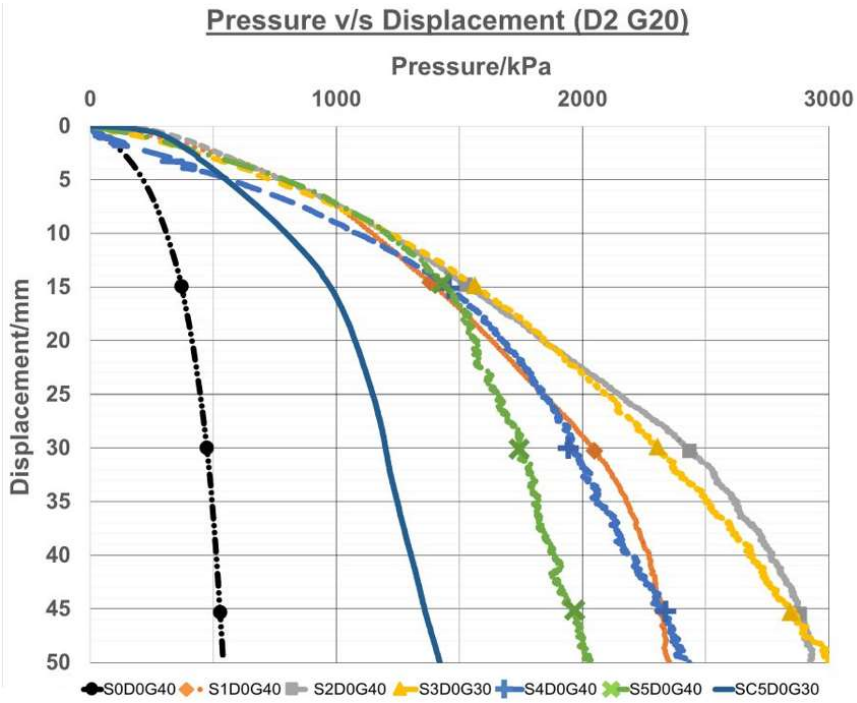

Figure G-10: Performance of stone columns in D2 configurations for G20 concrete.

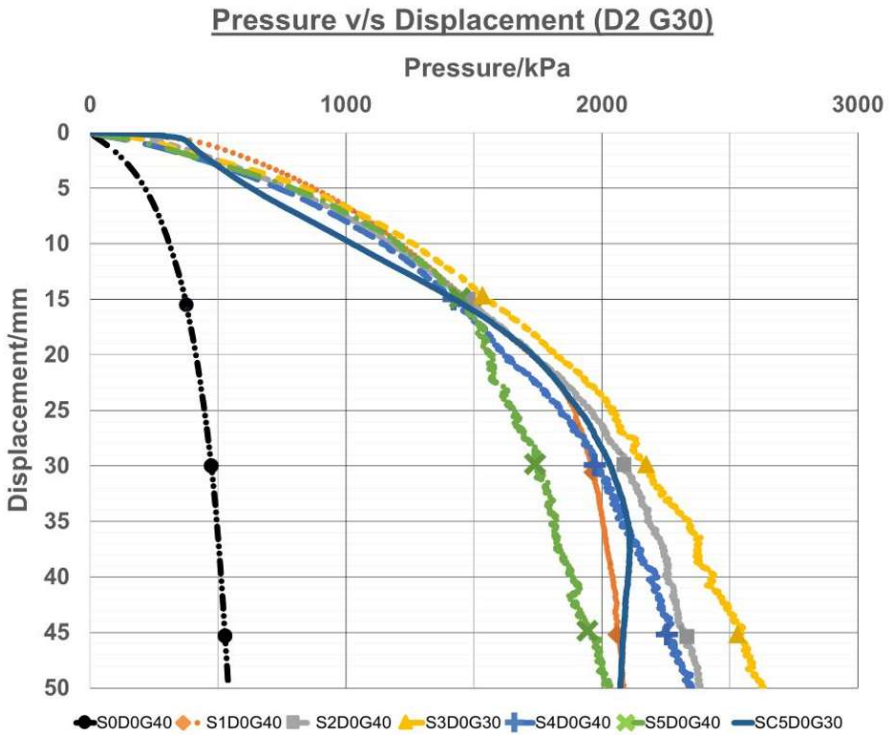

Figure G-11: Performance of stone columns in D2 configurations for G30 concrete.

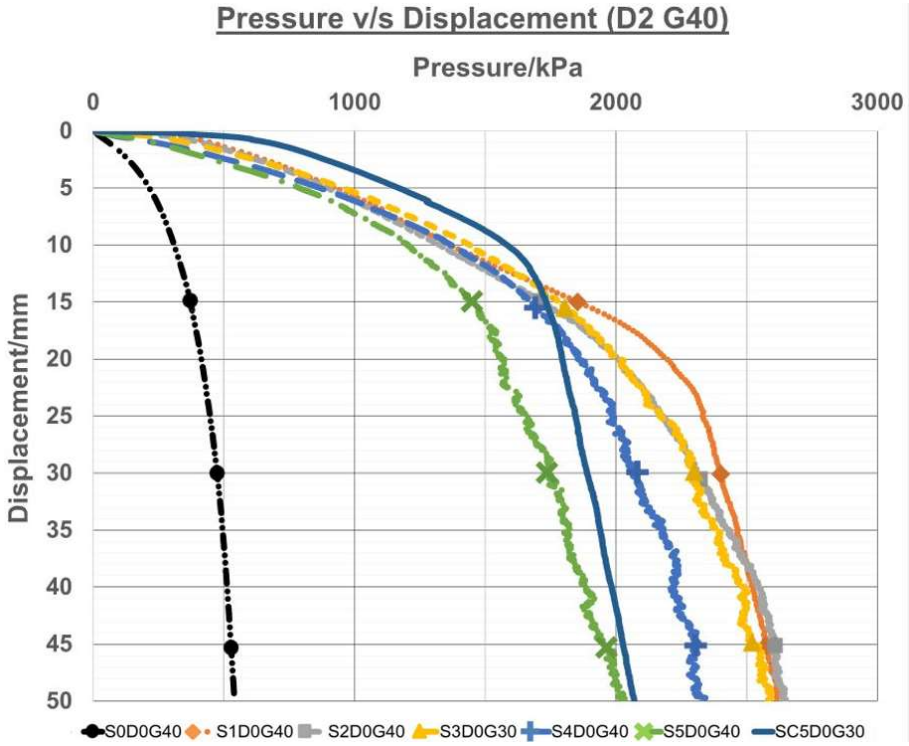

Figure G-12: Performance of stone columns in D2 configurations for G40 concrete.

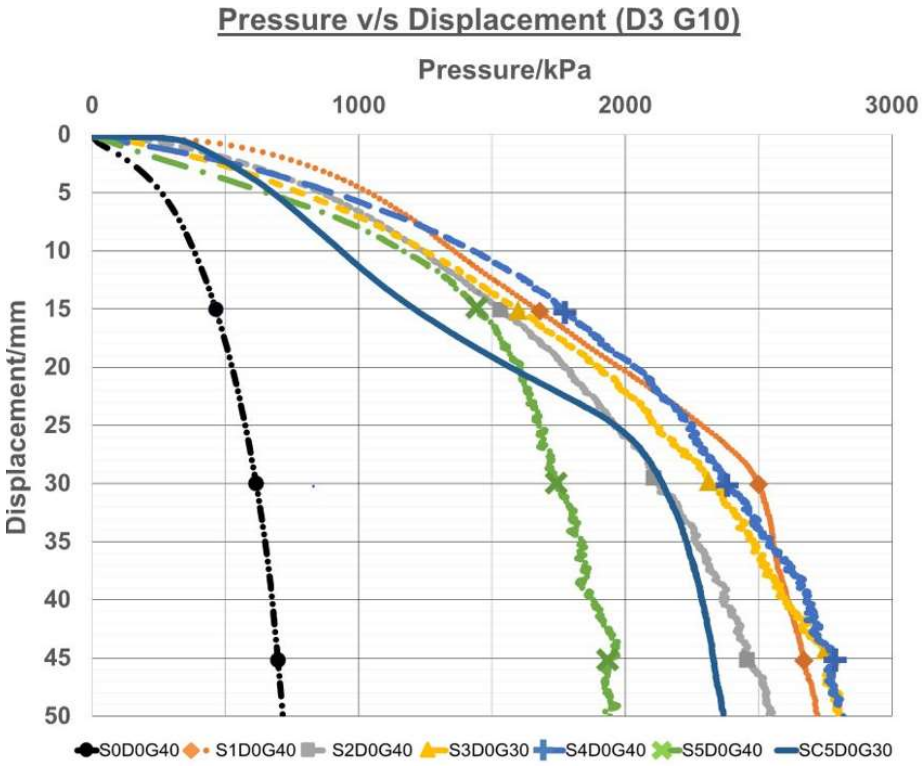

Figure G-13: Performance of stone columns in D3 configurations for G10 concrete.

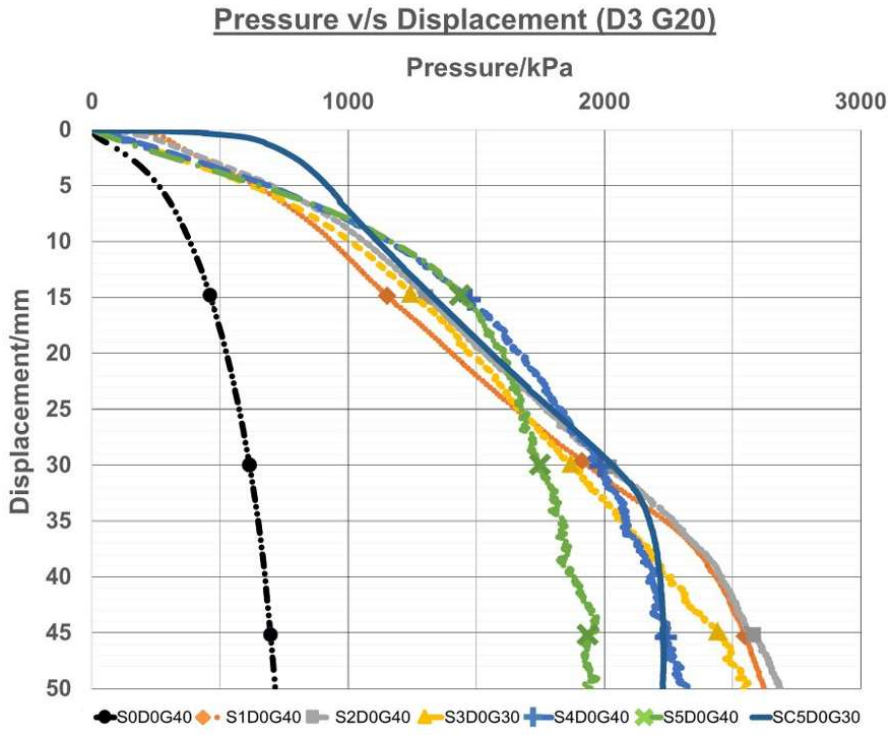

Figure G-14: Performance of stone columns in D3 configurations for G20 concrete.

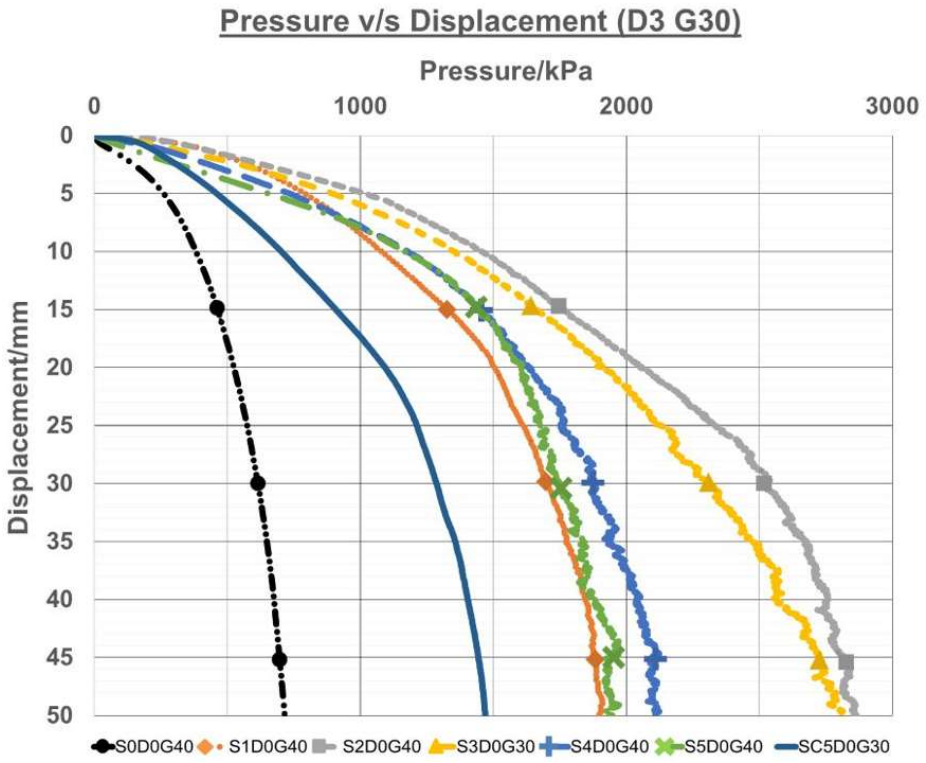

Figure G-15: Performance of stone columns in D3 configurations for G30 concrete.

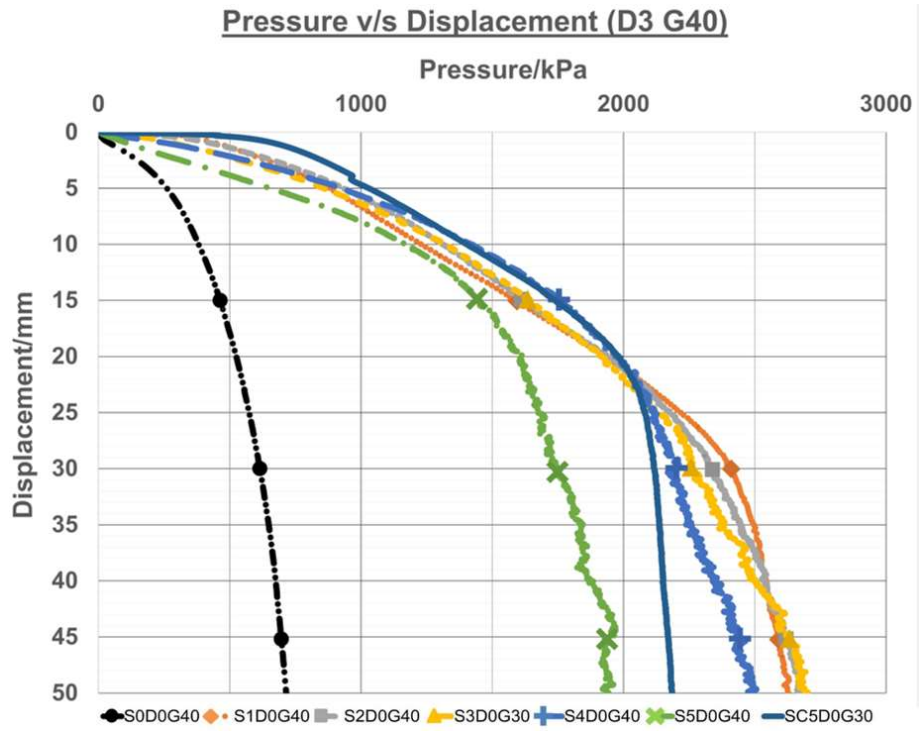

Figure G-16: Performance of stone columns in D3 configurations for G40 concrete.

References

1. AGARWAL, K. B. & GHANEKAR, K. D. 1970. Prediction of CBR from plasticity characteristics of soil. *Proceeding of 2nd south-east Asian conference on soil engineering*.
2. ARQ. 2014. *Port Louis Ring Road Design approach of post-failure stabilisation* [Online]. Available: https://arq.co.za/?p=1130 [Accessed 14 June 2017].
3. ASGARI, A., OLIAEI, M. & BAGHERI, M. 2013. Numerical simulation of improvement of a liquefiable soil layer using stone column and pile-pinning techniques. *Soil Dynamics and Earthquake Engineering,* 51**,** 77-96.
4. ASTM C127 2015. Standard Test Method for Relative Density (Specific Gravity) and Absorption of Coarse Aggregate. United States: ASTM International.
5. ASTM C128 2015. Standard Test Method for Relative Density (Specific Gravity) and Absorption of Fine Aggregate. United States: ASTM International.
6. ASTM D422 2007. Standard Test Method for Particle-Size Analysis of Soils. United States: ASTM International.
7. ASTM D698 2012. Standard Test Methods for Laboratory Compaction Characteristics of Soil Using Standard Effort. United States: ASTM International.
8. ASTM D854 2014. Standard Test Methods for Specific Gravity of Soil Solids by Water Pycnometer. United States: ASTM international.
9. ASTM D1557 2012. Standard Test Methods for Laboratory Compaction Characteristics of Soil Using Modified Effort (56,000 ft-lbf/ft3 (2,700 kN-m/m3))1. United States: ASTM International.
10. ASTM D1883 2016. Standard Test Method for California Bearing Ratio (CBR) of Laboratory-Compacted Soils. United States: ASTM International.
11. ASTM D2487 2011. Standard Practice for Classification of Soils for Engineering Purposes (Unified Soil Classification System). United States: ASTM International.
12. ASTM D3080 2011. Direct Shear Test of Soils Under Consolidated Drained Conditions. United States: ASTM international.
13. ASTM D4318 2010. Standard Test Methods for Liquid Limit, Plastic Limit, and Plasticity Index of Soils1. United States: ASTM International.
14. ASTM D6913 2009. Standard Test Methods for Particle-Size Distribution (Gradation) of Soils Using Sieve Analysis. United States: ASTM international.
15. AZA-GNANDJI, R. & KALUMBA, D. 2014. Experimental and Numerical Analysis of the Behaviour of Rammed Stone Columns Installed in a South African Soft Soil. *International Journal of Engineering Science and Innovative Technology (IJESIT),* 3.
16. BARKSDALE AND BACHUS 1983. *Design and construction of stone columns,* Virginia, Federal Highway Administration.
17. BOSELA, P., BRADY, P., DELATTE, N. & PARFITT, M. 2013. *Failure Case Studies in Civil Engineering,* United States of America., American Society of Civil Engineers.
18. BOWLES J.E 1997. *Foundation Analysis and Design,* Singapore, The McGraw-Hill Companies, Inc.
19. BS 1881-121 1983. Method for determination of elasticity in compression. London: BSI.

20. BS EN 12390-2 2000. Testing Hardened concrete: Making and curing specimen for strength test. Brussels, Germany: European Committee for Standardisation.

21. BS EN 12390-3 2001. Testing Hardened Concrete: Compressive strength of test specimens. Brussels, Germany: European Committee for Standardisation.

22. BYRNE, G. & BERRY, A. D. 2008. *A guide to practical geotechnical engineering in Southern Africa,* South Africa, VIVO Design Associates.

23. CARTER, M. & BENTLEY, S. P. 1991. *Correlations of Soil Properties,* London, Pentech Press.

24. CEMENT & CONCRETE INSTITUTE 1999. Strength development curves for SA cements. Midrand: Cement & Concrete institute.

25. CHAI, J., SHEN, S., DING, W., ZHU, H. & CARTER, J. 2014. Numerical investigation of the failure of a building in Shanghai, China. *Computers and Geotechnics,* 55**,** 482-493.

26. CHEN, J.-F., LI, L.-Y., XUE, J.-F. & FENG, S.-Z. 2015. Failure mechanism of geosynthetic-encased stone columns in soft soils under embankment. *Geotextiles and Geomembranes,* 43**,** 424-431.

27. CRAIG, R. & KNAPPETT, J. 2012. *Craig's Soil Mechanics,* London, Spon Press.

28. DAS, B. M. & SOBHAN, K. 2014. *Principles of Geotechnical Engineering,* USA, Global Engineering.

29. DASH, S. K. & BORA, M. C. 2013. Improved performance of soft clay foundations using stone columns and geocell-sand mattress. *Geotextiles and Geomembranes,* 41**,** 26-35.

30. DEB, K. 2008. Modeling of granular bed-stone column-improved soft soil. *International Journal for Numerical and Analytical Methods in Geomechanics,* 32**,** 1267-1288.

31. DEB, K. & MOHAPATRA, S. R. 2012. Analysis of stone column-supported geosynthetic-reinforced embankments. *Applied Mathematical Modelling,* 37**,** 2943-2960.

32. DEB, K., SAMADHIYA, N. K. & NAMDEO, J. B. 2011. Laboratory model studies on unreinforced and geogrid-reinforced sand bed over stone column-improved soft clay. *Geotextiles and Geomembranes,* 29**,** 190-196.

33. DEFIMEDIA.INFO. 2016. Autoroute terre-rouge-verdun : l'entrée en opération totale pas avant 1 an. *LeDEFIMEDIAGROUP*, 27th September.

34. DHEERENDRA BABU, M. R., NAYAK, S. & SHIVASHANKAR, R. 2012. A Critical Review of Construction, Analysis and Behaviour of Stone Columns. *Geotechnical and Geological Engineering,* 31**,** 1-22.

35. FRANKI 2010. Deep Vibro techniques. Pretoria, South Africa: Franki Africa.

36. GHAZAVI, M. & JAVAD, N. A. 2013. Bearing capacity of geosynthetic encased stone columns. *Geotextiles and Geomembranes,* 38**,** 26-36.

37. GNIEL, J. & BOUAZZA, A. 2009. Improvement of soft soils using geogrid encased stone columns. *Geotextiles and Geomembranes,* 27**,** 167-175.

38. GNIEL, J. & BOUAZZA, A. 2010. Construction of geogrid encased stone columns: A new proposal based on laboratory testing. *Geotextiles and Geomembranes,* 28**,** 108-118.

39. GOVERNMENT INFORMATION SERVICE. 2015. *Remedial works on Ring Road Phase 1 to be completed by February 2016* [Online]. Available: http://www.govmu.org/English/News/Pages/Remedial-works-on-Ring-Road-Phase-1-to-be-completed-by-February-2016.aspx [Accessed 14 June 2017].

40. HONG, Y.-S., WU, C.-S. & YU, Y.-S. 2015. Model tests on geotextile-encased granular columns under 1-g and undrained conditions. *Geotextiles and Geomembranes,* 44**,** 13-27.
41. HUYBRECHTS, N. & DENIES, N. 2013. General Report of TC 211. Proceedings of the 18th International Conference on Soil Mechanics and Geotechnical Engineering.
42. IS 15284 2003. Design and Construction for ground improvement- guidelines. *15284-1.* New Delhi: Prabhat Offset Press.
43. KAYTECH ENGINEERED FABRIC 2015. Technical Data Sheet. *In:* FABRIC, K. E. (ed.) *Creep tests on Rockgrid PC composite geotextile.* UK.
44. KAZEMIAN, S. & HUAT, B. B. K. 2010. Assessment of stabilization method for soft soils using admixtures. *Conference of Science and Social research*.
45. KEYKHOSROPUR, L., SOROUSH, A. & IMAM, R. 2012. 3D numerical analyses of geosynthetic encased stone columns. *Geotextiles and Geomembranes,* 35**,** 61-68.
46. KIRSCH, K. & BELL, A. 2012. *Ground Improvement,* London, CRC Press.
47. L'EXPRESS. 2015. Terre-Rouge-Verdun se dégrade de jour en jour. *L'express,*, 3rd February.
48. LE ROUX, D. 2016. Slope stability assessment associated with the Kirkwood Formation in the Southern Cape. *University of Cape Town*.
49. MANI, K. & NIGEE, K. 2013. A study on ground improvement using stone column technique. *International Journal of Innovative Research in Science Engineering and Technology,* 2.
50. MARSH B K 1997. *Design Of Normal Concrete Mixes Second Edition,* Watford, United Kingdom, Building Research Establishment Ltd.
51. MITCHELL, J. & SOGA, K. 2005. *Fundamentals of Soil Behavior,* USA, John Wiley & Sons.
52. MURUGESAN, S. & RAJAGOPAL, K. 2006. Geosynthetic-encased stone columns: Numerical evaluation. *Geotextiles and Geomembranes,* 24**,** 349-358.
53. NICHOLSON, P. G. 2015. *Soil improvement and ground modification methods,* U.S.A, Elsevier.
54. OVERSEAS ROAD NOTE 31 1993. Overseas Road Note 31. *Transport research laboratory*.
55. OWENS, G. 2009. *Fulton's concrete technology,* Midrand, South Africa,, Cement & Concrete Institute.
56. PUZRIN, A., ALONSO, E. & PINYOL, N. 2010. *Geomechanics of Failures,* London, Springer.
57. RAJ, P. 1999. *Ground Improvement Techniques,* New Delhi, Laxmi Publications.
58. SHUKLA, S. K. 2002. *Geosynthetics and their applications,* London, Thomas Telford.
59. SOBHEE-BEETUL, L. 2012. An Investigation using rammed stone columns for the improvement of South African Silty Clay. *University of Cape Town*.
60. TAFRESHI, S. N. M. & DAWSON, A. R. 2010. Comparison of bearing capacity of a strip footing on sand with geocell and with planar forms of geotextile reinforcement. *Geotextiles and Geomembranes,* 28**,** 72-84.

61. WONDEROPOLIS. 2012. *Is the Leaning Tower of Pisa Falling?* [Online]. NCFL. Available: http://wonderopolis.org/wonder/is-the-leaning-tower-of-pisa-falling [Accessed 14 June 2017].

62. XANTHAKOS, P., ABRAMSON, L. & BRUCE, D. 1994. *Ground Control and Improvement* New York, John Wiley & Sons.